HF PROPAGATION OVER HORIZONTALLY UNIFORM FIRST YEAR SEA ICE

KEN KLEIN

KENNETH A. BUTT

Technical Report
C-CORE Publication No. 83-13
December, 1983

C-CORE

CENTRE FOR COLD OCEAN RESOURCES ENGINEERING
MEMORIAL UNIVERSITY OF NEWFOUNDLAND
ST. JOHN'S, NEWFOUNDLAND, CANADA, A1B 3X5
TELEX 016 4794 TELEPHONE (709) 737-8354

The Centre for Cold Ocean Resources Engineering (C-CORE) was established at Memorial University of Newfoundland in St. John's in 1975. Its initial funding was provided by the Devonian Group of Charitable Foundations of Calgary. Ongoing funding now comes from government and industry.

The Centre's mandate is to undertake research that will assist the safe and orderly development of Canada's resources in cold and ice frequented oceans.

Ken Klein
Research Scientist, Radar Group
C-CORE

Kenneth A. Butt
Leader, Radar Group
C-CORE
(until June 1983 - now with INSTRUMAR Ltd.)

ISBN 0-88901-112-5

ABSTRACT

Transmission loss measurements (Pond Inlet, N.W.T., 1982) of vertically polarized waves at 25.4 MHz, propagating across horizontally uniform first year sea ice are compared with theoretical loss calculations.

Theoretical loss is calculated from a model based on the work of Walsh (1982) and Wait (1970) applying the concept of surface impedance.

Surface impedance is calculated from the vertical dielectric profile of the medium of propagation, assuming a series of horizontally uniform layers, each layer characterized by a permittivity and conductivity at the frequency of interest.

The dielectric properties are calculated from an empirical relationship relating the measured salinity and temperature profiles of the medium to permittivity and conductivity.

The objective is the development of a realistic model of propagation, for future application in C-CORE's ongoing program to develop an H.F. ground wave radar that will remote-sense ice conditions to a range beyond the optical horizon.

ACKNOWLEDGEMENTS

This project was funded by Department of Supply and Services contract: OSS81-00129, file number 31SS.FP802-1-2139 from Ocean Science and Surveys of the Department of Fisheries and Oceans. In addition, funding was received through the Department of Fisheries and Oceans support of an Ocean Remote Sensing Program at C-CORE.

Success of the field experiment and data collection was the product of a strong team effort. Special thanks to Terry Ridings, Ernest Reimer, and Deborah Diemand of C-CORE who provided special assistance for this program. Thanks to Phil Jeans, of C-CORE for his engineering of a special purpose HF radar control system, and to Eleanor Nesbitt-Friis who edited the report and prepared it for publication.

The authors gratefully acknowledge the contributions of John Walsh, Faculty of Engineering, and Joe Ryan, Graduate student, Engineering, Memorial University, for their discussions and support of the overall program and specifically for implementing a model of HF propagation.

The local staff of Arctic Research Establishment, Pond Inlet, N.W.T., provided necessary logistic support to carry out the field work.

TABLE OF CONTENTS

	PAGE
Abstract	i
Acknowledgements	ii
Table of Contents	iii
List of Figures	v
List of Tables	vi
1. Introduction	1
2. Project Description	3
3. Hardware Description	5
3.1 Transceiver	5
3.2 Transmit Power Amplifier	6
3.3 Transmit Antenna	7
3.4 Multiplexer Box	7
3.5 Transponder	7
3.6 HF Control Box	8
4. Field Work (Pond Inlet, N.W.T.)	9
4.1 Personnel	9
4.2 Preparation and Operational Testing	9
4.3 Measurement Along the Line of Interest	11
5. Theory	15
5.1 Propagation of a Vertically Polarized E/M Wave over Horizontally Homogeneous Media	15
5.2 Transmission Loss	16
5.3 Vertical Infinitesimal Dipoles	18
6. Computerized Model	21
6.1 Calculation of Normalized Surface Impedance	21
6.2 Evaluating F(w)	22
7. Transmission Loss Measurements and Signal Processing	25
7.1 The Decoded Transponder Signal	25
7.2 Processing Out Noise Background	26
7.3 Calculating Transmission Loss	27
8. Modelling Sea Ice and Snow as Series of Horizontally Uniform Dielectric Layers	29
8.1 Available Data Relating Dielectric Properties to Salinity and Temperature	30
8.2 Empirical Approach	31
8.3 The Average Salinity Profile of the Sea Ice on the Line Line of Interest	34
8.4 The Observed Temperature Profiles	38
8.5 The Resulting Dielectric Profile	38

9. Results and Discussion 41
9.1 Transmission Loss: Observed vs. Theoretical 41
9.2 Antenna Efficiency: Corrections to Calculated Transmission Loss 43
9.3 Sensitivity of Calculated Loss to ϵ_r, σ and the Depth of Sea Ice 46

10. Conclusions 51

11. Recommendations 53

References 55

Figures 57

Appendix A Salinity Measurements of Ice Cores Taken Along the Line of Interest 91

Appendix B Temperature Data 97

Appendix C Calculation of Receiver Gains 101

Appendix D Intermediate Results from Intigrated Digital I & Q Wave Forms 103

Appendix E Computerized Model 123

LIST OF FIGURES

		PAGE
Figure 1	Field Operational Configuration	57
Figure 2	HF Doppler Radar - Photo	58
Figure 3	Transceiver Block Diagram	59
Figure 4	Transmit Power Amplifier Block Diagram	60
Figure 5	CODAR Transponder - Block Diagram.....	61
Figure 6	Scope Display of Noise Floor for Two Receive Antenna Locations	62
Figure 7	Scope Display of Noise Floor (a) and Decoded Transponder Signal (b)	63
Figure 8	Map of Eclipse Sound and Line of Interest	64
Figure 9	Experimental Test Sites Along Line of Interest....	65
Figure 10	Location of Near Field Propagation Measurements...	66
Figure 11	Pond Inlet - Crossing Tidal Crack with Komatik ...	67
Figure 12	Komatik and Transponder	67
Figure 13	Coring the Sea Ice	68
Figure 14	HF Radar in Operation	68
Figure 15	View of Tent and Transmit Antenna out on the Ice	69
Figure 16	View of Transmit Antenna Overlooking Line of Interest	69
Figure 17	Quarter Wave Monopole Receive Antenna and Mux box	70
Figure 18	Coordinate System for Infinitesimal Dipole above Complex Medium	70
Figure 19	Decoded Transponder Signal	71
Figure 20	Receiver Output Before (a) and After (b) Transponder Locks onto Transmit Pulse.....	72
Figure 21	Output from HP 5451B Fourier Analyzer used as basis for calibration	73

Figure 22 Block Diagram Modelling Transmission Loss Calculations 74

Figure 23 Graph of Empirical Formulae 75

Figure 24 Observed Salinities, Graph (a-d)..... 76

Figure 25 Salinity Profile (C-CORE Data)..... 80

Figure 26 Ice Profile Overview 81

Figure 27 Final Model of Salinity Profile 82

Figure 28 Rescaled Temperature Profile TM-1 83

Figure 29 Rescaled Temperature Profiles TC-1 84

Figure 30 Transmission Loss: Observed vs Theoretical..... 85

Figure 31 Variation of Calculated loss with ϵ_r 86

Figure 32 Variation of Calculated Loss at 5 km as individual parameters are varied..... 87

Figure 33 Variation of Calculated Loss with σ (graph) 88

Figure 34 Variation of Calculated Loss with h_{ice} (graph) ... 89

LIST OF TABLES

PAGE

Table I Ice Core and Temperature String Locations..... 13

Table II Ice Thickness and Surface Temperature Measurements 14

Table III Calculated Transmission Loss 29

Table IV Extracted Data from C-CORE Technical Report 77-6 . 33

Table V Coefficients for Empirical Formulae 33

Table VI Grouping Salinities for the Surface Layer 34

Table VII Ice and Snow Thickness Measurements Along Line of Interest 36

Table VIII Temperature/Salinity Profiles Modelling Sea Ice and Snow 39

Table IX Resultant Dielectric Profiles 39

Table X Observed Transmission Loss vs Theoretical Transmission Loss..... 42

Table XI Calculated Relative Loss vs Observed Relative Loss..... 43

Table XII Sensitivity of Calculated Loss to Single Parameter Variation..... 47

1. INTRODUCTION

HF radar has many of the attributes potentially necessary to remote-sense ice conditions beyond the optical horizon. Safe operations in cold oceans will require almost immediate knowledge of ice conditions. Sensitivity to changing ice conditions determines the range of remote sensing and the detail of information required.

Navigation in the Arctic, involving optimum route selection, hazard detection and avoidance requires a shipboard remote sensor capable of target detection and identification beyond the optical horizon. The ice conditions observed off the east coast of Newfoundland in the winter and spring of 1983 demonstrated the need for the province to have its own early warning sensor capable of beyond-the-horizon monitoring of icebergs and pack ice.

HF radar, whose wavelength is orders of magnitude longer than conventional marine radar, propagates in a groundwave mode not limited in range to the optical horizon. The interaction of HF radiation with ice targets relies on the electrical dissimilarity between the target and its surroundings.

Because of these attributes C-CORE is actively investigating the limitations and capabilities of remote sensing of ice conditions in the HF band.

One part of the much larger investigation is the assessment of the operational range of HF radar over already existing ice cover, to delineate hazardous ice features in the ice cover or beyond. In addition, a general theory in the form of a model is

required for propagation loss, radar cross-section at HF, range predictions and many other fundamental issues.

This report describes the measurement of propagation loss at HF over first year sea ice, comparing it with predictions from an HF layered media propagation model developed at Memorial University. The long term objective of the HF radar program is the specification of an optimum HF radar for remote sensing of ice conditions.

2. PROJECT DESCRIPTION

In March, 1982, C-CORE conducted transmission loss measurements of a vertically polarized electromagnetic wave travelling over first sea ice in the vicinity of Pond Inlet, N.W.T. The frequency of interest was 25.4 MHz.

Salinity and temperature profiles of the sea ice and snow cover were to be measured along the path of propagation. These measurements would be used to model the ice and snow as a horizontally uniform medium whose electrical properties varied only with depth.

A theoretical model of propagation (flat earth) based on the work of J. Walsh (1982) was computerized at Memorial University. Using the vertical profile of the electrical properties of the sea ice and snow, and assuming a horizontally uniform medium, the theoretical transmission loss would be calculated for the frequency of interest. A successful comparison of the observed transmission loss with the calculated theoretical loss would verify the modelling of the electrical properties of sea ice at 25.4 MHz and the theoretical model of propagation. C-CORE would then have a reliable mechanism for performance predictions in the HF range, for use in its ongoing HF radar program for sea ice detection.

3. DESCRIPTION OF HF RADAR SYSTEM

The HF radar system used in Pond Inlet is actually part of C-CORE's Coastal Ocean Dynamics Application Radar system (CODAR), (K. Butt and P. Jeans, 1981) as originally developed by NOAA with the addition of a digital control box in place of the computer used during CODAR operations.

This section describes the equipment as it was arranged (Figure 1) for the propagation study in Pond Inlet (Figures begin on page 57).

3.1 Transceiver

C-CORE's transceiver is shown in the centre of Figure 2. Although labelled "receiver" it also provides the reference pulse to the transmitting amplifier, hence "transceiver". Built by ERBTEC ENGINEERING INC. and sold by C.T.I., it was a custom design specifically for CODAR operation and was made as a series of plug-in printed circuit boards of modular design for ease of maintenance. A block diagram of operation is presented in Figure 3.

The transceiver contains the basic reference oscillator of the entire radar. All of the required frequencies for the mixers are derived from this 10 MHz quartz crystal oscillator. It is oven stabilized and contained in a hermetically sealed module mounted on a card in the transceiver. On command, a transmit pulse at the transmit frequency is generated and subsequently boosted by a power amplifier and radiated by the transmit antenna. The return signal from the receive antenna is first amplified by

the multiplexer box and then routed to the input of the receiver strip in the transceiver. The signal is then coherently demodulated and heterodyned down to baseband using the reference frequencies derived directly from the transmitter portion.

3.2 Transmit Power Amplifier

The output of the radar transmitter in the transceiver is a short CW pulse of 10 dBm (10mW) power. This output must be boosted up to 70 dBm (10 kW) before being fed to the transmit antenna. A block diagram of this amplifier is shown in Figure 4.

C-CORE's transmit power amplifier is a modified 1 kW linear power amplifier, (intended for CW amateur use in the CB bands). The unmodified amplifier is a model ALPHA 76CA supplied by ENRHORN TECHNOLOGICAL OPERATION INC. and modified for CODAR operation by C.T.I. and ERBTEC ENGINEERING INC.

The front end consists of a custom built solid state pre-amplifier with an output of 100 W. The signal is then boosted up another 5 dB by an intermediate stage power amplifier custom built around a ceramic triode tube. The final output power amplifier consists of 3 tubes of this same type in parallel, and provides the additional 15 dB gain required. A custom built control circuit is included to monitor the operation of the unit and to shut it down if any abnormal conditions exist. A DC status signal is returned to the transceiver by using the RF signal input cable as a bidirectional line.

3.3 Transmit Antenna

The transmit antenna, a three element Yagi array, radiates the transmit radar pulse received from the transmit power amplifier via 60m of cable.

3.4 Multiplexer Box

The multiplexer box (MUX) shown in Figure 1 contains the antenna multiplexer or antenna switcher, a pre-amplifier, a transmit - receiver (TR) switch and a bandpass filter. The purpose of the multiplexer box is to switch sequentially from one antenna element to another (during CODAR operation) and to filter and boost the radar return signal for input to the transceiver via 60m of coaxial cable. For the purposes of this experiment only one receive antenna was used, and the MUX box was readjusted always to sample that antenna.

3.5 Transponder

A transponder is a radio receiver and transmitter which transmits an identifiable signal automatically whenever the proper interrogation signal or command has been received.

C-CORE's transponder was built by ERBTEC ENGINEERING INC. and sold by CTI. It is a refined version of the original SEVEN OAKS RESEARCH design used by NOAA and is completely contained on one printed circuit board. A block diagram of C-CORE's transponder is shown in Figure 5. The receiver portion is a narrow band AGC (automatic gain control) amplifier tuned to 25.40 MHz. For the

purposes of this experiment the 1 Hz modulation of the output pulse was disabled.

3.6 HF Control Box

The control box turns the CODAR transceiver on and off and adjusts its gains. This was accomplished by building a TTL based circuit hardwired to an operator panel.

Detailed hardware specifications are presented by Butt et al., (1983).

4. FIELD WORK AT POND INLET, N.W.T. 72° 42'N, 77° 58'W approx.

This section desribes conditions at the experimental test site, the chronological order of events, the problems that arose during the course of the experiment, and the measurements made.

4.1 Personnel

The C-CORE personnel involved in the field operations were:

Radar Group: Ken Klein - Principal Investigator
Terry Ridings - Field Technologist

Ice Properties Group: Ernie Reimer - Field Management
Deborah Diemand - Core Analysis

4.2 Preparation and Operational Testing

On March 8, 1982 the last of the personnel and equipment arrived in Pond Inlet. The radar, which had been shipped in advance of personnel, was stored in a heated hut on the coast. This hut was intended to serve as both storage and operational test facility throughout the experiment.

In practice, very little operational testing of the radar could be performed at the hut owing to an unknown noise source which saturated the receiving section of the radar at the lowest gain settings.

Most operational tests of the radar were therefore conducted at the experimental test site, a tent on the ice approximately one kilometre west of the coastline.

At this distance from the local community the radar, no longer saturated, still observed a strong noise floor at close

range. This initially prevented operational testing of the transponder since the transponder signal could not be observed above it. Initial operational testing was also hindered by generator voltage fluctuations (from 112 to 119 V.a.c.). However, the observed noise floor at close range was found to be significantly decreased (over 25 dB) by moving the position of the receive antenna about 25 metres. (See Figure 6). The close range noise was attributed to direct path coupling of the transmission decay transient with the receive antenna; once a minimum noise position was found for the receive antenna (within the radius of its 60m cable) the receiver gain could be increased while still keeping the noise floor at an acceptable level. The transponder signal was then clearly observed and preparations made to start the actual measurements. (See Figure 7).

One last attempt was made to improve operating conditions and reduce the noise floor further before we proceeded with the actual measurements.

A replacement generator, which gave us the voltage stability required, was located outside the tent in an effort to minimize its noise contribution. The generator was then screened in and grounded through the ice to the sea water; the transceiver chassis was similarly grounded. This, however, did not decrease the noise floor noticeably. The addition of a grounded plane of fine wire screening immediately below the four ground whips of the transponder antenna also gave no observable improvement. (Skidoo ignitions did not appear to affect the noise floor either).

4.3 Measurements Along the Line of Interest

Prior to our arrival, a straight line extending roughly west from Pond Inlet was surveyed and marked on the ice by the Arctic Research Establishment, (A.R.E.). All measurements were made along this line, (See Figure 8), hereafter called the 'Line of Interest'.

4.3.1 Propagation Measurements

(March 11 to March 12, 1982) All the far field measurements were made during this time period. This was accomplished by moving the transponder and its antenna by komatik to a known point on the line. With the transponder antenna stationary the transmitter was then enabled and the receiver's "I" (in phase) and "Q" (quadrature) outputs recorded onto magnetic tape using a **Racal Store 4D tape recorder.** At the same time, the I & Q output displayed by a **Tektronix 465B scope** was photographed. (An attempt was made to maximize either the I or the Q output, prior to recording, by moving the transponder antenna a few metres along the line, but the noise floor made it difficult to identify a maximum condition accurately. Additional local wavelength measurements were attempted by moving the transponder antenna along the line while counting maxima in either the I or Q channel and then measuring the distance travelled for five successive maxima. The noise floor, however, obscured maxima, thus increasing the experimental error on this particular measurement.

The locations of the transponder during measurements are shown in Figure 9. The maximum range of operation for the

transponder was found to be 7.91 km from the transmit antenna; at this point the transponder could only lock onto the transmit pulse intermittently. The transponder was moved out to almost 9 km but from that distance it could not lock on to the transmit pulse.

(March 13, 1982) All the near-field propagation measurements were recorded in one day on a short line surveyed by C-CORE personnel (see Figure 10). The experimental procedure was the same as for the far field measurements except that the distance over which local wavelength measurements were made was reduced to permit only one cycle of either the I or the Q output. Figures 11 to 17 illustrate the terrain, the equipment layout, and typical operations.

(March 14, 1982) Our time had expired; the equipment was packed in preparation for our departure on March 15, 1982.

4.3.2 Salinity and Temperature Measurements:

Ice Cores: A total of 33 ice cores were pulled along the line of interest (see Figure 9), between March 3, 1982 and March 12, 1982. A complete list of core sites, dates, and the agency involved is given in Table I. The ice core salinities measured as a function of depth are given in Appendix A, which also includes the methods of measurement, and correlation between the different methods.

4.3.3 Temperature profiles:

Thermocouple strings supplied, installed, and read by A.R.E. personnel, were located at 6.88 and 15.33 km from the transmit

antenna. A double overlapping thermistor string was installed at 0 km and read by C-CORE personnel (see Table I). The recorded ice temperatures as functions of depth are given in Appendix B.

4.3.4 Ice Thickness and Surface Temperatures:

Ice thickness measurements along the line of interest were taken March 4, 1982. Additional ice thicknesses were measured in the vicinity of the transmit antenna on March 14, 1982, as well as surface temperature measurements for this location. The data is given in Table II.

TABLE I

Ice Core and Temperature String Locations

Ice Core	Distance from Transmit Antenna	Date Pulled	Agency
C1 - C9	0 km	03/03/82	C-CORE
C10, C11	0.67	12/03/82	C-CORE
C12	1.35	06/03/82	C-CORE
C13, C14	1.35	12/03/82	C-CORE
C15	1.45	06/03/82	C-CORE
C16	1.55	06/03/82	C-CORE
C17	1.65	06/03/82	C-CORE
C18	1.75	06/03/82	C-CORE
C19, C20	1.85	12/03/82	C-CORE
C21	1.95	06/03/82	C-CORE
C22	2.45	06/06/82	C-CORE
C23, C24	2.45	12/03/82	C-CORE
C25, C26	3.02	12/03/82	C-CORE
C27	3.54	06/03/82	C-CORE
C28, C29	3.54	12/03/82	C-CORE
C30, C31	4.61	12/03/82	C-CORE
C32	6.88	10/03/82	ARE
C33	15.33	10/03/82	ARE

Thermocouple String	Distance from Transmit Antenna	Date of Recorded Data	Agency
TC-1	6.88 km	10/03/82	ARE
TC-2	15.33 km	10/03/82	ARE

Thermistor String			
TM-1	0.0 km	Feb. 28/82 thru Mar. 10/82	C-CORE

TABLE II

Ice Thickness Measurements March 4, 1982

Marker	Thickness (cm)	Distance from Transmit Antenna (km)
2	85	1.35
3	93	2.45
4	100	3.54
5	102	4.61
6	95	5.73
7	86	6.88
8	94	7.91
9	93	8.98
10	91	10.03
11	91	11.06
12	95	12.13
13	106	13.18
14	96	14.24
15	96	15.33

Ice Thickness and Surface-Temperatures March 14, 1982

Along receive antenna line

d	ice thickness	freeboard	snow depth	ice surface temp. ±(0.2° + interpolation error*)
30 m	95 cm	5 cm	14 cm	-15°C
60 m	95 cm	5 cm	14.7 cm	-15°C
90 m	95 cm	4 cm	10.0 cm	-17°C
120 m	91 cm	4 cm	15.5 cm	-14.5°C
150 m	94 cm	6 cm	14.7 cm	-15.5°C
180 m	95 cm	6 cm	10.0 cm	-16.0°C
210 m	95 cm	7 cm	15.0 cm	-16.5°C

*Using YSI 44005 (green tip) thermistor and fluke meter).

5. THEORY

For the derivation of the particular form of the equation of the vertical electric field contained in section 5.1, (see Walsh, 1982). We will simply state his results and make a few comments; in Section 5.2 transmission loss is defined in a useable form.

5.1 Propagation of a Vertically Polarized E/M Wave Over Horizontally Homogeneous Media

(See Figure 18) For an infinitesimal vertical dipole in free space, a distance h above a semi-infinite medium in the lower half space, the far field approximation to the vertical electric field E_z at $(x, y, {}^{+}z)$ is given by Walsh, (1982);

$$E_z = \frac{k^2 I dl}{j\omega\epsilon_o 4\pi}\left[\frac{e^{-jkR_o}}{R_o}\cos^2\phi + \cos^2\theta\left(\frac{R_v e^{-jkR_1}}{R_1} + (1-R_v)(1-\Delta^2)F(w)\frac{e^{-jkR_1}}{R_1}\right)\right] \quad (1)$$

where θ, R_o, R_1 are as defined in Figure 18,

I is the current in the dipole of length dl,

and $k = \frac{2\pi}{\lambda}$

R_v is the reflection coefficient at the interface between free space and the semi-infinite medium.

$$R_v = \frac{\sin\theta - \Delta}{\sin\theta + \Delta} \quad (2)$$

F(w) is the Norton attenuation function,

$$F(w) = 1 - j(\pi w)^{1/2} e^{-w} \operatorname{erfc}(jw^{1/2}) \tag{3}$$

where erfc is the complementary error function,

$$W = \frac{-jkR_1\Delta^2}{2} \left(1 + \frac{z^+ + h}{\Delta R_1} \right)^2 \tag{4}$$

and Δ = normalized surface impedance of the semi infinite medium.

Note that when h = o (grazing incidence), $\cos\theta = 1$, $\cos\phi = 1$, $R_v = -1$, and

$$E_z \text{ reduces to, } \frac{k^2 Idl}{jw\varepsilon_o 4\pi} \left[2 \quad (1 - \Delta^2) \; F(w) \; \frac{e^{-jk\rho}}{\rho} \right] \tag{5}$$

5.2 Transmission Loss

We must develop a form for transmission loss which will allow us to compare theoretical predictions of loss based on the formula in section 5.1 with the actual observed loss.

Consider a current source in free space and an identical source in some complex medium. The fields of the sources are measured at the same arbitrary point (away from the sources) in both systems. Then we can write,

$$\frac{\text{Loss (free space)}}{\text{Loss (complex medium)}} = \frac{\left[\frac{\text{Power Radiated}}{\text{Power Received}}\right]_{\text{free space}}}{\left[\frac{\text{Power Radiated}}{\text{Power Received}}\right]_{\text{complex medium}}} \qquad (6)$$

Since the power radiated is the same in both systems This gives

$$\frac{\text{Loss (free space)}}{\text{Loss (complex medium)}} = \frac{(\text{Power received})_{\text{complex medium}}}{(\text{Power received})_{\text{free space}}} \qquad (7)$$

Let us denote the electric field at the point of reception by E_c for the complex medium and E_o for free space.

Then, since in general power received $\propto E^2$

$$\frac{\text{Loss (free space)}}{\text{Loss (complex medium)}} = \frac{E_c^2}{E_o^2} \qquad (8)$$

$$\text{or Loss (complex medium)} = (E_o^2 / E_c^2)\ \text{Loss (free space)} \qquad (9)$$

For the specific case of two antennas in free space, one being the source with a gain G_t and the other the receiving antenna with a gain G_r, the loss is given by, (Antenna Engineering Handbook, 1961);

$$\text{Loss (free space)} = \left[\frac{4\pi d}{\lambda}\right]^2 \frac{1}{G_t G_r} \qquad (10)$$

Where it is assumed that the receiving antenna is in the far field and its effective area depends only on its geometry.

Then for two antennas separated by d,

$$\text{Loss (complex medium)} = \frac{E_o^2}{E_c^2} \left(\frac{4\pi d}{\lambda}\right)^2 \frac{1}{G_t G_r} \qquad (11)$$

5.3 Vertical Infinitesimal Dipoles:

We shall now evaluate the theoretical transmission loss between two vertical infinitesimal dipoles both in free space above a complex medium (Figure 18) where the elevations of the dipoles are small compared to the distance of separation. Since the dipoles are vertical we are only concerned with the z component of the electric field.

For an infinitesimal vertical dipole in free space the vertical component of the electric field in a plane passing through the dipole axis perpendicular to the axis is (to first order), (Lorraine and Corson, (1970)),

$$E_{oz} = \frac{k^2 Idl}{j\omega\varepsilon_o 4\pi} \frac{e^{-jkr}}{r} \qquad \text{(far field)} \qquad (12)$$

In our case (Figure 18) $r \doteq R_o$ for $h, z^+ \ll R_o$.

Therefore, under the following conditions,

i) vertical infinitesimal dipoles

ii) separation much greater than antenna elevations

iii) separation equivalent to the far field

$$E_o = E_{oz} \ (r = R_o), \ E_c = E_z$$

Then the theoretical transmission loss is,

$$\text{Loss} = \left[\cos^2\phi + \cos^2\theta \ \left(R_v \frac{R_o}{R_1} e^{-jk(R_1-R_o)} + (1-R_v) \ (1-\Delta^2) F(w) \frac{R_o}{R_1} e^{-jk(R_1-R_o)}\right]^{-2} \left(\frac{4\pi R_o}{\lambda}\right)^2 \frac{1}{G_t G_r} \right. \tag{13}$$

In the case of glancing incidence and $\rho >> h$, z^+, $\cos^2\theta \doteq 1$, $\cos^2\phi \doteq 1$ and $\frac{R_o}{R_1} \doteq 1$ yielding,

$$\text{Loss} = \left[\frac{1}{G_t G_r} \ \frac{\lambda}{4\pi R_o} \ \left(1 + R_v e^{-jk(R_1-R_o)} + (1-R_v) \ (1-\Delta^2) \ F(w) e^{-jk(R_1-R_o)}\right)\right]^{-2} \tag{14}$$

6 COMPUTERIZED MODEL

This section describes the software used to calculate transmission loss, based on the dielectric profiles arrived at in section 9, and the loss equation (14) calculated in section 5. The program, written in Fortran, has been documented with appropriate comments throughout, and is listed as Appendix E.

6.1 Calculation of Normalized Surface Impedance:

The complex medium is characterized as a series of M horizontally uniform layers above a semi-infinite medium (sea water). Layer M is the first layer above sea water and layer 1 corresponds with the surface. Associated with each layer is a triplet (ϵ_{rm}, σ_m, h_m) where,

ϵ_{rm} = relative permittivity of layer m,
σ_m = conductivity of layer m,
h_m = thickness of layer m.

It is assumed that for all layers $\mu_m = \mu_o$.

The calculation of transmission loss requires the calculation of A, the normalized surface impedance of the medium in the lower half space. Based on the work of Wait, (1970) A is given by,

$$= \frac{Z_1}{120\pi} \qquad (15)$$

where Z_1 is calculated from the recursion relationship

$$Zm = Km \left(\frac{Z_{m+1} + K_m \tanh (U_m h_m)}{K_m + Z_{m+1} \tanh (U_m h_m)} \right) \quad (16)$$

and,

$$Km = \frac{Um}{\sigma_m + \imath\omega\varepsilon_{rm}\varepsilon_o} \quad (17)$$

$$Um = \sqrt{k_o^2 + \gamma_m^2} \quad (18)$$

$$\gamma_m^2 = \imath\sigma_m\mu_m\omega - \varepsilon_{rm}\varepsilon_o\mu_m\omega^2 \quad (19)$$

$$k_o^2 = \omega^2\varepsilon_o\mu_o \quad (20)$$

In this particular form Δ represents the normalized surface for a plane wave at grazing incidence to the complex medium.

To calculate Z_1, the program must iterate Z_m upwards from the semi-infinite medium, requiring the properties of the layers to be read in starting with the **lowest** layer above sea water.

6.2 Evaluating F(w)

The calculation of transmission loss also requires evaluation of the Norton Attenuation function F (w); (see Section 5.1).

From the work of Wait, (1970) the method of evaluating F(w) is determined from the values of the magnitude and argument of w written in the form:

$$W = |W| \, e^{-jb} \quad (21)$$

When $|w| < 10$ a convergent series expansion is used,

$$F(w) \doteq 1 - j\sqrt{\pi w}e^{-w} - 2w + \frac{(2w)^2}{1.3} - \frac{(2w)^2}{1.3.5} + \ldots \qquad (22)$$

For $|w| \geq 10$ two asymptotic expansions based on the argument of w are used;

$|w| \geq 10$ and $-2\pi < b < 0$;

$$F(w) \doteq \frac{-1}{2w} - \frac{1.3}{(2w)^2} - \frac{1.3.5}{(2w)^3} \qquad (23)$$

$|w| \geq 10$ and $0 < b < 2\pi$

$$F(w) \doteq -2j\sqrt{\pi w}e^{-w} - \frac{1}{2w} - \frac{1.3}{(2w)^2} - \frac{1.3.5}{(2w)} \qquad (24)$$

7. TRANSMISSION LOSS MEASUREMENTS

This section describes the initial electrical measurements, the subsequent data processing and the calculations to arrive at an estimate of the observed transmission loss as a function of path length along the line of interest.

7.1 The Decoded Transponder Signal:

Although the original transponder signal is only 16 μ sec long, the decoding of the transponder signal generates "I" (in phase) and "Q" (quadrature) components extending over 32 μ secs. This is evidenced in Figure 19 by both I & Q (especially Q).

In calculating the average voltage associated with the observed I and Q for a specific range, a 32 μ sec window is therefore required for the purposes of integrating the area under each component.

It must be noted from Figure 19 that when the "in phase" component has been minimized, this does not result in a flat baseline (zero response) in the quadrature component: but the integral of the area under Q should still be zero. This indicates that in integrating either component the integration would, in general, proceed as a normal integral. Then the absolute average voltage output of the receiver normalized to 16 μ sec is given by:

$$V_{avg} = \left[\left[\frac{1}{16\mu sec} \int_{to}^{to+32\mu sec} I(t)\,dt \right]^2 + \left[\frac{1}{16\mu sec} \int_{to}^{to+32\mu sec} Q(t)\,dt \right]^2 \right]^{1/2} \qquad (25)$$

where, t_o represents the beginning of the decoded transponder signal, and I(t), Q(t) are the I and Q voltages respectively as a function of time.

7.2 Processing out the Noise Background;

The transponder signal was all but lost in the noise floor at a range of three km (Figure 20). Fortunately, recordings of the I and Q outputs (with a synchronization signal) were made at the time using a **Racal Store 4-D analogue tape recorder.**

An HP 5451B Fourier analyzer was used to digitize successively both the I and Q signals from the tapes played back on the Racal. The digitized versions of both I and Q were each added sequentially for n samples, then normalized to average out the noise floor. The results were acceptable; the resultant waveforms are shown in Appendix D.

To obtain a scaling relationship between the waveform after processing and the original signal before recording, 100 samples of I for a range of 210.6 m were digitized from the analogue tape and averaged. The resultant waveform was compared with the photograph shown in Figure 19, which shows the original "I" signal during the analogue recording.

For the 2-volt scale used on the Racal at the time of recording, a ratio of 4:1 between input and output (playback) was expected. The observed ratio was 6:1 (see Figure 21), so all the integrated and normalized results were scaled upwards by a factor of 6:4.

In order to sample the analogue tape properly it was necessary to play back at one quarter the speed of recording. No appreciable change in the waveform between the recording speed (60 ips) and the playback speed (15 ips) was observed. However, as the time scales of the resultant waveforms are magnified by a factor of 4, this fact was taken into account in the data processing. Each digital channel represented a 1.25 μsec interval, resulting in the approximation,

$$\frac{1}{16\mu\text{sec}} \int_{to}^{to+32\mu\text{sec}} I(t)\, dt \doteq \frac{1}{16\mu\text{sec}} \left[\sum_{i=n}^{n+26} \right] I_i \times 1.25\mu\text{sec} \qquad (26)$$

with a similar equation for the integral of Q, (I_i = the "in phase" voltage in channel i in the HP 5451B).

The resulting relationship is;

$$V_{avg}\ (\text{dB}) = -22.14\ \text{dB} + 20\ \text{Log} \sqrt{\left(\sum_i I_i \right)^2 + \left(\sum_i Q_i \right)^2} \qquad (27)$$

A list of integration intervals on the Fourier analyzer along with intermediate values such as ΣI, ΣQ is given in Appendix D.

7.3 Calculating Transmission Loss:

The experimental transmission loss was calculated, based on the value of V_{avg} as defined in Section 7.2, and known system gains.

Referring to Figure 22 the power at the input to the transceiver, P_{in}, is the sum in dB,

$$P_{in} = P_{received} + G_{mux} + G_{cables} \qquad (28)$$

where P_t = Power output of transponder, 3dB

G_{mux} = Multiplexer gain, 9.2 dB

G_{cables} = cable loss, -1.6 dB

$P_{received}$ = power at receive antenna

$$\therefore P_{in} = P_{received} + 7.6 \text{ dB} \qquad (29)$$

We have a second expression for P_{in} in terms of V_{avg}, Z_{in} (= 50 Ω), and the voltage gain G_{rec} of the receiver,

$$P_{in} \text{ (dB)} = 10 \text{ Log} \left[\frac{V_{avg}^2}{G_{rec}^2 \; 50\Omega} \right] \qquad (30)$$

With transmission loss (T.L.) defined as $\left[\frac{P_{transmitted}}{P_{received}} \right]$ we get,

$$\text{T.L.} = -20 \text{ Log } V_{avg} + 20 \text{ Log } G_{rec} + 27.6 \text{ dB} \qquad (31)$$

Table III lists calculated transmission loss as a function of range.

Appendix C describes the voltage gain calculations for the receiver, and lists the results.

TABLE III

Calculated Transmission Loss

Range km	Gr Vavg dB	Receiver Gain Gr (dB)	Transmission Loss (dB)
0.64	15.68	91.45	103.4
0.67	11.96	91.45	107.1
1.32	8.66	101.05	120.0
1.87	9.12	104.65	123.1
1.90	12.68	108.55	123.5
2.45	9.31	111.15	129.4
2.97	6.96	110.15	130.8
3.00	6.19	110.15	131.6
3.51	-0.33	110.15	138.1
3.54	1.55	110.15	136.2
5.73	-0.73	110.15	138.5
6.88	-5.11	110.15	142.9
(m)			
210.0	4.38	62.75	86.0
180.0	4.65	62.75	85.7
150.5	2.84	55.55	80.3
120.4	7.48	55.55	75.7
89.6	9.44	51.65	69.8
59.7	12.36	47.65	62.9

8. MODELLING SEA ICE AND SNOW AS A SERIES OF HORIZONTALLY UNIFORM DIELECTRIC LAYERS:

Modelling the snow and sea ice as a dielectric medium requires relationships between permittivity, conductivity, salinity and temperature for the frequency of interest, 25.4 MHz.

Although, much work has been reported in general on this subject (eg. Vant, Ramseier, Makios, 1978, very little data exists for the H.F. range.

The relevant reported works are discussed, leading into the empirical relations used. Finally, the dielectric equivalent of the snow and sea ice is modelled.

8.1 Available Data Relating Dielectric Properties to Salinity and Temperature

The works of J.L. Davis (1979) and of Wentworth and Cohn (1964) both indicate that the dielectric properties of sea ice will vary as the direction of polarization of a propagating E/M wave, referenced to the growth direction of the ice, changes from horizontal to vertical. Ideally, we would seek dielectric information where the method of measurement used a vertically polarized E/M wave.

The observed sea ice temperature and salinity profiles during the experiment ranged from -27° C to -1.87°C and from 17°/oo to 4.2°/oo respectively.

No single scientific work to date contains sufficient salinity, temperature, permittivity, and conductivity measurements at or near 25.4 MHz for a vertically polarized E/M wave in sea ice, to cover our area of interest entirely. A significant amount of data was measured by J.R. Addison (1969) on the subject of electrical properties of sea ice and also by Wentworth and Cohn, (1964). Calculations were made based on the graphs in both publications for vertical polarization at approximately 25 MHz.

Unfortunately, Wentworth and Cohn's data only covers the two salinities 7.5% and 4.8% between -5°C and -40°C. Calculations based on their published graphs did not produce similar curves when conductivity was plotted as a function of temperature for constant salinity. To generate reliable artificial curves for higher salinities would require a larger family of curves.

J.R. Addison's measurements cover three salinities, 5.12°/oo, (-12.5 to -33°C), 12.5°/oo and 15.8°/oo (-15°C to -35°C). However, our calculations based on the published graphs, indicated the observed conductivities did not always increase with salinity for fixed temperature and frequency.

Dr. Addison pointed out (pers. comm., 1982) that more emphasis should be placed on the shapes of the individual curves than on the actual numbers.

In general no data could be found for temperatures above -5°C, (which is approximately the temperature range of the lower third of the profile of the ice during our experiment).

8.2 Empirical Approach:

The following assumptions were made, in order to generate empirical relationships between ε_r, σ, salinity and temperature for 25.4 MHz.

i) A graph of ε_r or σ as a function of temperature for fixed salinity would be a smooth curve, with ε_r or σ increasing with higher temperature.

ii) The values of ε_r and σ would approach 80 and 4 mhos/m respectively as the temperature approached 0°C for all salinities.

iii) For fixed salinity, the general form of the equations for both ε_r and σ could be approximated by:

$$\varepsilon_r \text{ or } \sigma = a\,|T|^b + c \text{ (mhos/m)} \qquad (32)$$

where, a, b and c are constants, different in each case

Calculation of these constants required some average values for ε_r and σ for different temperatures and salinities. The report by Parashar, Dawe and Worsfold (1977) includes a table containing average values for these quantitites as a function of 4 salinities and 3 temperatures. **By using this data the condition of vertical polarization with respect to ice growth, was probably sacrificed.**

An extract of their data is presented in Table IV where values of calculated conductivity based on $\sigma = \omega\varepsilon_o\varepsilon''_r$ (for 25 MHz) have also been included.

NOTE: The relationship between σ and ε''_r stems from a notational difference in the equation for k^2, where k is the complex wave number.

Parashar, Dawe and Worsfold (1977) use,

$$k^2 = \frac{w^2}{c^2}(\varepsilon'_r - j\varepsilon''_r) \qquad (33)$$

whereas this report uses, $k^2 = \frac{w^2}{c^2}(\varepsilon_r - j\frac{\sigma}{\omega\varepsilon_o})$ (34)

Table V lists the calculated values of a, b and c based on the data extract.

Figure 25 graphs the empirical relations as well as the data points from Table IV.

TABLE IV

Extract of Data from C-CORE Technical Report 77-6

$T = -5^{o}C$

S(^{o}/oo)	ϵ_r'	ϵ_r''	Calculated σ ($= 1.39 \times 10^{-3}\epsilon_r''$)
1.0	4.853	0.967	1.344 x 10-3
5.0	5.425	2.556	3.553 x 10-3
10.0	6.141	4.541	6.312 x 10-3
15.0	6.856	6.527	9.073 x 10-3

$T = -10^{o}C$

S(^{o}/oo)	ϵ_r'	ϵ_r''	σ
1.0	4.785	0.779	1.083 x 10-3
5.0	5.086	1.614	2.243 x 10-3
10.0	5.462	2.657	3.693 x 10-3
15.0	5.838	3.701	5.144 x 10-3

$T = -15^{o}C$

S(^{o}/oo)	ϵ_r'	ϵ_r''	σ
1.0	4.763	0.716	9.952 x 10-4
5.0	4.973	1.300	1.807 x 10-3
10.0	5.236	2.030	2.822 x 10-3
15.0	5.499	2.760	3.836 x 10-3

TABLE V

Comparison of Coefficients for $\epsilon_r = a|T|^{b}+c$, $= d|T|^{e} + f$ for Different Salinities.

So/oo	≈ a	≈ b	c
1.0	-75.02	1.09 x 10-3	80
5.0	-73.92	5.50 x 10-3	80
10.0	-72.55	11.09 x 10-3	80
15.0	-71.20	16.73 x 10-3	80

So/oo	≈ d	≈ e	f
1.0	-3.998	7.9 x 10-5	4
5.0	-3.994	39.8 x 10-5	4
10.0	-3.989	79.5 x 10-5	4
15.0	-3.983	119.4 x 10-5	4

8.3 The Average Salinity Profile of the Sea Ice on the Line of Interest:

Appendix A contains a complete list of all the salinity measurements, with the depth of the sample and the date when the ice core was pulled.

The distance to be characterized along the line of interest is from 0 to 6.9 km, since the transponder failed to lock onto the transmitted pulse past 6.9 km.

For a particular depth the following procedure was used to describe the salinity of the first 4.6 km of the medium.

The data was first grouped, based on the date and location at which the samples were taken. As an example, refer to Salinity Measurements (C-CORE), Appendix A. Twenty-eight salinity measurements exist for the "Surface" layer over 4.6 km. A description of the grouping of data is given in Table VI for this layer.

TABLE VI

Grouping the Salinities for the "Surface" Layer (0 to 4.6 km)

Date 1982	Distance (km)	# Samples	Average Values °/oo
Mar. 3	0.00	8*	9.3
Mar. 12	0.67	2	12.5
Mar. 12	1.35	2	10.95
Mar. 6	1.35, 1.45	5	12.58
Mar. 6	1.55, 1.65		
Mar. 6	1.95		
Mar. 12	1.85	2	13.75
Mar. 6	2.45	1*	-
Mar. 12	2.45	2	16.0
Mar. 12	3.0	2	11.3
Mar. 6	3.5	1	14.0
Mar. 12	3.5	1	12.7
Mar. 12	4.6	2	12.1

*Note: Data contained one anomolous salinity measurement which was discarded.

This grouping produced 10 separate salinities for the surface layer. The average value of these grouped salinities is 12.52 ± 1.84°/oo.

In a similar manner the salinities for all the other layers were calculated for the range 0 to 4.6 km. (Figure 24 shows grouped salinities for each layer as a function of distance where grouping was done only for ice cores with common extraction dates).

The result of grouping the data as described produced the salinity profile graphed in Figure 25.

From measurements taken March 4, 1982 (See Table VII) the ice thickness from 1.35 to 7.9 km was 93.6 cm ± 6.4 cm and from 1.35 to 15.3 km it was 94.5 cm ± 5.65 cm. On March 14, 1982 the ice thickness at 0 km was 94.3 cm ± 1.5 cm. For the purposes of modelling the ice, the thickness was taken to be 93.6 cm.

Figure 26 illustrates the thickness and temperature information contained in Table VII.

Between 4.6 km and 6.9 km only one other ice core was pulled, C-32. The salinity measurements are listed and graphed in Appendix A. This data was used to provide an extension to the salinity profile in Figure 25 for depths greater than 85 cm.

Since the true length of C-32 was 110 cm the required values for extending the salinity profile were found by rescaling the thickness of C-32 to 93.6 cm and using

$$\text{rescaled depth} = \text{depth} \times \frac{93.6 \text{ cm}}{110 \text{ cm}} \qquad (35)$$

TABLE VII

Ice and Snow Thickness Measurements Along Line of Interest

Distance	Date 1982	# Samples	Ice Thickness
0 km	Mar. 14	7	94.3 cm ± 1.5 cm
1.35	Mar. 4	1	85
2.45	Mar. 4	1	93
3.5	Mar. 4	1	100
4.6	Mar. 4	1	102
5.7	Mar. 4	1	95
6.9	Mar. 4	1	86
7.9	Mar. 4	1	94
9.0	Mar. 4	1	93
10.0	Mar. 4	1	91
11.0	Mar. 4	1	91
12.1	Mar. 4	1	95
13.2	Mar. 4	1	106
14.2	Mar. 4	1	96
15.3	Mar. 4	1	96

Distance	Date 1982	# Samples	Snow Depth
0 km	Mar. 4	7	13.4 cm ± 2.4 cm

Ice Surface Temperatures March 14, 1982

Distance	# Samples	Average Temperature (°C)
0 km	7	-15.6°C ± 0.9

to locate those rescaled salinity depths between 85 and 93.6 cm to extend the salinity profile.

3 points below 85 cm were added to the profile shown in Figure 25:

89.5 cm, 4.8°/oo; 91.5 cm, 5.5°/oo; and 93.5 cm, 7.3°/oo

(NOTE: Although it would have been unjustified to average the profile of C-32 directly with the grouped salinities of 0 to 4.6 km, because of the great difference in the number of samples represented by each, since C-32 was the only source of salinity data below 85 cm, that section of C-32's profile had to be used.)

8.3.1 Estimating the Salinity of the Snow Layer:

The snow samples were melted in order to measure the salinity. The high salinity observed, of about 17°/oo (due to salt migrating from the ice) is exaggerated by the change in density.

Assuming a snow density of 0.4 gms/cc for granular snow (S. Evans, 1965) and knowing the density of sea water (1.025 gms/cc) the average salinity of the snow before melting can be estimated as

$$17^{o}/oo \times \frac{0.4 \text{ gms/cc}}{1.025 \text{ gms/cc}} = 6.6^{o}/oo$$

From the data in Table VII the average snow depth was 13.4 cm, so the snow was modelled as a uniformly saline medium of 6.6°/oo salinity, 13.4 cm deep.

The resulting salinity profile of both the ice and snow is shown in Figure 27.

8.4 The Observed Temperature Profiles:

A complete list of the raw temperature data is given in Appendix B, with graphs of the temperature profiles for March 10, 1982. Since, the area of interest is the first 6.9 km, there are three relevant temperature profiles, two at 0 km (March 10, 1982; 9:57 and 15:51 hrs local time) and one at 6.9 km (March 10, 1982, 15:20 hrs).

The profiles at 0 km indicate an ice thickness of approximately 104 cm. The profile at 6.9 km indicates an ice thickness of 90 cm. Therefore, allowing for local variations in ice thickness, an average ice thickness of 93.6 cm is reasonable.

The three profiles were rescaled to 93.6 cm in a similar manner to the salinity profile. The results are shown in Figures 28 and 29.

The temperature profiles, and the final salinity profile, model the ice and snow within the first 6.9 kms of the line of interest as a horizontally uniform medium with 3 possible configurations.

The resultant salinity/temperature profiles are given in Table VIII. Temperatures for depths between thermocouple or thermistor locations were calculated by interpolation.

8.5 The Resulting Dielectric Profile

The family of curves for ϵ_r, σ (Table V and Figure 23) and the salinity/temperature profiles arrived at in Sections 8.3 and 8.4 (Table VIII) were combined to produce three estimates of the dielectric profile of the ice and snow medium. Interpolation was

required as most salinities did not lie directly on any of the four curves. The results are listed in Table IX.

TABLE VIII

Temperature/Salinity Profiles Modelling Sea Ice and Snow as Horizontally Uniform Medium

Depth (cm)	Salinity (o/oo)	Temperature °C March 10, 1982 TM-1 (9.57)	Tm-1 (15.51)	TC-1 (15.20)
13.4	6.6	-27.0	-35.0	-27.4
10	6.6	-25.75	-32.75	-23.3
5	6.6	-23.75	-28.0	-18.4
0	12.5	-22.5	-25.0	-15.5
-5	5.6	-20.5	-21.5	-15.0
-10	4.9	-19.5	-19.0	-14.0
-15	5.3	-18.0	-17.0	-13.5
-20	5.3	-16.5	-15.5	-12.5
-25	5.1	-15.0	-14.0	-12.0
-35	4.2	-12.5	-11.5	-10.0
-40	4.2	-11.5	-10.7	-9.5
-45	4.3	-10.5	-10.0	-8.0
-55	4.7	-10.0	-10.0	-6.2
-60	4.5	-8.0	-8.0	-6.0
-65	4.5	-6.0	-5.7	-5.5
-75	4.8	-5.0	-4.7	-4.0
-80	4.6	-4.0	-4.0	-3.5
-85	4.7	-3.0	-3.0	-3.0
-89.5	4.8	-2.0	-2.0	-2.5
-91.5	5.5	-1.87	-1.87	-2.45
-93.5	7.3	-1.87	-1.87	-1.87

TABLE IX

PROFILE #1

SAL °/oo	TEMP	SIGMA	EPSILON	THICKNESS
6.6	-27.00	0.8989E-03	4.7356	0.034
6.6	-25.75	0.9986E-03	4.7616	0.050
6.6	-23.75	0.1168E-02	4.8059	0.050
12.5	-22.50	0.1716E-02	4.9456	0.050
5.6	-20.50	0.1373E-02	4.8599	0.050
4.9	-19.50	0.1378E-02	4.8616	0.050
5.3	-18.00	0.1561E-02	4.9090	0.050
5.3	-16.50	0.1708E-02	4.9471	0.050
5.1	-15.00	0.1828E-02	4.9783	0.100
4.2	-12.50	0.1888E-02	4.9942	0.050
4.2	-11.50	0.1999E-02	5.0230	0.050
4.3	-10.50	0.2153E-02	5.0627	0.100
4.7	-10.00	0.2352E-02	5.1143	0.050
4.5	- 8.00	0.2605E-02	5.1798	0.050
4.5	- 6.00	0.3016E-02	5.2862	0.100
4.8	- 5.00	0.3443E-02	5.3964	0.050
4.6	- 4.00	0.3658E-02	5.4520	0.050
4.7	- 3.00	0.4150E-02	5.5788	0.045
4.8	- 2.00	0.4840E-02	5.7563	0.020
5.5	- 1.87	0.5548E-02	5.9388	0.020
7.3	- 1.87	0.7102E-02	6.3400	0.020

TABLE IX (Continued)
PROFILE #2

SAL °/oo	TEMP	SIGMA	EPSILON	THICKNESS
6.6	-35.00	0.3543E-03	4.5931	0.034
6.6	-32.75	0.4940E-03	4.6296	0.050
6.6	-28.00	0.8227E-03	4.7156	0.050
12.5	-25.00	0.1298E-02	4.8356	0.050
5.6	-21.50	0.1288E-02	4.8378	0.050
4.9	-19.00	0.1419E-02	4.8721	0.050
5.3	-17.00	0.1657E-02	4.9340	0.050
5.3	-15.50	0.1813E-02	4.9744	0.050
5.1	-14.00	0.1940E-02	5.0073	0.100
4.2	-11.50	0.1999E-02	5.0230	0.050
4.2	-10.70	0.2096E-02	5.0480	0.050
4.3	-10.00	0.2219E-02	5.0800	0.100
4.7	-10.00	0.2352E-02	5.1143	0.050
4.5	- 8.00	0.2605E-02	5.1798	0.050
4.5	- 5.70	0.3090E-02	5.3051	0.100
4.8	- 4.70	0.3537E-02	5.4208	0.050
4.6	- 4.00	0.3658E-02	5.4520	0.050
4.7	- 3.00	0.4150E-02	5.5788	0.050
4.8	- 2.00	0.4840E-02	5.7563	0.020
5.5	- 1.87	0.5548E-02	5.9388	0.020
7.3	- 1.87	0.7102E-02	6.3400	0.020

PROFILE #3

SAL °/oo	TEMP	SIGMA	EPSILON	THICKNESS
6.6	-27.40	0.8681E-03	4.7275	0.034
6.6	-23.30	0.1208E-02	4.8164	0.050
6.6	-18.40	0.1704E-02	4.9456	0.050
12.5	-15.50	0.3198E-02	5.3336	0.050
5.6	-15.00	0.1929E-02	5.0046	0.050
4.9	-14.00	0.1895E-02	4.9957	0.050
5.3	-13.50	0.2046E-02	5.0349	0.050
5.3	-12.50	0.2176E-02	5.0685	0.050
5.1	-12.00	0.2189E-02	5.0722	0.100
4.2	-10.00	0.2186E-02	5.0714	0.050
4.2	- 9.50	0.2254E-02	5.0891	0.050
4.3	- 8.00	0.2524E-02	5.1589	0.100
4.7	- 6.20	0.3067E-02	5.2991	0.050
4.5	- 6.00	0.3016E-02	5.2862	0.050
4.5	- 5.50	0.3140E-02	5.3183	0.100
4.8	- 4.00	0.3783E-02	5.4842	0.050
4.6	- 3.50	0.3854E-02	5.5023	0.050
4.7	- 3.00	0.4150E-02	5.5788	0.045
4.8	- 2.50	0.4500E-02	5.6688	0.020
5.5	- 2.45	0.5076E-02	5.8176	0.020
7.3	- 1.87	0.7102E-02	6.3400	0.020

9. RESULTS AND DISCUSSION

This section will be devoted to a comparison of the observed transmission loss with the transmission loss predicted by the model.

The sensitivity of the transmission loss model to the thickness of the medium, the permittivity and the conductivity will also be examined. Discrepancies between observation and theory will be evaluated and explanations offered.

9.1 Transmission Loss: Observed vs. Theoretical

The computerized model described in section 6, and the three dielectric profiles of the sea ice and snow (arrived at in section 8, Table IX) produces an estimate of transmission loss based on the theoretical loss equation, (14). It should be noted that the calculations were made assuming $G_t = G_r = 1$ (G = efficiency x directivity). Therefore the freespaceloss term (10) incorporated into the transmission loss equation 14) is for 100% efficient isotropic radiators as transmit/receive antennas, and not for the quarter wave monopole antennas actually used. The correction to the calculated transmission loss curve will be given in section 9.2, from an estimate of antenna efficiency over a lossy medium such as sea ice.

The estimated transmission loss is plotted as a function of range in Figure 30. The observed transmission loss data points (listed in Table III) are plotted as well.

The 3 dielectric profiles produced almost identical transmission loss curves (of such small numerical difference that

visually they overlie on the graph).

Examination of the spacing between the data points and the graph indicate that the observed and calculated transmission loss differ by an average of 9.48 dB. (The numerical values of both observed loss and calculated loss and their difference at each range of interest are listed in Table X).

Apart from a constant, the observed loss compares very favourably with the calculated loss, exhibiting the same range dependence within normal experimental variation If relative loss was graphed (see Table XI) the observed points would lie on the calculated curve with an acceptable scatter. This however, places too much emphasis on the observed loss at 60 m.

It remains to ascertain the cause of the apparent constant difference of 9.48 dB between the observed loss and the calculated loss.

TABLE X

OBSERVED TRANSMISSION LOSS VS THEORETICAL TRANSMISSION LOSS

Range km	Theoretical (dB) (Gt=Gr=1)	Observed (dB)	Difference (dB)
.060	53.7	62.9	9.2
.090	61.0	69.8	8.8
.120	66.2	75.7	9.5
.150	70.1	80.3	10.2
.180	73.4	85.7	12.3
.210	76.1	86.0	9.9
0.64	95.6	103.4	7.8
0.67	96.3	107.1	10.8
1.32	108.2	120.0	11.8
1.87	114.3	123.1	8.8
1.90	114.5	123.5	9.0
2.45	119.0	129.4	10.4
2.97	122.3	130.8	8.5
3.00	122.5	131.6	9.1
3.51	125.2	138.1	12.9
3.54	125.4	136.2	10.8
5.73	133.7	138.5	4.8
6.88	136.9	142.9	6.0

Average Difference = 9.48 dB ± 2.0 dB

TABLE XI

Calculated Relative Loss vs Observed Relative Loss

[Calculated Loss - Calculated Loss @ 60m] vs [Observed Loss - Observed Loss @ 60m].

Range km	Calculated (dB) (Gt=Gr=1)	Observed (dB)	Difference (dB)
0.060	0	0	0
0.090	7.3	6.9	-0.4
0.120	12.5	12.8	0.3
0.150	16.4	17.4	1.0
0.180	19.7	22.8	3.1
0.210	22.4	23.1	0.7
0.64	41.9	40.5	-1.4
0.67	42.6	44.2	1.6
1.32	54.5	57.1	2.6
1.87	60.6	60.2	-0.4
1.90	60.8	60.6	-0.2
2.45	65.3	66.5	1.2
2.97	68.6	67.9	-0.7
3.00	68.8	68.7	-0.1
3.51	71.5	75.2	3.7
3.54	71.7	73.3	1.6
5.73	80.0	75.6	-4.4
6.88	83.2	80.0	-3.2

9.2 Antenna Efficiency: Corrections to Calculated Transmission Loss

We must now discuss what G_t, G_r represent. In our case they represent the net forward gain of quarter wave monopoles in free space. However, as the model does not take antenna efficiency into account (ie. it assumes 100% efficiency) G_t and G_r must be made to reflect the antenna efficiency as it existed during the experiment.

Since the receive antennas were both quarter wave monopoles, with 4 quarter wave ground whips,

$$G_t = G_r = 10 \log [(\text{directivity (in free space)} \times \text{antenna efficiency (over sea ice)})]$$

where the free space directivity of a quarter wave monopole is 1.637, (Graf, 1974).

If antenna efficiency is the source of the constant difference between observed and calculated loss, then,

average loss difference (9.48 dB) = -10 log (1.637 x antenna efficiency)^2

i.e. The average difference between calculated loss ($G_t = G_r = 1$) and observed loss result from an effective antenna gain less than unity for both the transponder antenna and the receive antenna.

This translates into an antenna efficiency of 20.5%.

9.2.1 Supplementary Information

The efficiency of the antenna in question resting on a lossy medium such as sea ice was discussed with Dr. Walsh (Memorial University) who felt that over sea ice as described one could expect an antenna efficiency between 25 and 50% for the antennae described.

Dr. J.R. Wait (U. of Arizona) (pers. comm.) has indicated that in our case we have "an extremely lossy situation" and could expect only a few % efficiency. He was mildly surprised that the calculated efficiency was as much as 20.5%.

Actual experimental evidence of poor efficiency was made available to C-CORE through private communications (May/83) with Mike Evans (Codar Technology Inc.).

In the process of performing propagation experiments at the identical H.F. frequency, Mike discovered a 5/8 λ antenna installed above 1.7 m sea ice layer gave a 7 dB improvement over a $\lambda/4$ monopole in the same location. The $\lambda/4$ monopole was almost identical in construction to those used in Pond Inlet except that

his $\lambda/4$ monopole had 8 radial ground whips, twice that of the C-CORE's antennas. The theoretical difference in directivity between a $5/8\lambda$ and a $1/4\lambda$ monopole is 3dB. This leaves 4dB which can only be attributed to different antenna efficiencies over sea ice.

Don Barrick (N.O.A.A.) in private communication (May, 1983) pointed out that the $1/4\lambda$ has its current distribution at a maximum at the feed point of the antenna (very close to the ground plane) and therefore will be more affected by the presence of the sea ice than a $5/8\lambda$ antenna whose current distribution reaches a maximum approximately $\lambda/8$ above the feed point.

If we assume the $5/8\lambda$ monopole to be fairly efficient, 90%, then a $1/4\lambda$ monopole, 4dB down in efficiency will have an efficiency of 36%.

Then of the 9.48 dB between calculated and observed data, 10 Log $(1.637 \times 0.36)^2$ = 4.6 dB is attributable to antenna inefficiency, leaving 4.88 dB still to be accounted for.

Section 9.3 will illustrate the model's sensitivity to the choice of relative permittivity for sea ice and to the overall ice depth and in particular show that underestimating ice depth or relative permittivity could easily produce a significant discrepancy between observed and calculated data of the order of 3 to 4 dB.

9.3 Sensitivity of Calculated Loss to ε_r , σ , and the Depth of Sea Ice

Let us now examine how calculated transmission loss varies as a function of ε_r , σ and the overall depth of sea ice. In each case, we will start with dielectric profile #1 derived in Section 8 (see Table IX). Only one of the three parameters ε_r , σ , h (h = layer thickness) will be changed at any one time, so that the change in transmission loss can be directly related to it.

9.3.1 Variation of Transmission Loss with ε_r.

Transmission Loss was calculated using the following profile:

layer "n" (ε_{rn} x scale factor, σ_n, h_n)

Therefore the layer thickness and conductivity of each layer in profile #1 remain unchanged. The relative permittivity of each layer is increased by the value of the constant, "scale factor".

The transmission loss is graphed in Figure 31 for 5 scale factors, 0.75, 1.00, 1.25, 1.50, 1.75. The scale factor 1.00 is of course the original calculated transmission loss as shown in Figure 30.

From Table XII it is apparent that if the values of ε_r in the profile had been chosen 25% larger the calculated loss would have increased by about 4 dB, whereas a decrease of 25% in ε_r would decrease the loss by 4 dB. Note also that a 50% increase in the original value of ε_r from the original profile appears to be no different than a 75% increase. Therefore the loss increase associated with increasing ε_r is not uniform.

Since the curve shape does not change appreciably with

changing ε_r we will take the loss at 5 km to represent the position of the total loss curve.

The transmission loss at 5 km for different scale factors is listed in Table XII part (i) and graphed in Figure 32 part i.

TABLE XII

Sensitivity of Calculated Loss to Single Parameter Variation
(σ, ε_r, h = individual layer thickness)

i) ε_r x scale factor
σ,h unchanged from original profile

scale factor	Loss (dB) @ 5 km
0.750	127.8
0.875	129.5
1.000	131.4
1.125	133.3
1.250	135.3
1.375	137.3
1.500	139.1
1.750	139.4

ii) σ x scale ε_r, h unchanged from original profile

scale factor	Loss (dB) @ 5 km
0.5	131.2
1.0	131.4
1.5	131.6
2.0	131.5
2.5	131.2
3.0	130.6
3.5	129.8
4.0	128.8

iii) h_{ice} x scale factor ε_r, σ, h_{snow} unchanged from original profile

scale factor	Loss (dB) @ 5 km
0.750	124.5
0.875	127.9
1.000	131.4
1.125	135.0
1.250	139.0
1.375	142.9
1.500	141.1
2.000	124.1

9.3.2 Variation of Transmission Loss with σ

Varying the conductivity by a constant scale factor between 0.5 and 4.0 while retaining the original ϵ_r and layer thickness did not produce much variation in Transmission Loss. In Figure 33 the Transmission Loss is graphed for the range of scale factor mentioned. There is a spread of approximately 3dB at 5 km over this range in σ, (see Table XII, part ii, and Figure 32 part ii. Again, the scale factor 1.00 gives the original calculated loss as in Figure 30.

9.3.3 Variation of Transmission Loss with Sea Ice Total Depth

Transmission loss was calculated using the following profile;

layer "n" (ϵ_{rn}, σ_n, h_n x scale factor)

where h_n is the thickness of the nth layer. In this case only the sea ice layers were scaled in thickness, while the 3 snow layers were always left at their original thickness. ϵ_r and σ retained their original value for each layer as in profile #1. In this way the effect on the transmission loss of changing the overall sea ice thickness, while retaining the relative permittivity and conductivity of each layer, could be examined.

Figure 34 shows transmission loss for 4 scale factors between 0.75 and 1.50 in graph form, where the scale factor 1.00 yields the original calculated loss as in Figure 30. Table XII and Figure 32 illustrate the loss at 5 km as a function of total sea ice depth.

From Table XII is is apparent that an increase or decrease of 12.5% in ice depth will increase or decrease the calculated loss by about 3.5 dB.

However, as the ice depth increases beyond 37.5% of the ice thickness used in the initial calculation of transmission loss the transmission loss begins to decrease with increasing depth. In fact, a 200% increase in ice depth or a 25% decrease in depth produce the same calculated transmission loss at 5 km.

9.3.4 Summary of Section 9

The observed transmission loss data points parallel the calculated curve, indicating that the model contains the correct range dependence. The discrepancy between the two is judged to be a constant, (allowing for experimental scatter) and is attributed to a combination of antenna efficiencies of 36% over sea ice and underestimation of the relative permittivity and/or ice depth.

Underestimation of ice thickness is a distinct possibility, as most of the ice thickness measurements occurred on March 4, 1982, 7 days before the far field transmission loss measurements were begun. Ice growth during that period was therefore, neglected. The characterization of relative permittivity was based on averaged data that may be more applicable to horizontal polarization than vertical. In general, vertically polarized measurements of sea ice permittivity at H F give higher values than horizontally polarized measurements.

On this basis the model is taken to be in agreement with observed data.

10 CONCLUSIONS

While C-CORE recognizes that one experiment is not sufficient to verify the theoretical model as 100% reliable, the correlation between theory and observation suggests the model is in a useable form exhibiting the correct properties such as range dependence and magnitude of transmission loss.

The process of modelling sea ice as a dielectric medium has given insight into the electrical properties of sea ice at H.F. In future it will be necessary to revise our estimates of relative permittivity upwards by 15 to 20%, until more data is available. The model has also shown that the insensitivity to changes in conductivity will not require the estimates of conductivity of sea ice to be revised. In particular, the empirical relationships between (ϵ_r, σ) and (5°/oo, T°C) will be retained until evidence to the contrary is presented. These values of ϵ_r and σ for sea ice will also be used in analytical work on H.F. backscatter from first year sea ice.

Antenna efficiency over sea ice will be modelled in the near future in an effort to develop expertise in that area.

The transmission loss model's prediction that transmission loss over thick sea ice (2m) is less than that for 1m sea ice for similar dielectric profiles, suggests that any future work would be most useful over thicker ($\approx$ 2m) sea ice.

11. RECOMMENDATIONS

(i) A second similar experiment is required over thicker first year sea ice for the following reasons;

a) The model predicts that 1 metre sea ice results in more transmission loss than either 1/2 or 2 metre ice. This should be verified if the model is to be used confidently for future calculations.

b) This report magnifies the lack of consistent reference data on permittivity and conductivity of sea ice at H F frequencies for the temperature range -2°C to -27°C. The results of a second experiment combined with the results in this report should eliminate the dielectric properties of sea ice as questionable variables. This would aid radar backscatter calculations that rely on an abrupt change of electrical properties, e.g. a multiyear ice target surrounded by first year ice.

c) Antenna efficiency over sea ice must be quantified if portable ground-based radar systems are to be considered viable, and to remove this variable from the calculations.

d) The natural northern H F power spectrum must be examined before the optimum operational frequency can be decided upon.

ii) The proposed second experiment

a) The cross-section of an iceberg or multi-year ice floe embedded in first year ice should be experimentally measured at the same time as the propagation measurements are carried out. This requires a judicious choice of test site.

b) Measurement technique can be improved by using a multi-element receiving array, (improving signal to noise), and by signal processing in the field to integrate out the effective noise floor. Minimizing excess data accumulation makes best use of available resources.

c) Antenna efficiency ($1/4\lambda$) over sea ice can be quantified by varying the antenna height above the sea ice, since efficiency is expected to increase with height. The model can be used to take the height difference into account, thus modelling efficiency versus height.

REFERENCES

Addison, J.R., (1969) "Electrical Properties of Saline Ice", **Journal of Applied Physics**, Vol. 40 #8, July 1969.

Butt, K.A. and Jeans, P.K. (1981). **H.F. Radar Technology Transfer Project - Evaluation Phase**, C-CORE Technical Report 81-14.

Butt, K.A., Jeans, P.K. and Raymond, R.C. (1983). **H.F. Radar Technology Transfer Project - Acquisition Phase March, 1982**, C-CORE Technical Report 83-8.

Davis, J.L., (1979). "Electrical Property Measurements of Sea Ice In-Situ Using a Wide-Band Borehole Radar and a Time-Domain Reflectometer", Proceedings of the International Workshop on the Remote Estimation of Sea Ice Thickness, St. John's, Nfld., Canada, September 25, 26, 1979.

Evans, S., (1965). "Dielectric Properties of Ice and Snow - A Review", **Journal of Glaciology**, Vol.5, 1965.

Gradshteyn, I.S. and Ryzhik, I.W., (1965). **"Tables of Series Integrals and Products"**, New York: Academic Press.

Graf, R.F. (ed.) (1974). **Electronic Databook - a guide for designers** (2nd ed.) New York: Van Nostrand Reinhold Co.

Jasik, H. (1961). "Fundamentals of Antennas", **Antenna Engineering Handbook**, ed. H. Jasik, New York: McGraw Hill Book Company.

Lorrain, P. and Carson, D. (1970). **Electromagnetic Fields and Waves**, (2nd ed.), San Francisco: W.M. Freeman and Company.

Parashar, S.K., Dawe, B.R. and Worsfold, R.D., (1977). **Stage 1, Evaluation of Potential Sea Ice Thickness Measuring Techniques Development of a Remote Sea Ice Thickness Sensor Phase I**, C-CORE Technical Report 77-6.

Vant, M.R., Ramseier, R.O. and Makios, V., (1978). The Complex-dielectric Constant of Sea Ice at Frequencies in the Range 0.1 - 40 GHz, **Journal of Applied Physics**, Vol.49 #3, March 1978.

Wait, J.R. (1970). "Reflection of Electromagnetic Waves from Horizontally Stratified Media", **Electromagnetic Waves in Stratified Media** (2nd ed.), Oxford: Pergamon Press.

Walsh, J., (1982) **A General Theory of the Interaction of Electromagnetic Waves with Isotropic, Horizontally Layered Media and Applications to Propagation over Sea Ice**, C-CORE Technical Report 82-9.

Wentworth, F.L. and Cohn, M., (1964). Electrical Properties of Sea Ice at 0.1 to 30 Mc/s, **Radio Science Journal of Research** NBS/USNC-URSI, Vol. 68D., No. 6, June 1964.

FIGURES

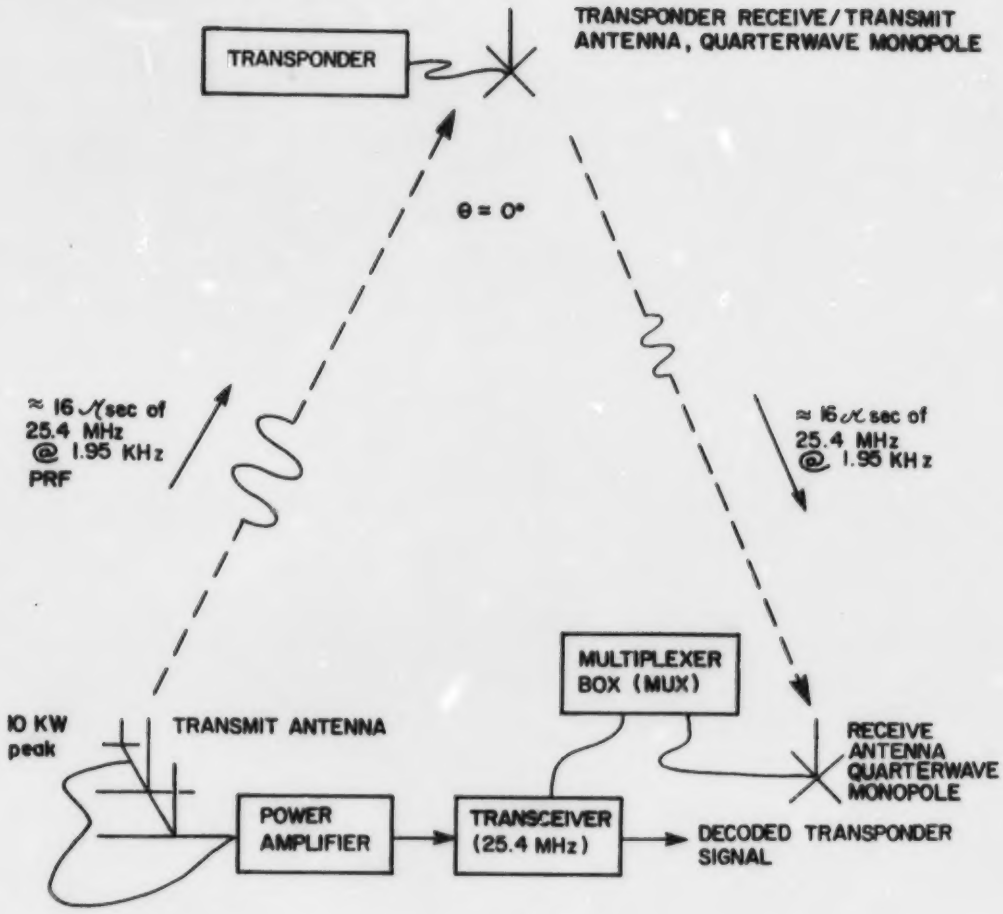
TRANSPONDER
TRANSPONDER RECEIVE/TRANSMIT ANTENNA, QUARTERWAVE MONOPOLE
θ = 0°
≈ 16 μsec of 25.4 MHz @ 1.95 KHz PRF
≈ 16 μsec of 25.4 MHz @ 1.95 KHz
MULTIPLEXER BOX (MUX)
10 KW peak
TRANSMIT ANTENNA
RECEIVE ANTENNA QUARTERWAVE MONOPOLE
POWER AMPLIFIER
TRANSCEIVER (25.4 MHz)
DECODED TRANSPONDER SIGNAL

Figure 1. Field Operational Configuration
Pond Inlet, March 1982

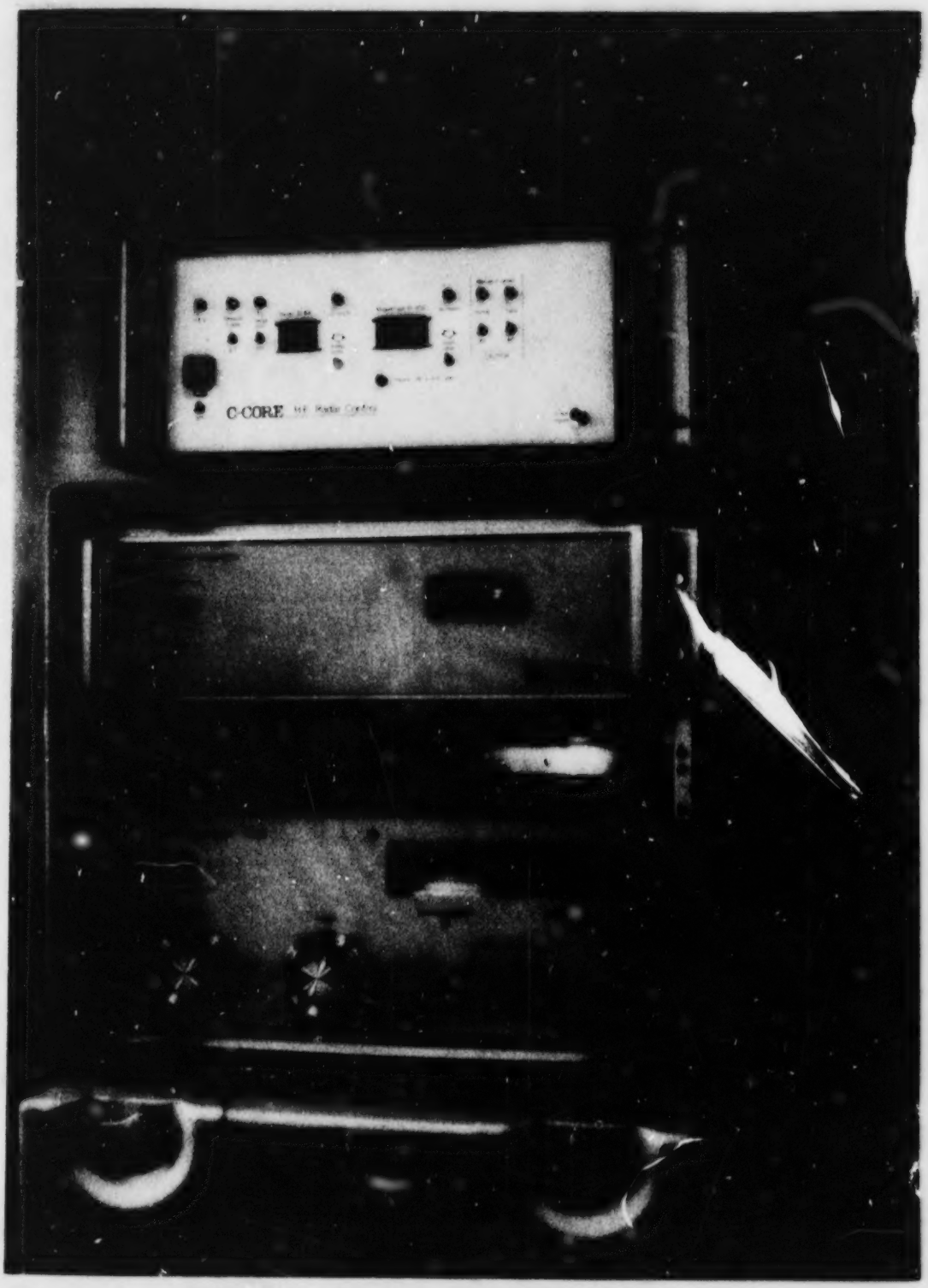

Figure 2 C-CORE H F Doppler Radar Equipment - Shown (top to bottom) are 4 signal multiplexer/filter; H.F radar control; H F transceiver; H.F. power amplifer.

Note: Only one receive antenna was used.

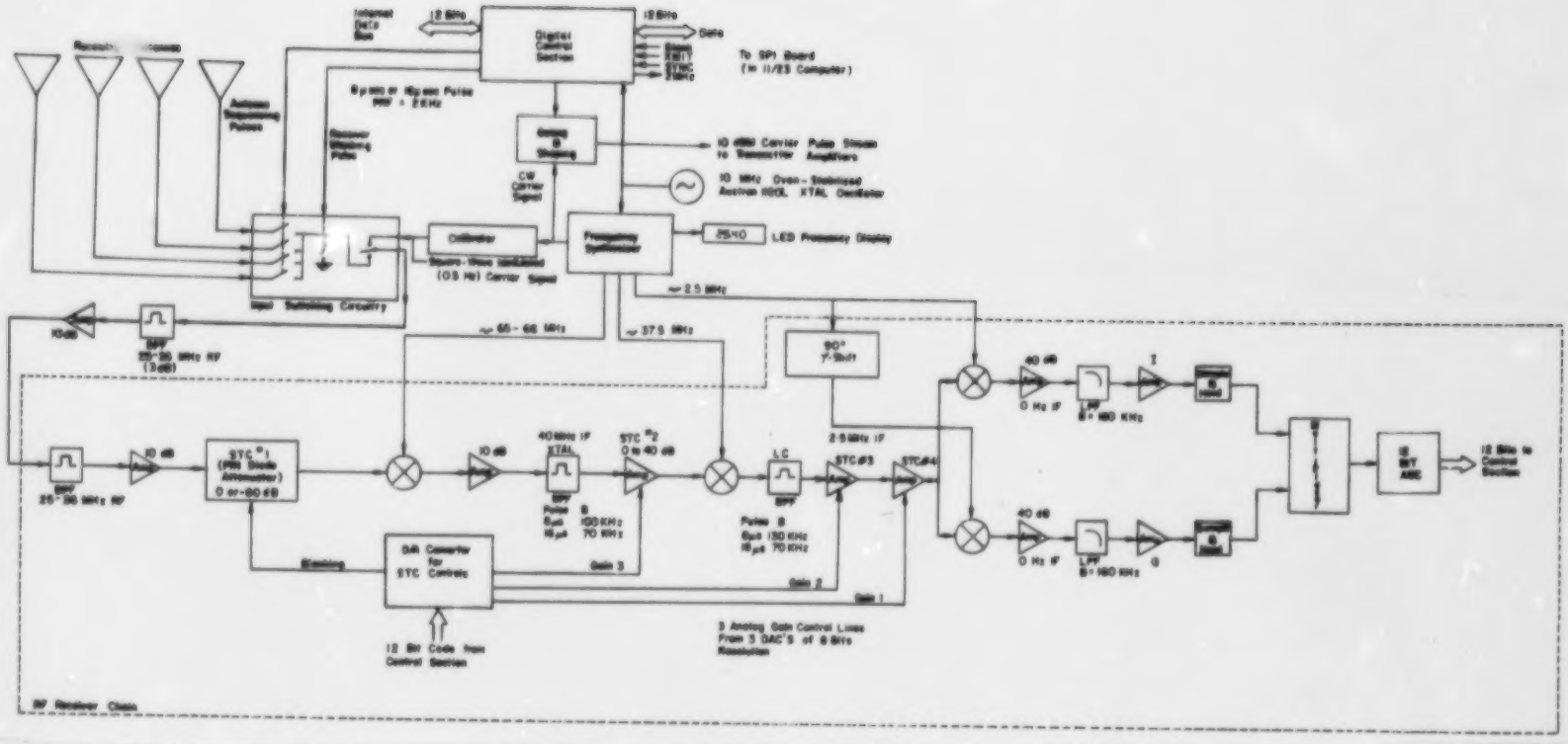

Figure 3: Transceiver Block Diagram

Note: Only one receive
antenna was used.

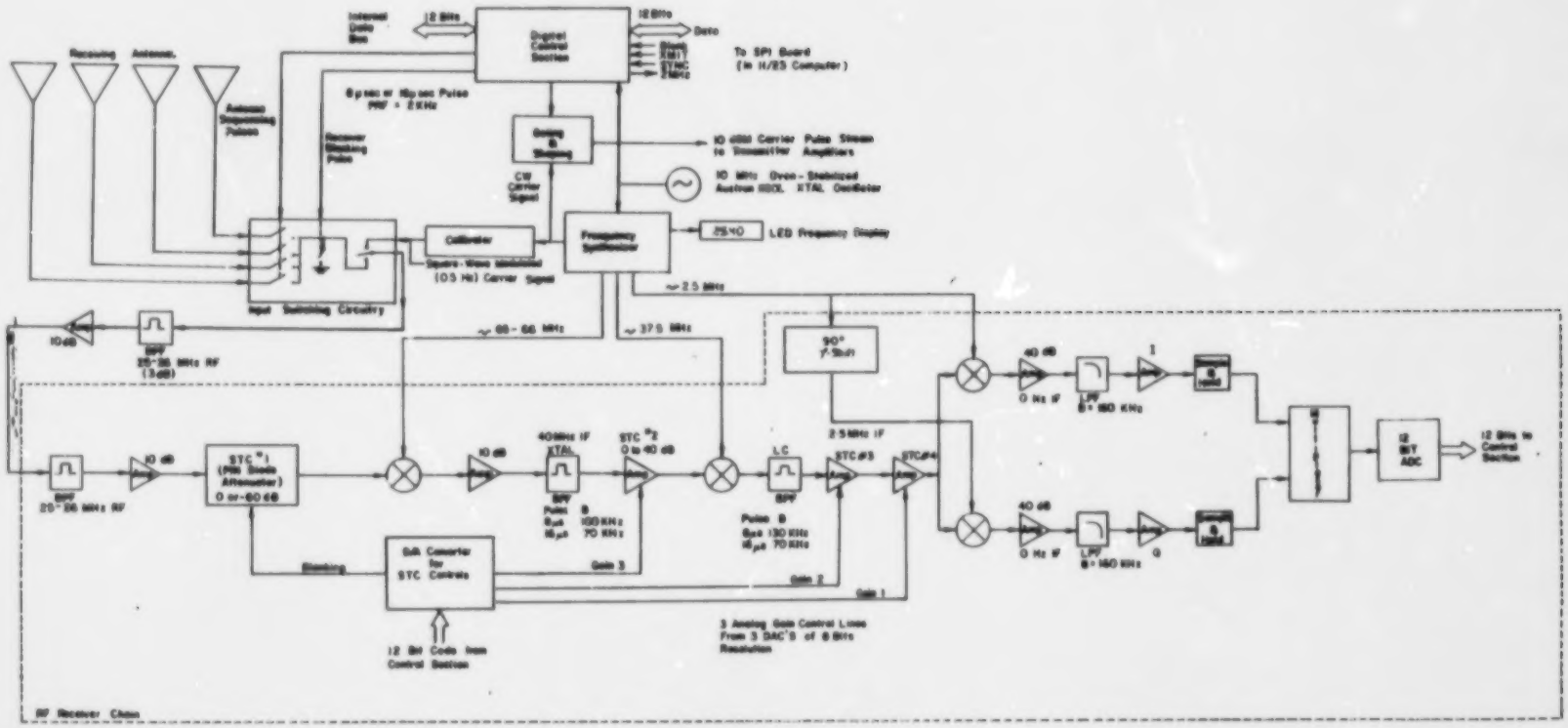
Digital Control Section
To SPI Board (In H/85 Computer)
Frequency Synthesizer
LED Frequency Display
Input Switching Circuitry
90° Y-Shift
STC #1 (PIN Diode Attenuator) 0 to -60 dB
STC #2 0 to 40 dB
STC #3
STC #4
40MHz IF XTAL
2.5MHz IF
0 Hz IF
LPF 8th 150 KHz
12 BIT ADC
12 Bits to Control Section
D/A Converter for STC Control
12 Bit Code from Control Section
3 Analog Gain Control Lines From 3 DAC's of 8 Bits Resolution
RF Receiver Chain

Figure 3: Transceiver Block Diagram

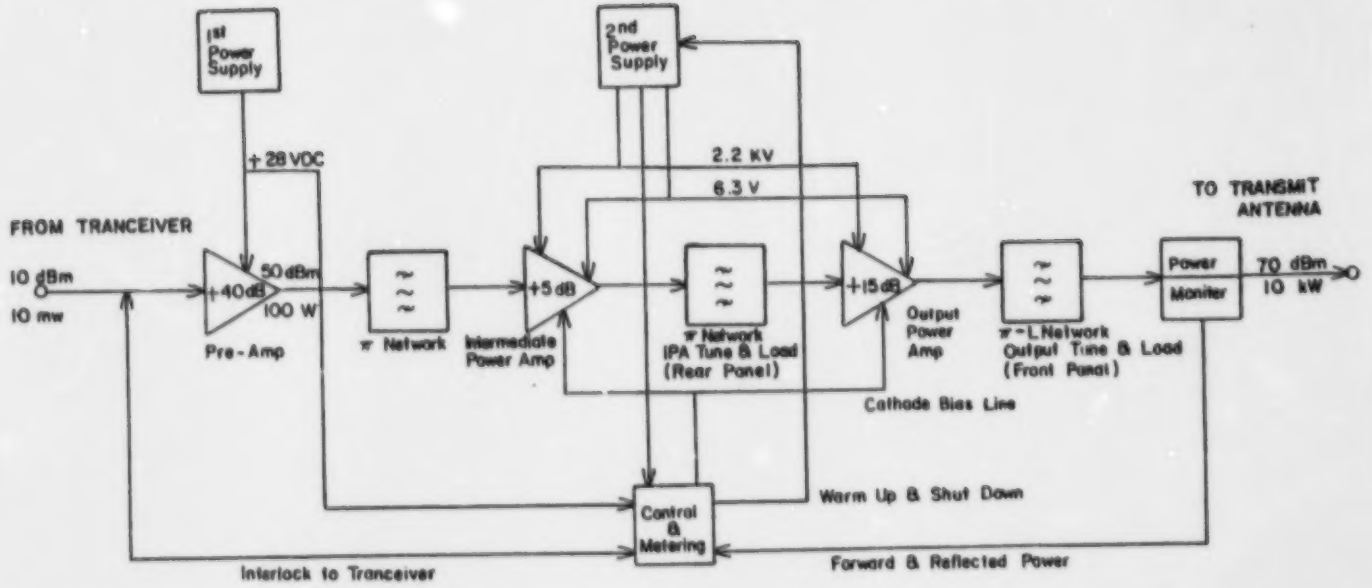

NOTES :

1. ALL POWER = PEAK
2. TUNING RANGE = 25 to 35 MHz
3. ALL LINES 50Ω IMPENDENCE
4. NOMINAL PLUSE WIDTH = 8μ sec (32μ sec MAX.)

Figure 4 : Transmit Power Amplifier Block Diagram

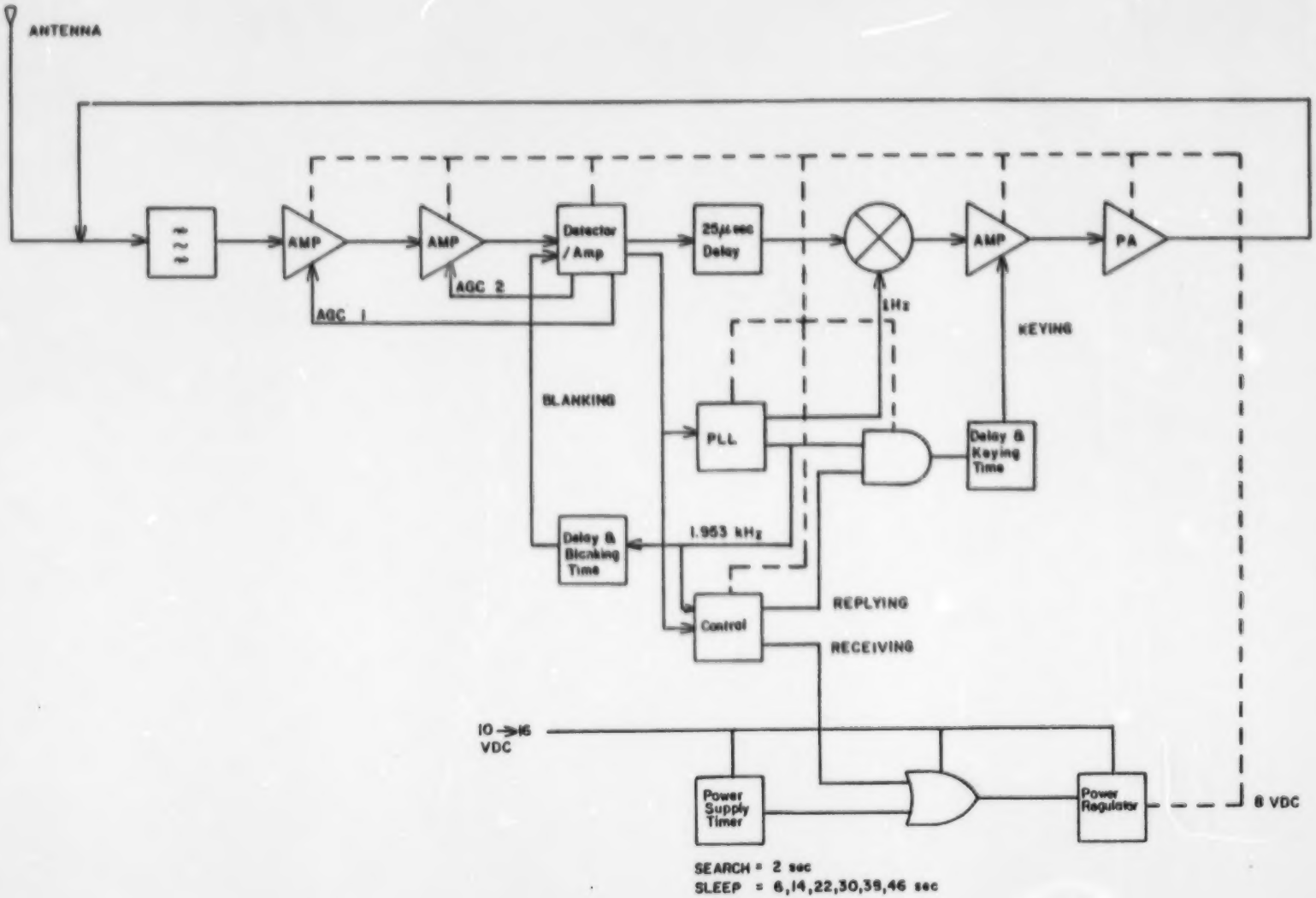

Figure 5 : CODAR Transponder-Block Diagram

a)
Initial receive antenna location
50μ sec/division
2 v/division
Receiver gain = 55.6 dB
Top trace - In phase
Bottom trace -
Quadrature

b)
Receive antenna location changed to minimize noisefloor
50μsec/division
2 v/division
Receiver gain = 80.8 dB
Top trace - Inphase
Bottom trace -
Quadrature

Figure 6 Scope Display of Noise Floor from two receive antenna locations. Proper location of the receive antenna eliminated a large part of the near range noise attributed to direct path coupling of the transmission decay transient. This permitted the use of higher receiver gains.

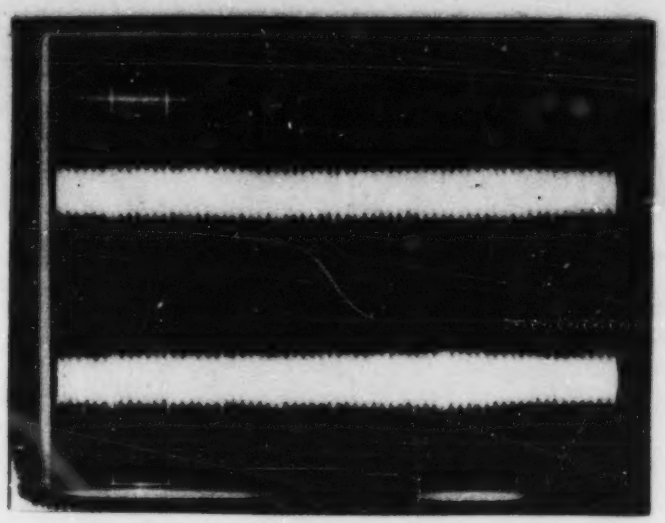

a)
Noise floor at final
receive antenna location
with transmitter disabled
50μsec/division
5 v/division
Receiver gain 101 dB
Top trace - Inphase
Bottom trace -
Quadrature

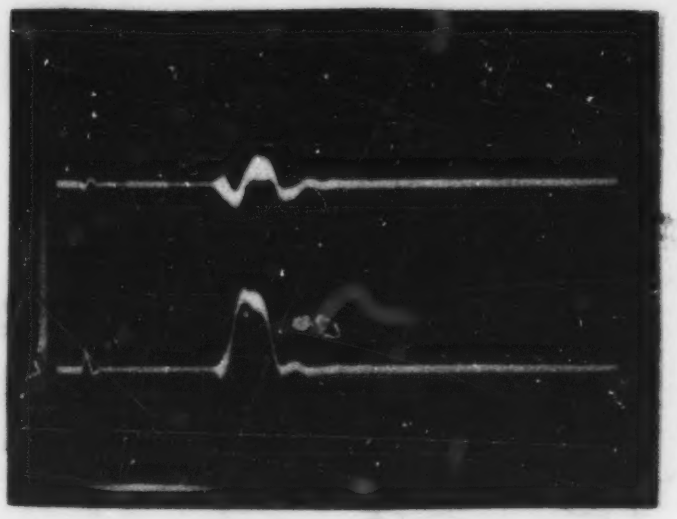

b)
Transponder signal
@ range 0.5 km
20 sec/division
2v/division
Receiver gain = 80.8dB
Top trace - Inphase
Bottom trace -
Quadrature

Figure 7 Scope Display of Noise Floor (a) and Decoded Transponder Signal (b)

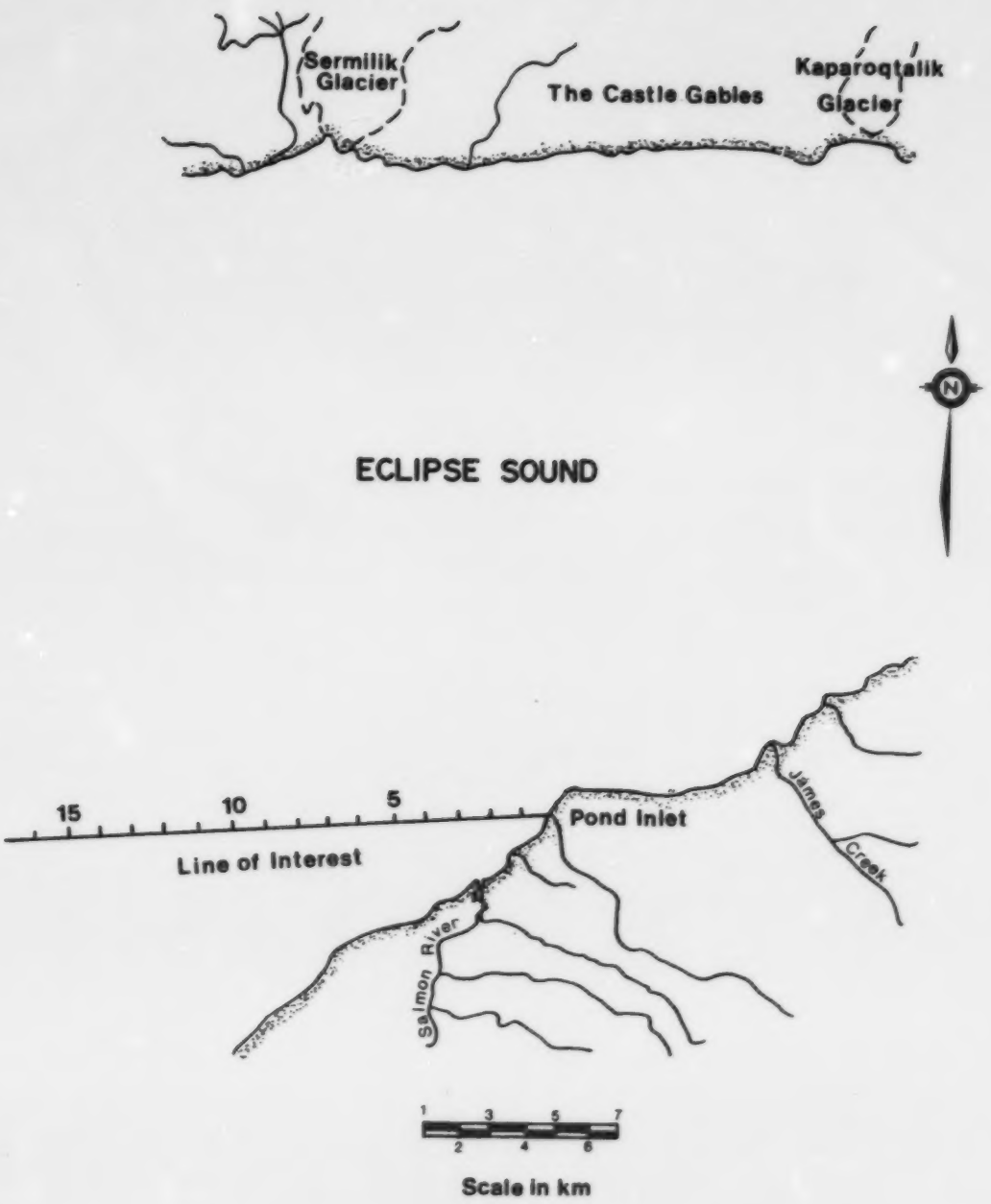

Figure 8 The Line of Interest over which propagation measurements were made.

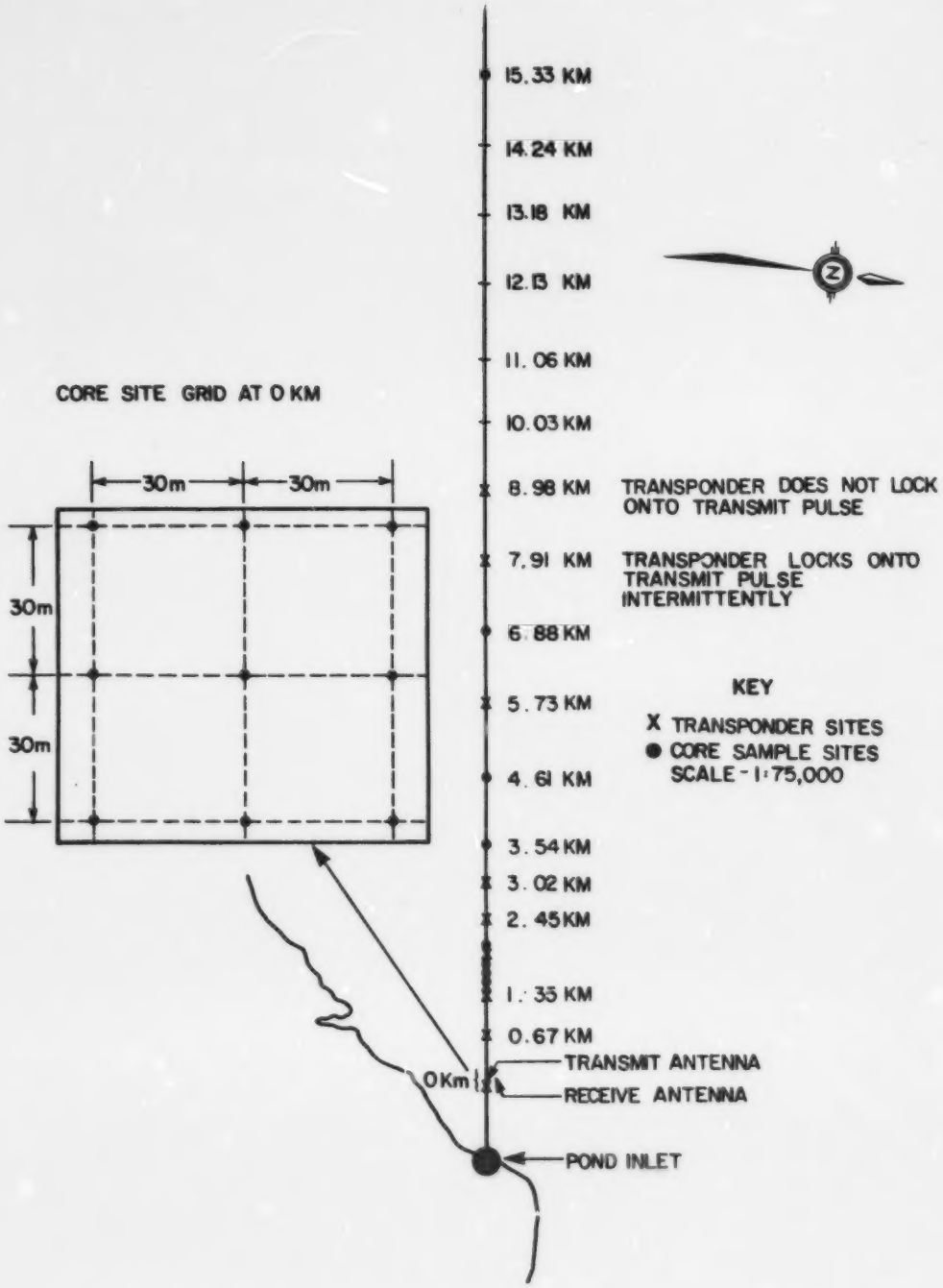

Figure 9 Experimental Test Sites Along Line of Interest

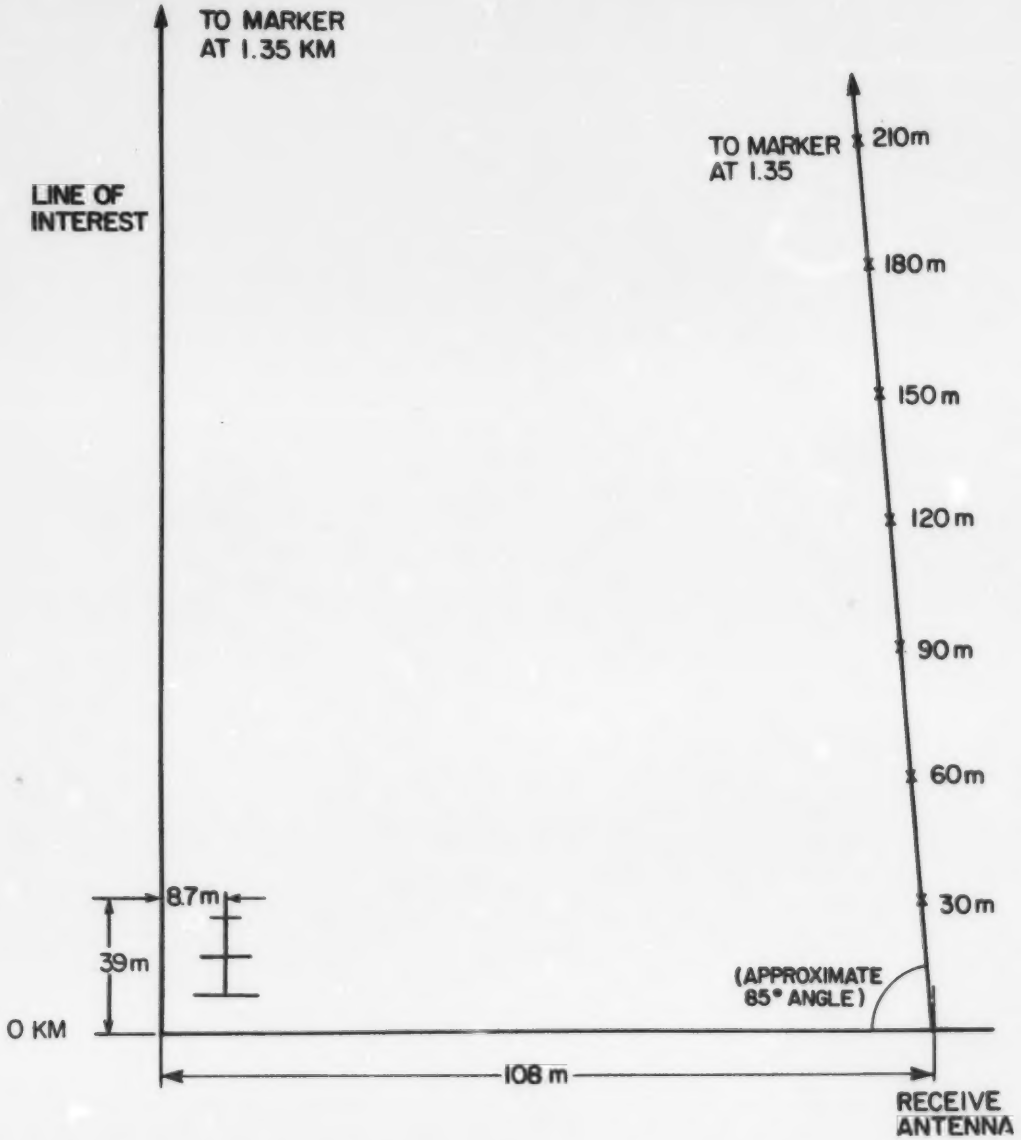

Figure 10 Location of Near Field Propagation Measurements

Figure 11 Pond Inlet - Crossing the Tidal Crack to take H F radar from a heated hut on the coast to the tent on the ice.

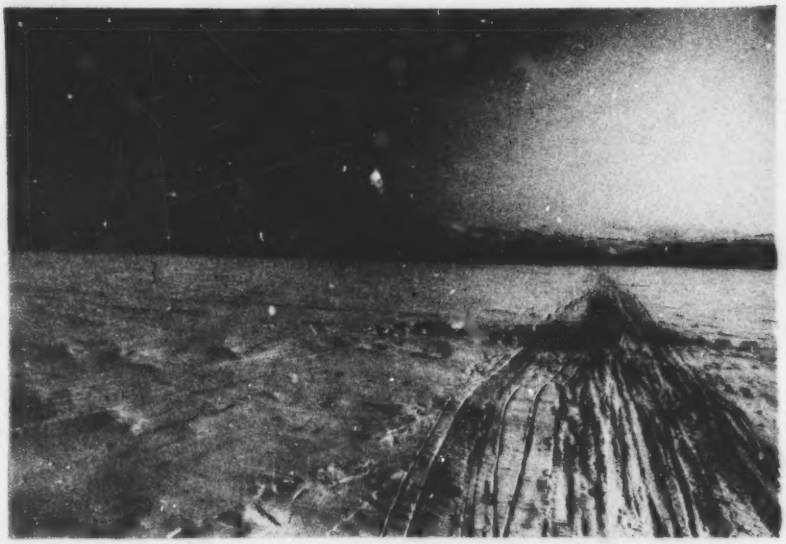

Figure 12 Komatik used to transport transponder and transponder antenna (quarter wave monopole) along line of interest. Pond Inlet lies in the background.

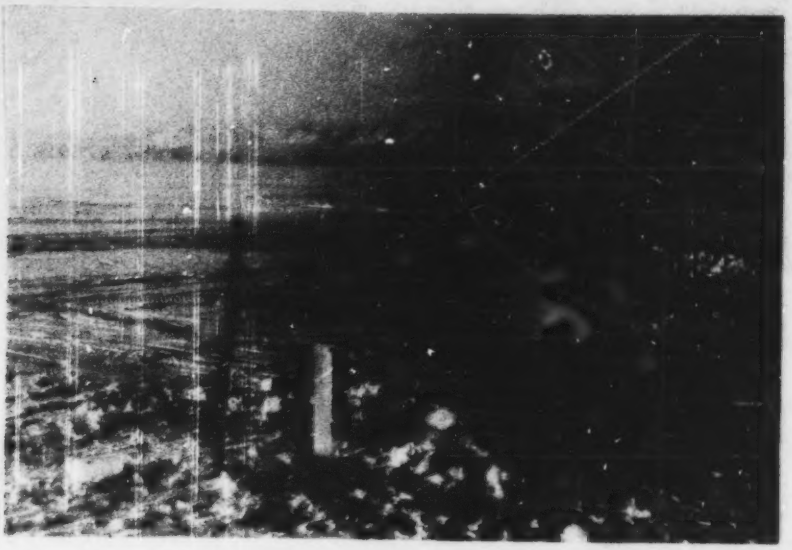

Figure 13 Coring the ice at one of the surveyed markers on the line of interest. Two cores were taken at each marker out to 4.6 km.

Figure 14 H F radar in operation. From top to bottom, 465B oscilloscope, H F control box, H F transceiver, H F power amplifier. The top of the Racal Store 4-D analogue tape recorder is just visible in the lower right hand corner.

Figure 15 The tent containing the H F radar with the 3 element Yagi transmit antenna in the foreground. The receive antenna, approximately 200 feet to the far side of the tent, is too thin to show up in this photo.

Figure 16 The 3 element Yagi transmit antenna looks out over the line of interest. The surface of the snow layer indicates general uniformity out to the horizon.

Figure 17 Quarter Wave monopole receive antenna sitting on surface of snow layer. The multiplexer (MUX) box can be seen in the lower right hand corner. The mountains in the background form the coast of Bylot Island.

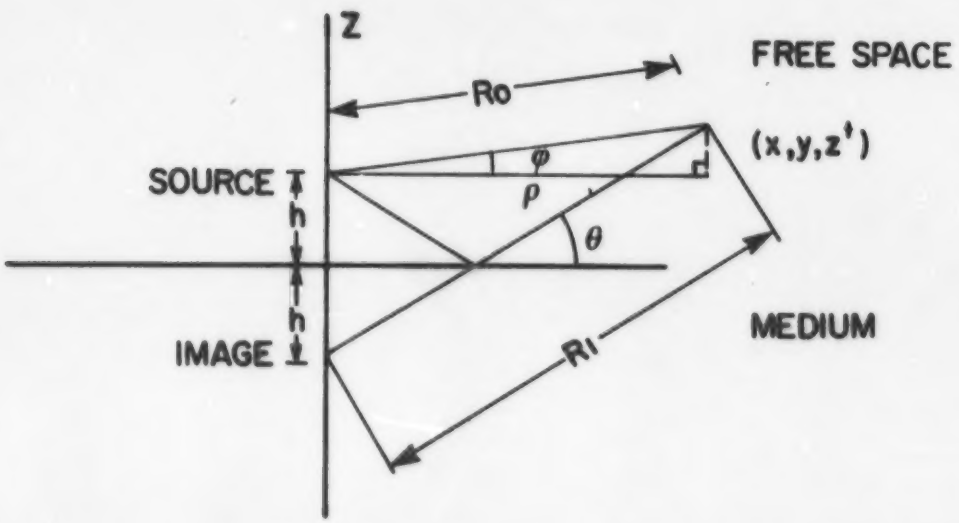

Figure 18 Coordinate System for Infinitesimal Dipole above Complex Medium. The medium in the lower half space is taken to be horizontally homogeneous. Its electrical properties may only vary in the vertical (z) direction.

In phase

Quadrature

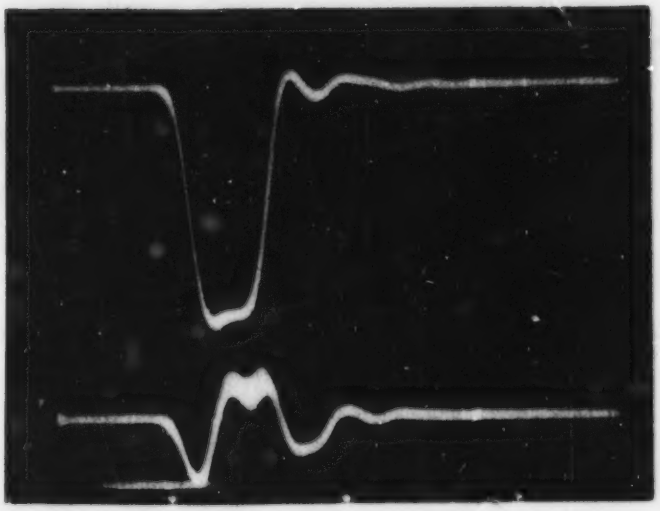

Figure 19 The transponder antenna was moved to minimize the in phase component, thus nulling the quadrature component. 210.6 metres separated the transponder and receive antennas.

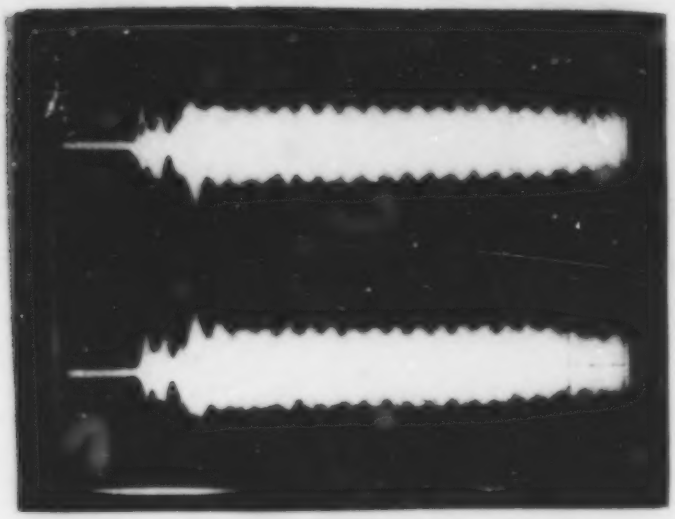

a)
20μsec/division
5v/division
Top trace - Inphase
Bottom trace -
Quadrature

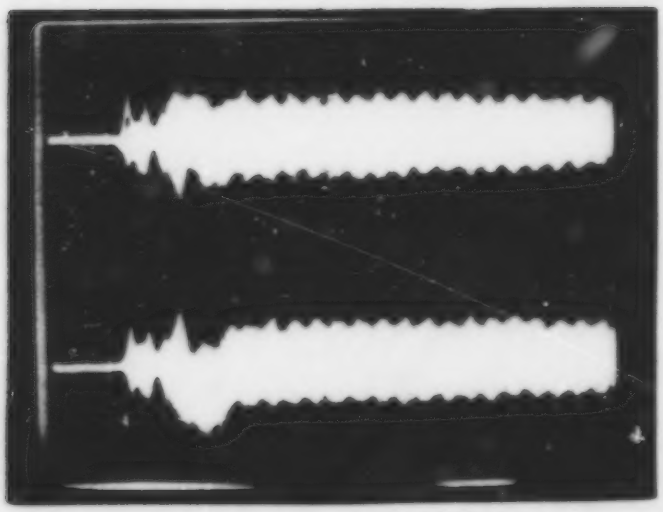

b)
20μsec/division
5v/division
Top trace - Inphase
Bottom trace -
Quadrature

Figure 20 Receiver Output Before (a) and After (b) the Transponder locks on to the transmit pulse (30 km separated the transponder and receive antenna

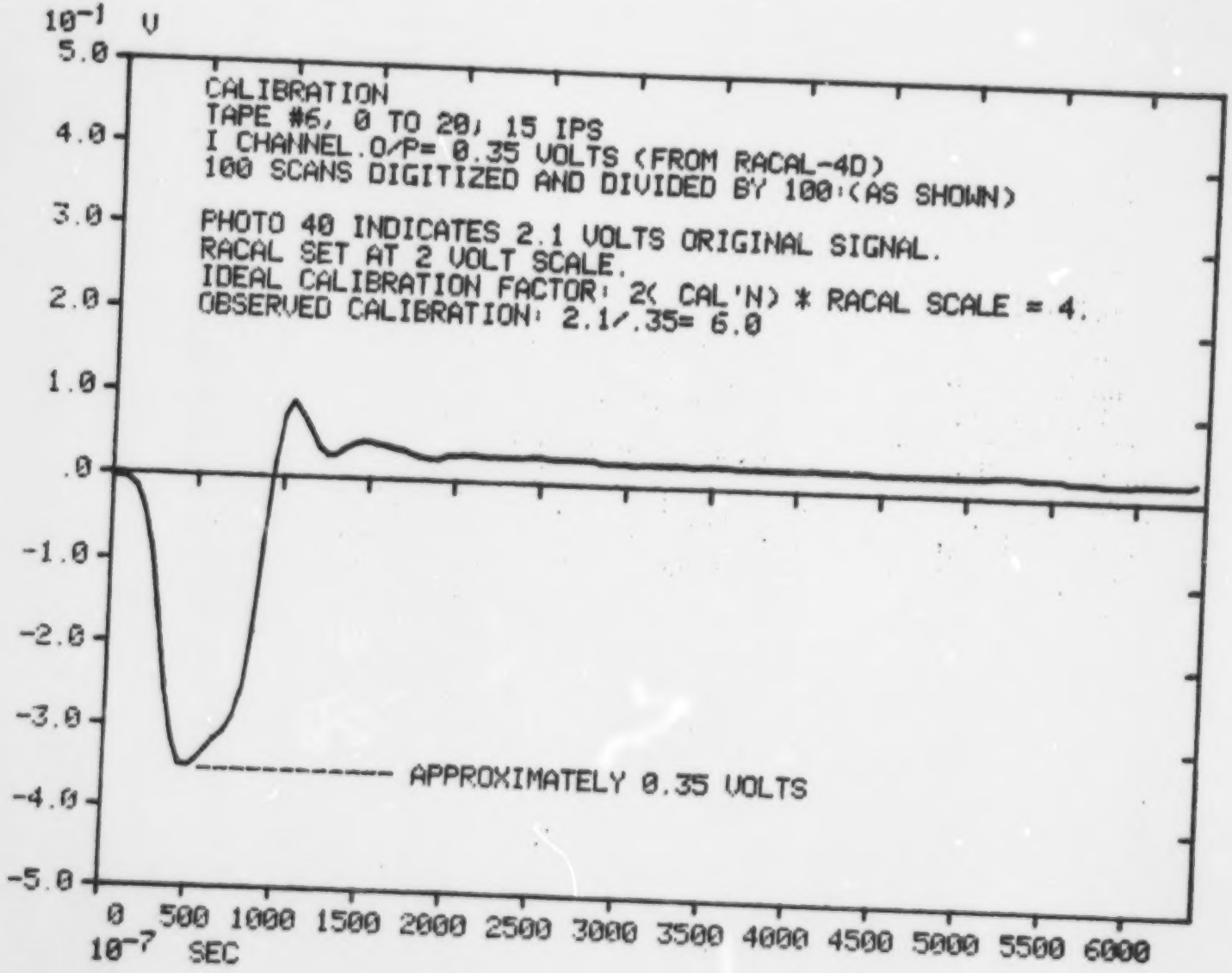

Figure 21 Output from HP5451B Fourier Analyzer used as basis for calibration

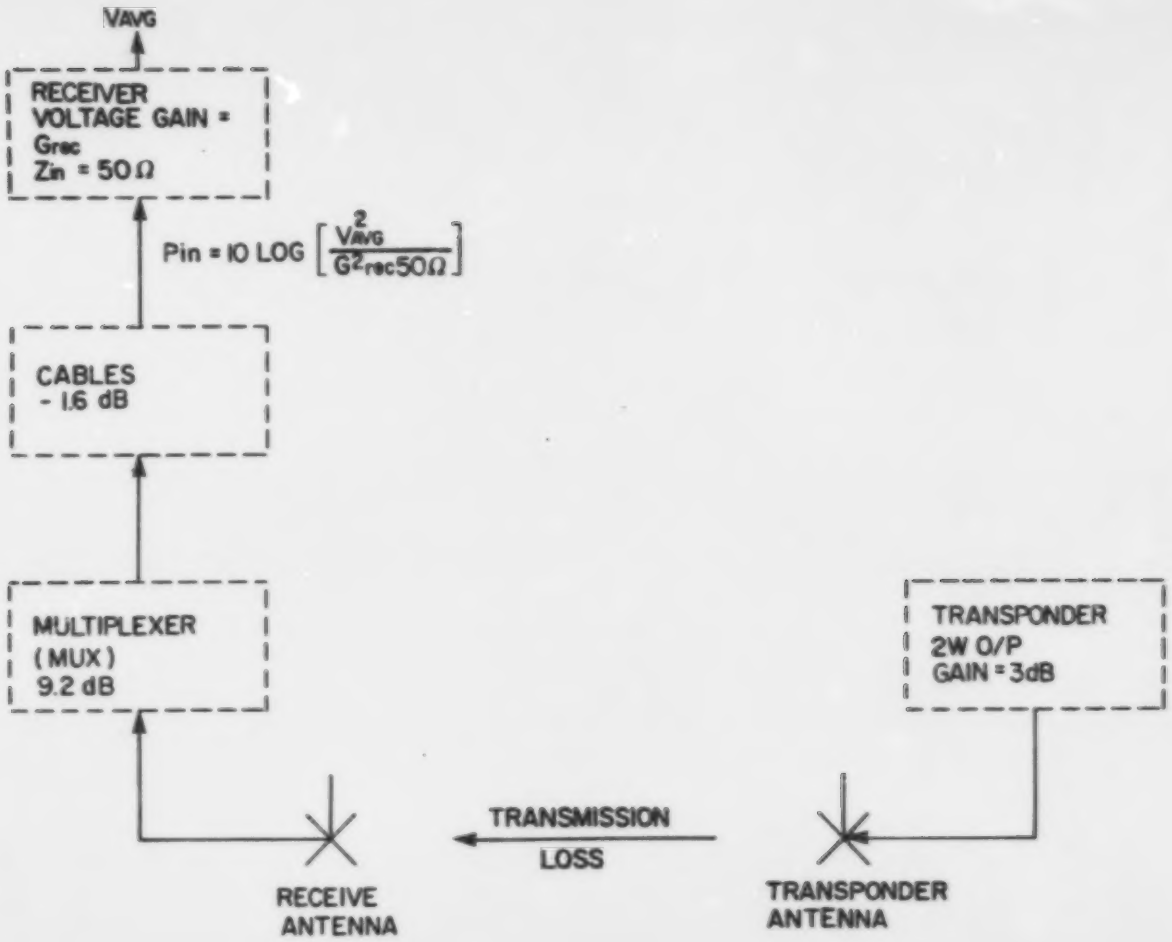

Figure 22 Block Diagram Modelling Transmission Loss Calculations

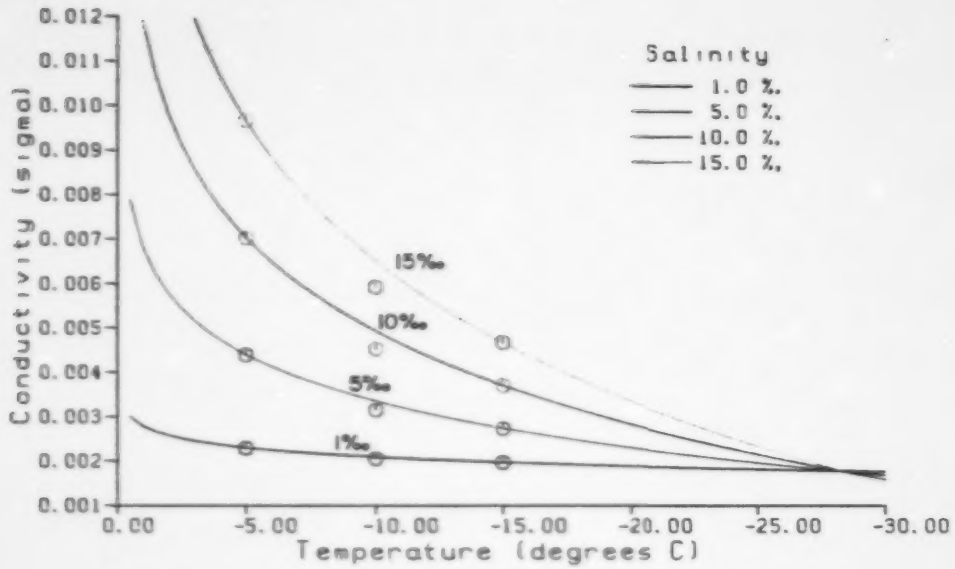

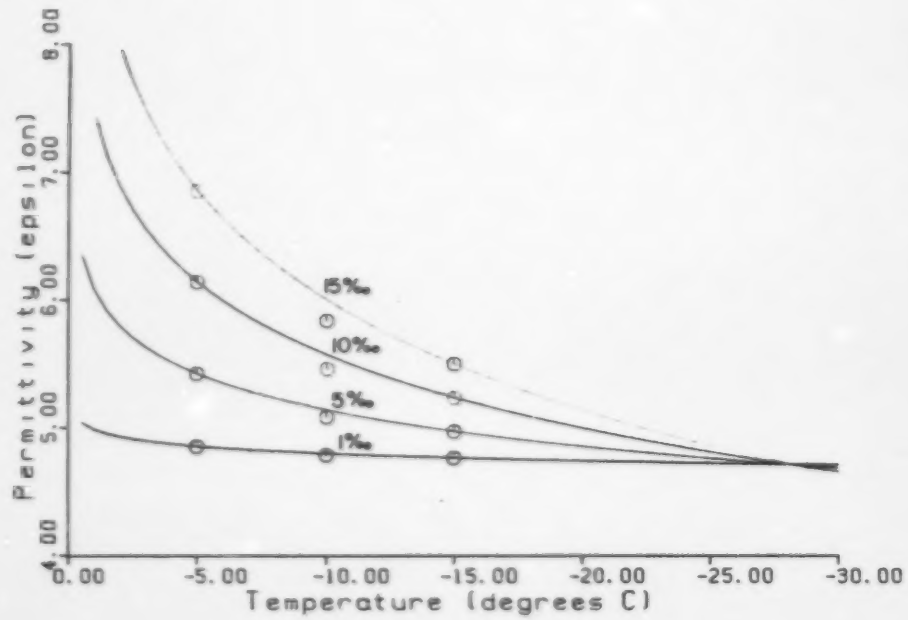

Figure 23 Graph of Empirical Formulae

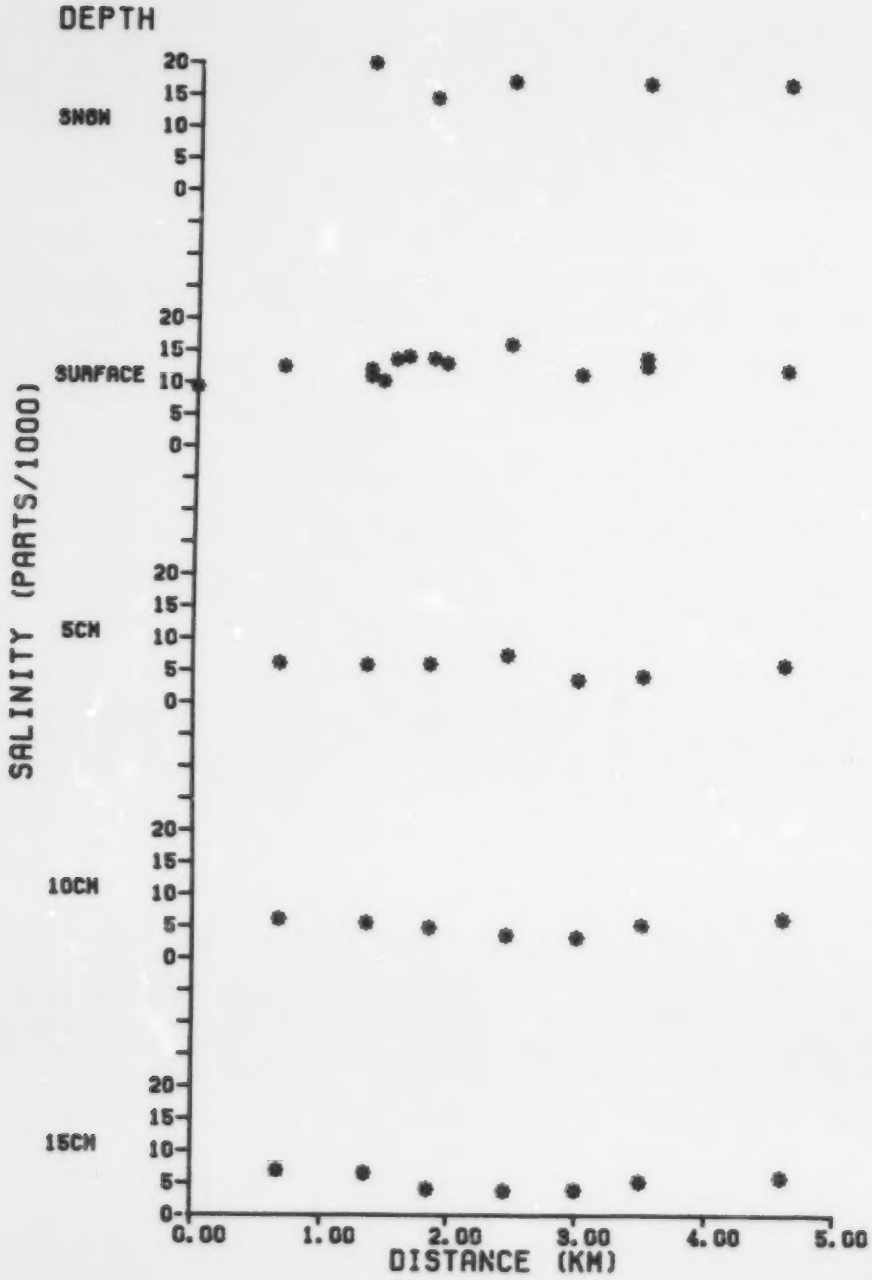

Figure 24(a) Observed Salinities grouped by ice core extraction date only.

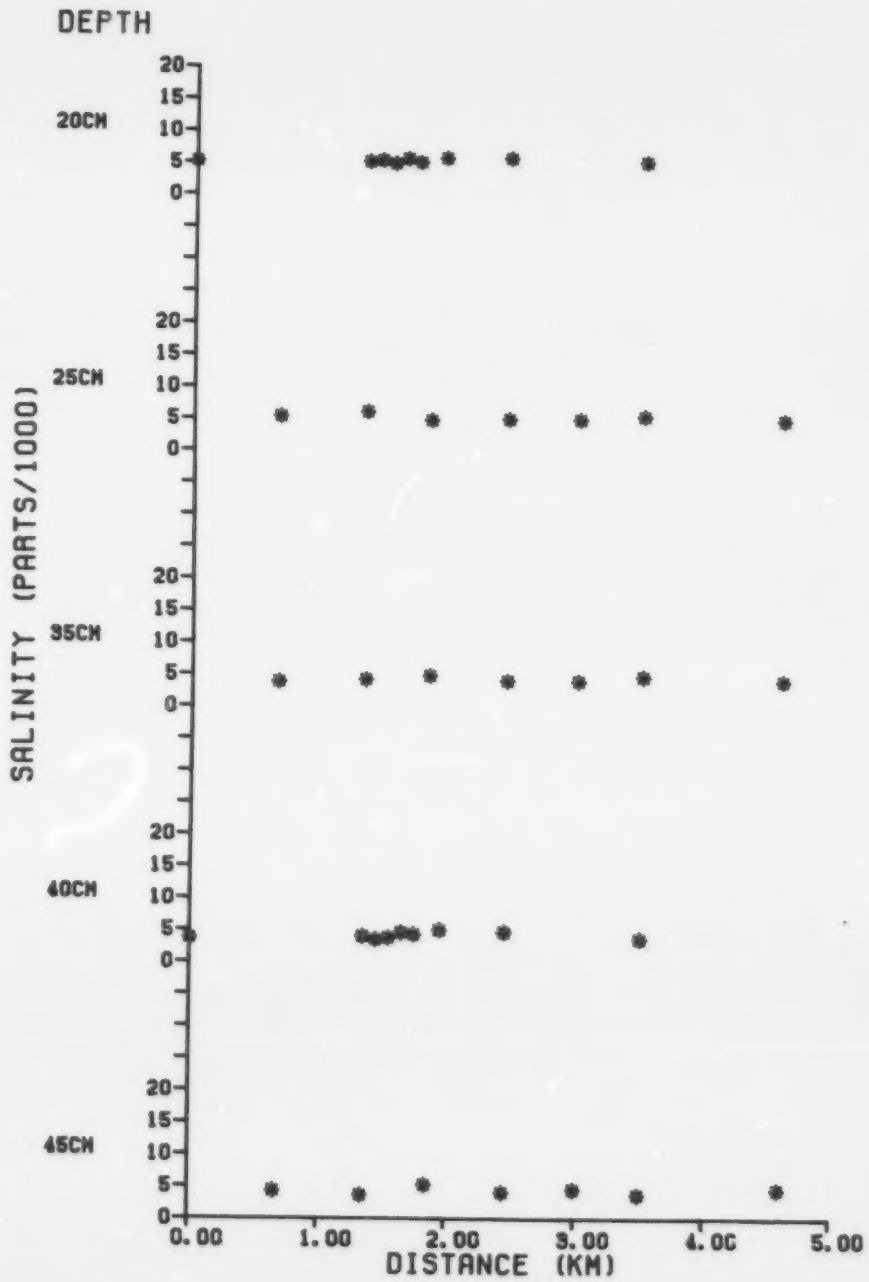
DEPTH
20CM
25CM
35CM
40CM
45CM
SALINITY (PARTS/1000)
20
15
10
5
0
0.00
1.00
2.00
3.00
4.00
5.00
DISTANCE (KM)

Figure 24(b)

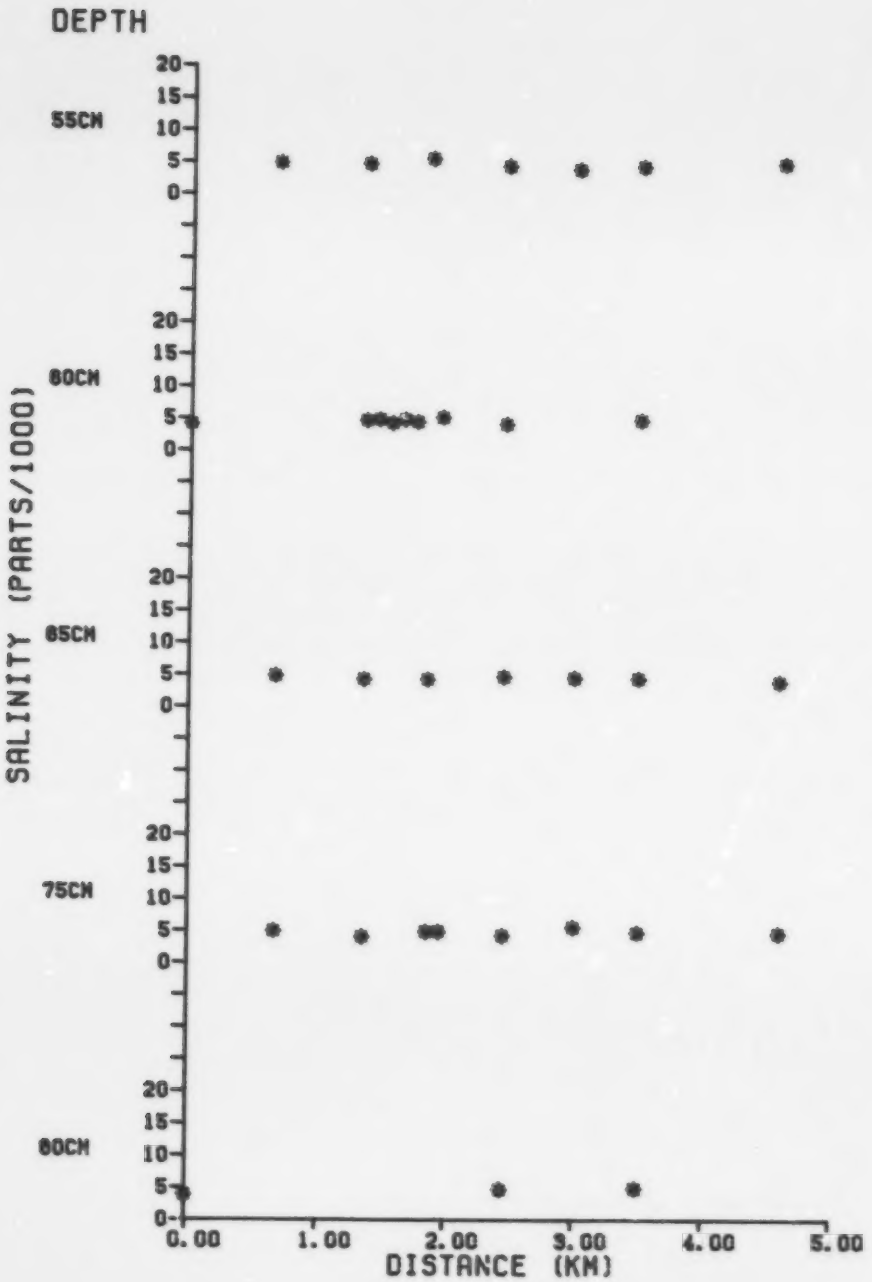
DEPTH
55CM
80CM
85CM
75CM
80CM
20
15
10
5
0
SALINITY (PARTS/1000)
0.00
1.00
2.00
3.00
4.00
5.00
DISTANCE (KM)

Figure 24(c)

DEPTH
SALINITY (PARTS/1000)
20
15
10
5
0
85CM
0.00
1.00
2.00
3.00
4.00
5.00
DISTANCE (KM)

Figure 24(d)

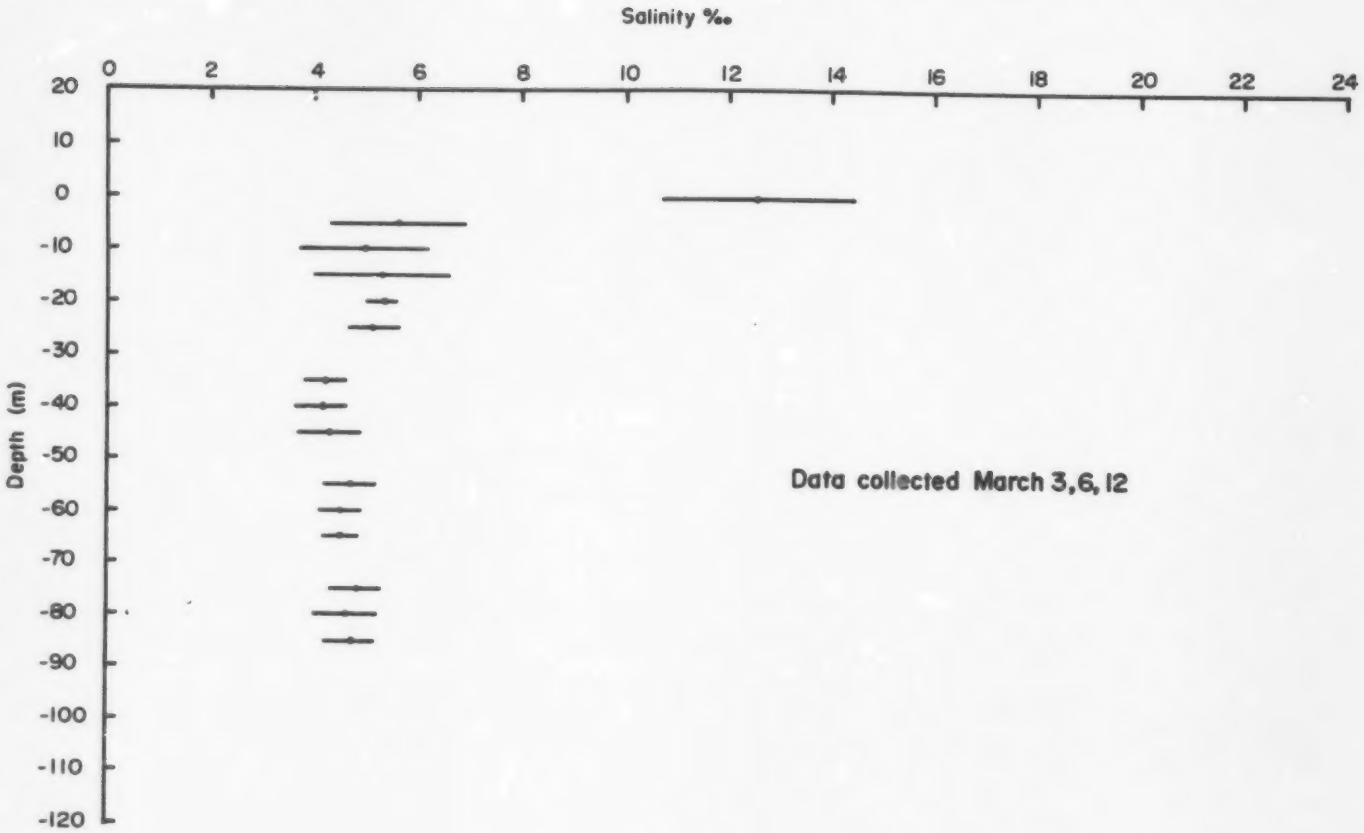

Figure 25 Salinity Profile (C-CORE Data)
Average Data (grouped over 0 to 4.6 km)

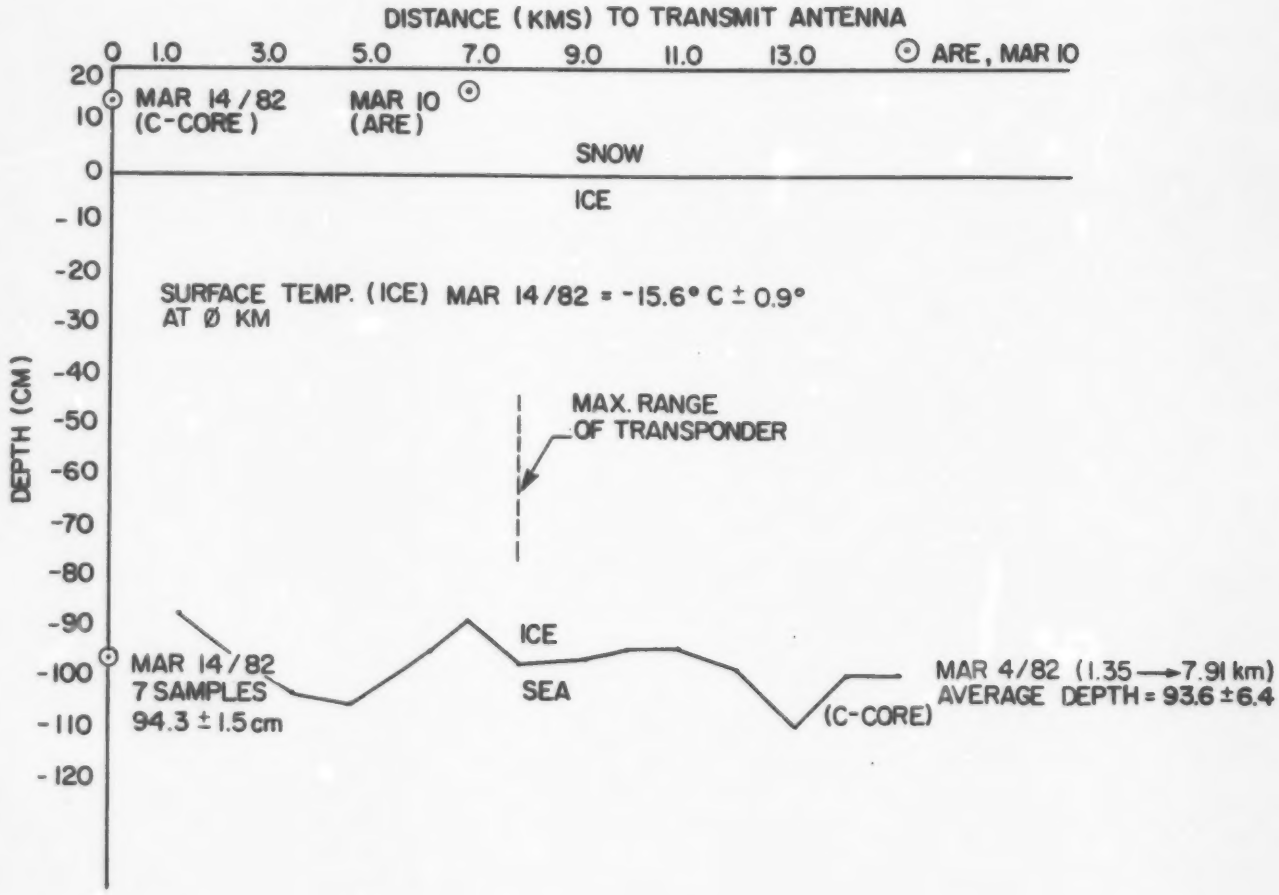

Figure 26 Ice Profile Overview

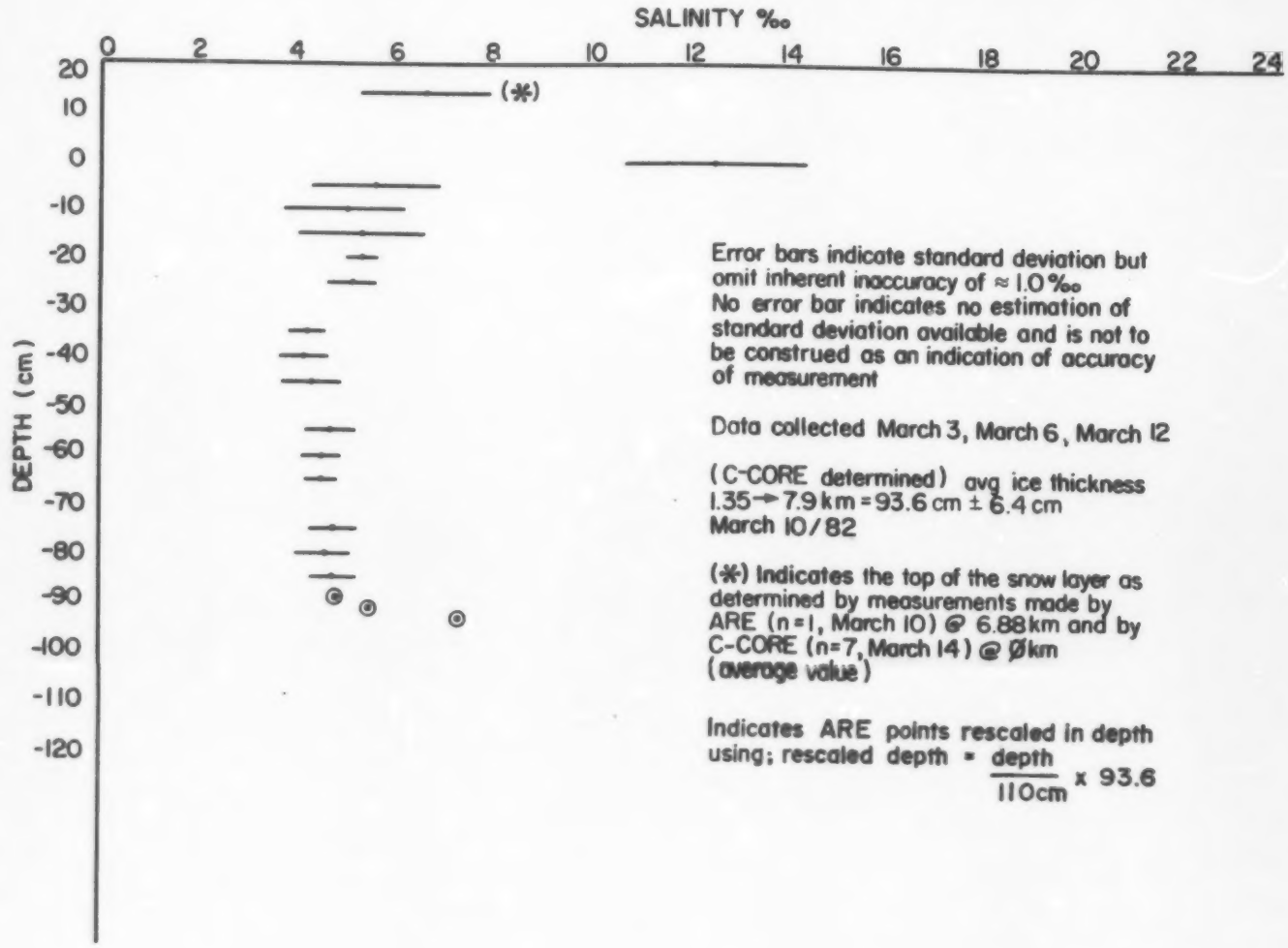
SALINITY ‰
0 2 4 6 8 10 12 14 16 18 20 22 24
20 10 0 -10 -20 -30 -40 -50 -60 -70 -80 -90 -100 -110 -120
DEPTH (cm)
(*)
Error bars indicate standard deviation but omit inherent inaccuracy of ≈ 1.0 ‰
No error bar indicates no estimation of standard deviation available and is not to be construed as an indication of accuracy of measurement
Data collected March 3, March 6, March 12
(C-CORE determined) avg ice thickness 1.35→7.9 km = 93.6 cm ± 6.4 cm March 10/82
(*) Indicates the top of the snow layer as determined by measurements made by ARE (n=1, March 10) @ 6.88 km and by C-CORE (n=7, March 14) @ Ø km (average value)
Indicates ARE points rescaled in depth using; rescaled depth = depth / 110cm x 93.6

Figure 27 Final Model of Salinity Profile

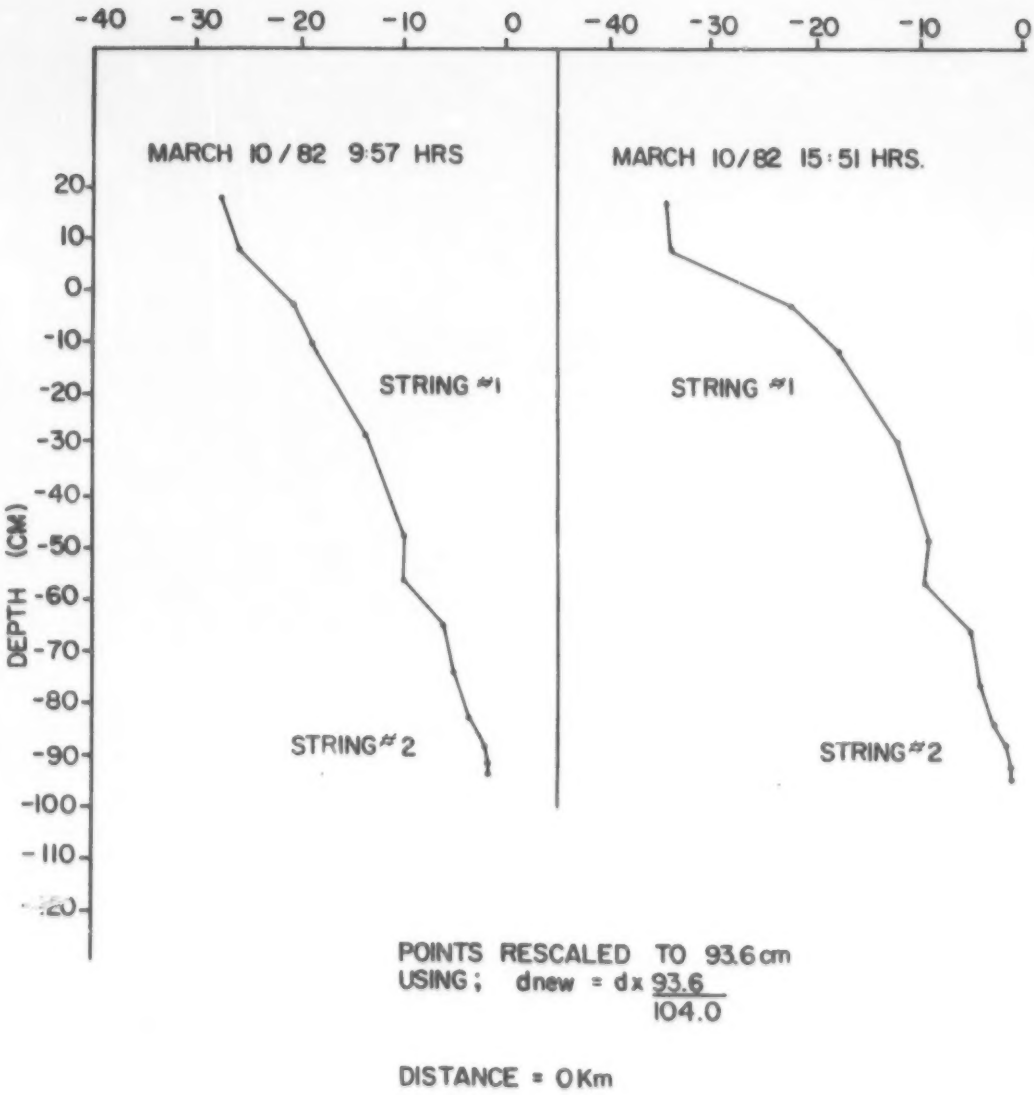

Figure 28 Temperature Profile
Rescaled to 93.6 cm
Thermistor String TM-1

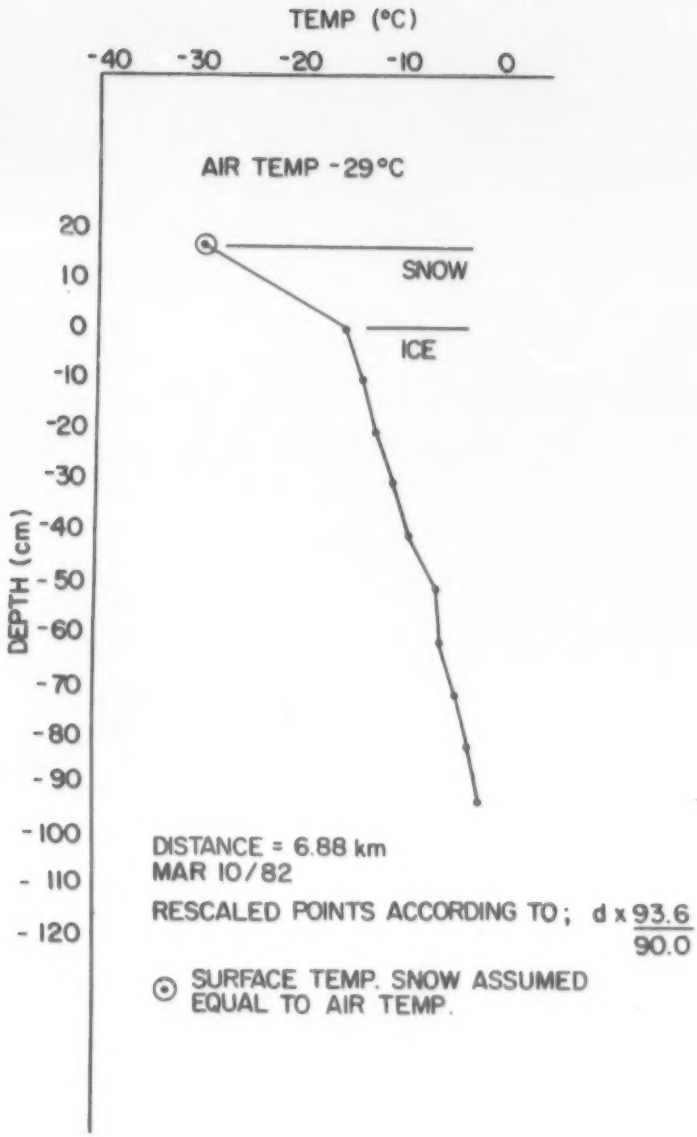

Figure 29 Temperature Profile
Rescaled to 93.6 cm
Thermocouple TC-1

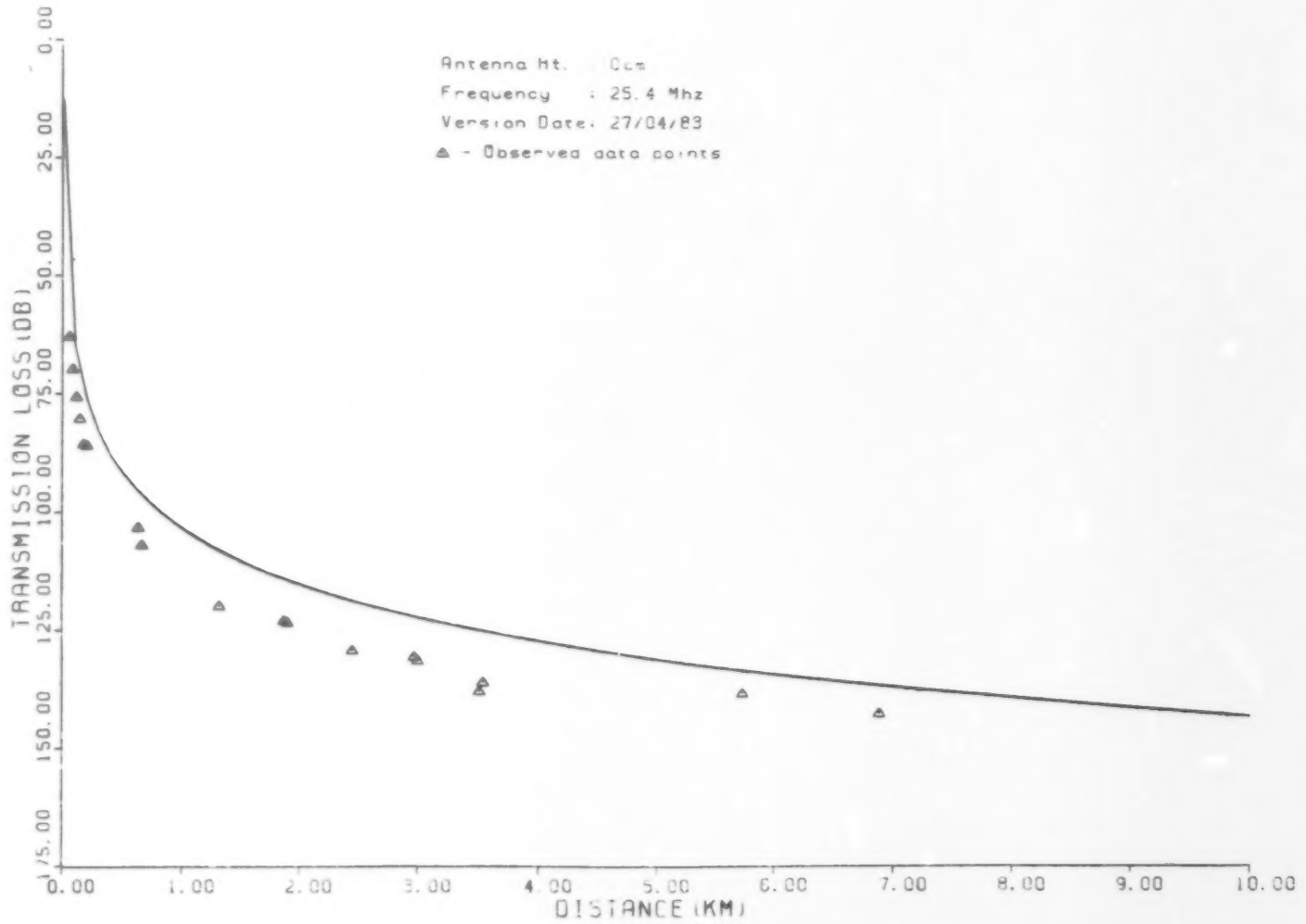

Figure 30 Transmission Loss: Observed vs Theoretical ($G_t = G_r = 1$)

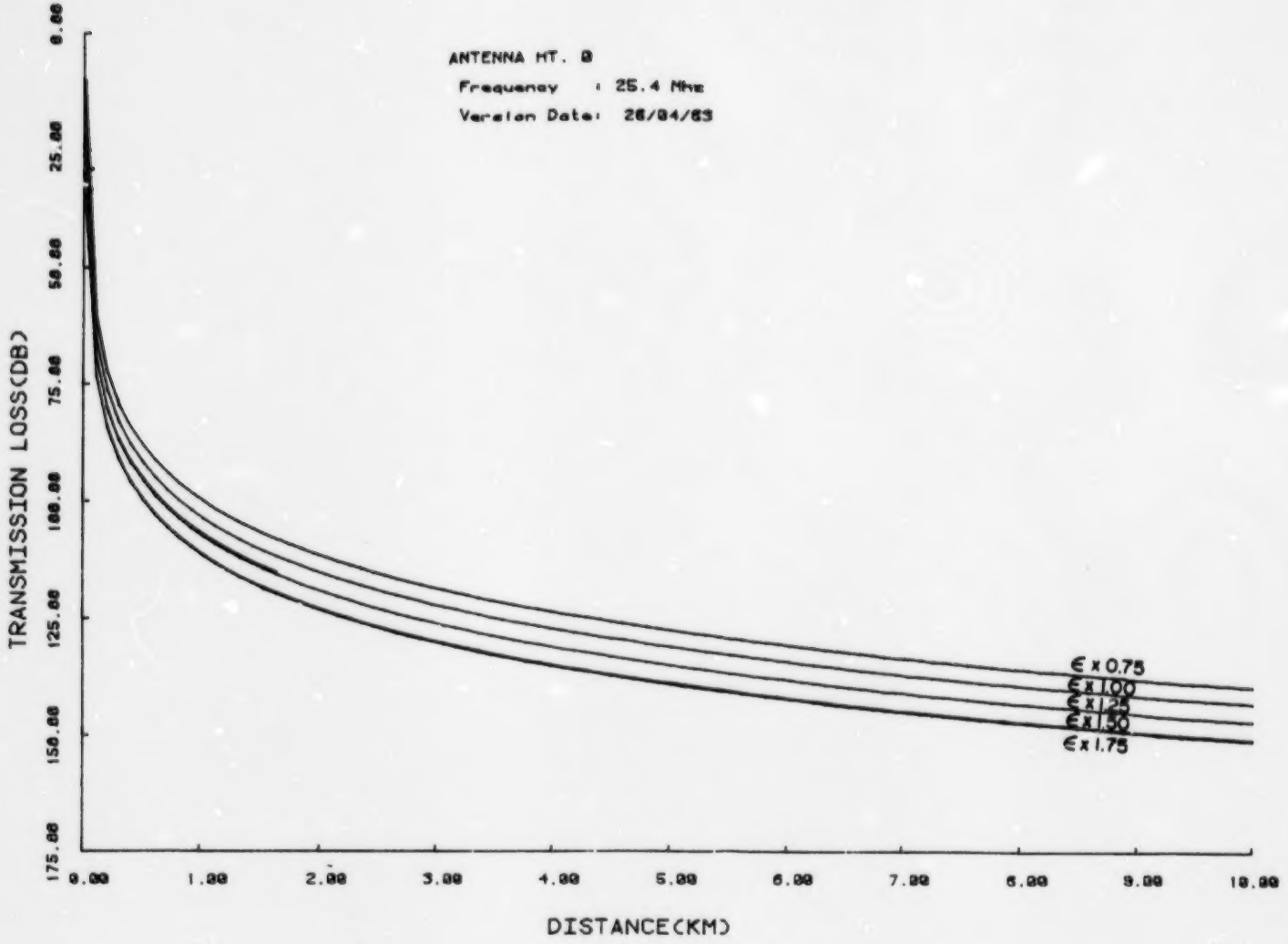

Figure 31 Variation of Calculated Loss With ε_r

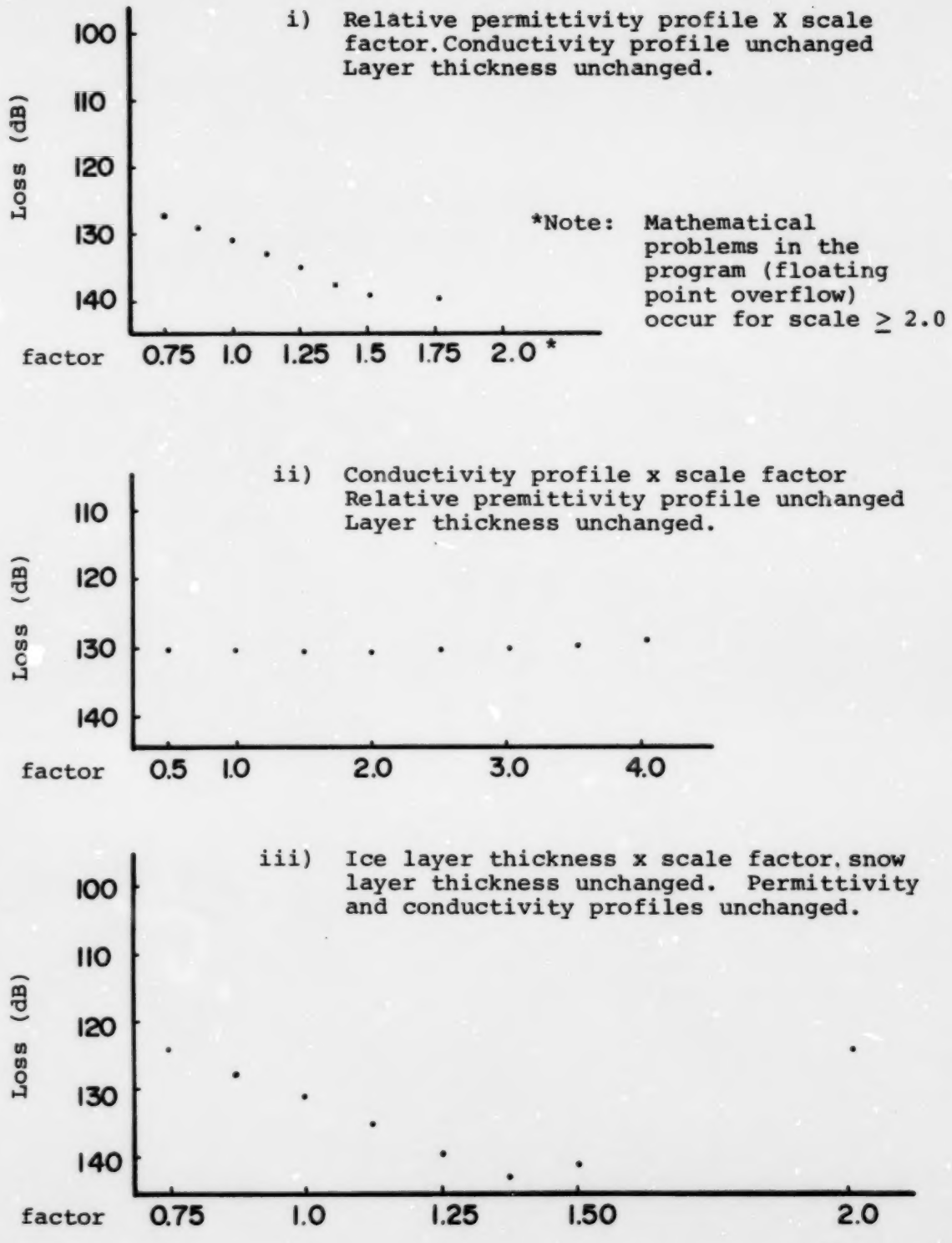

Figure 32 Variation of Calculated Loss at 5 km as individual parameters are varied.

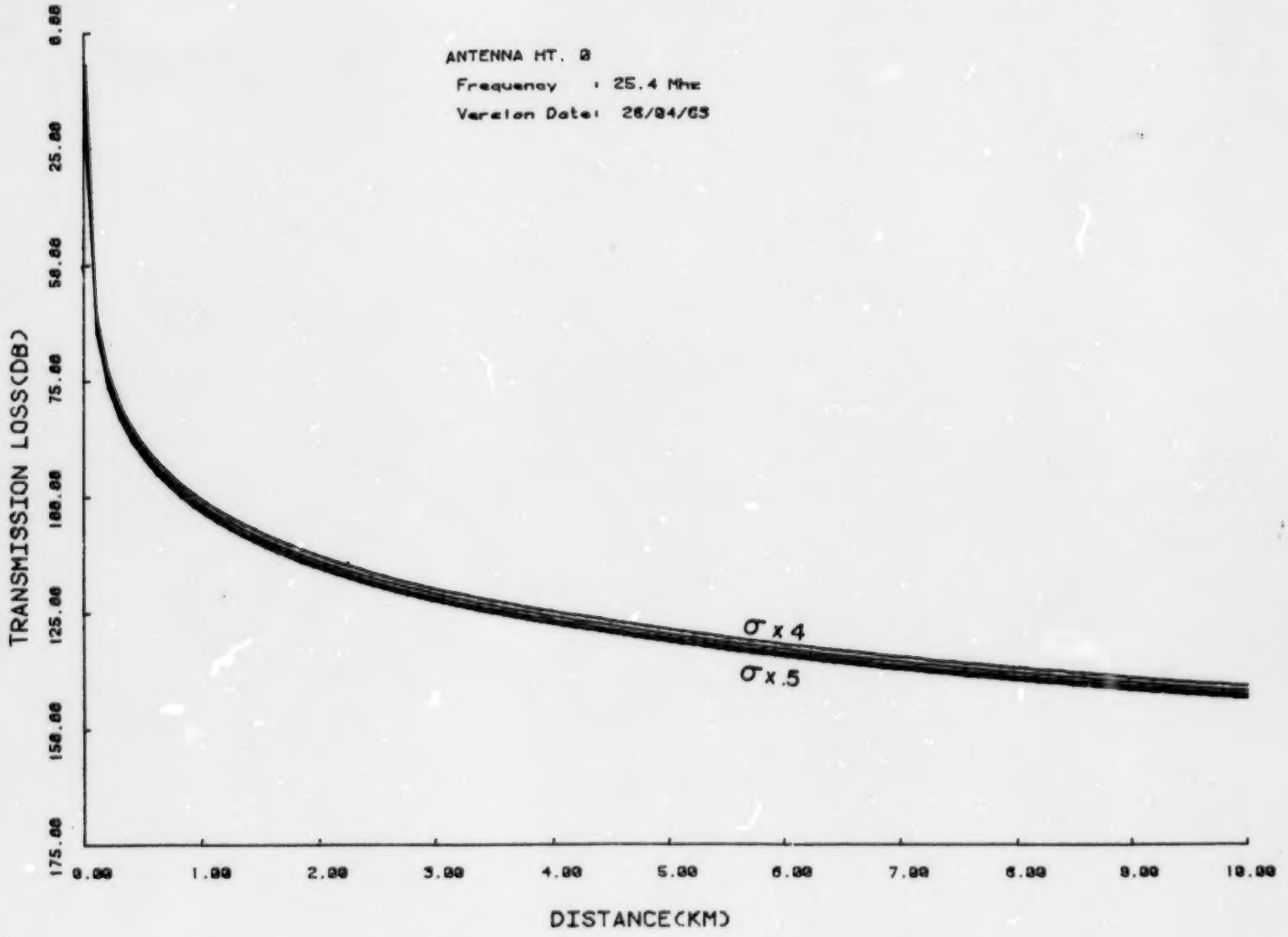

Figure 33 Variation of Calculated Loss with σ

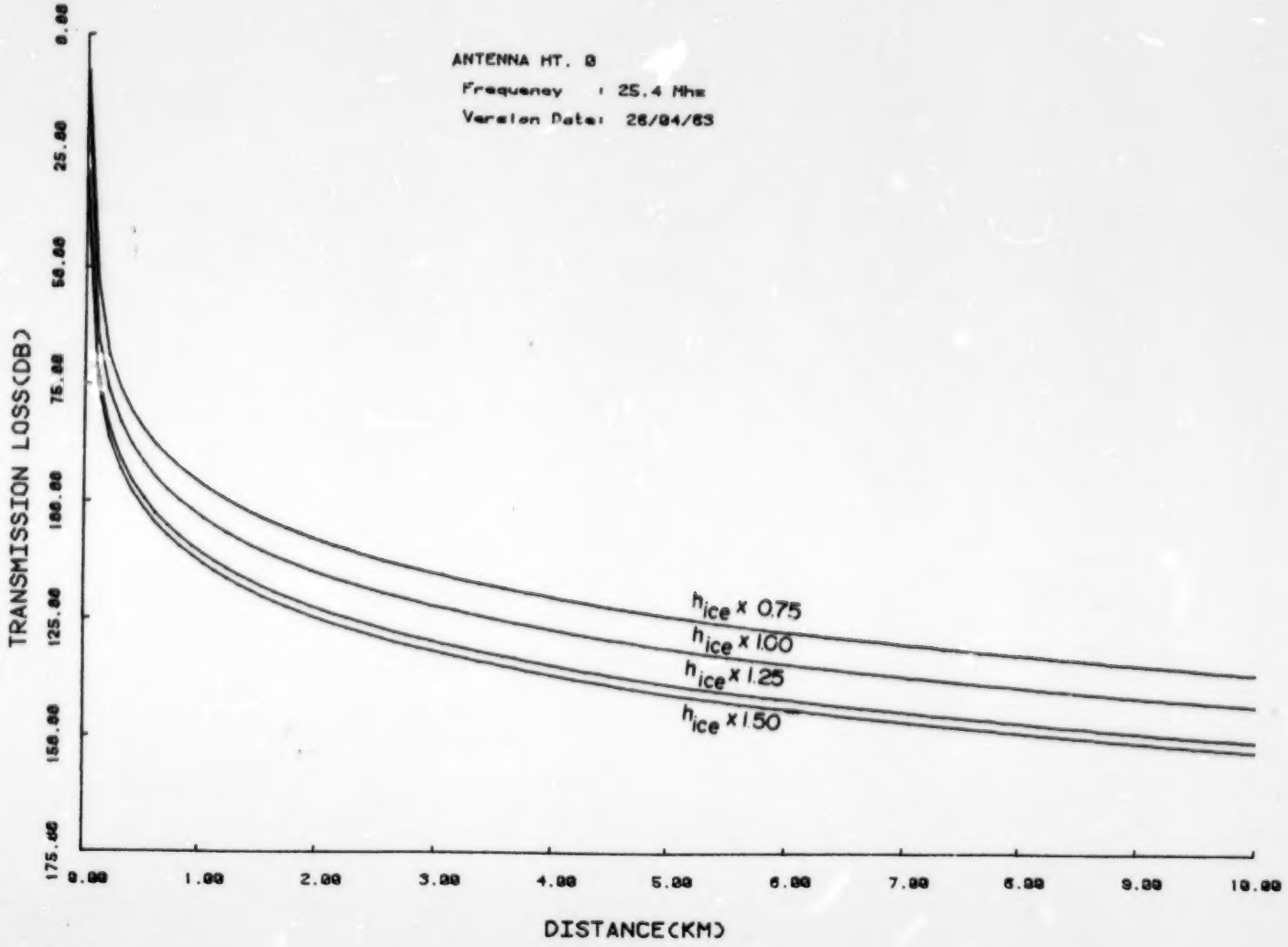

Figure 34 Variation of Calculated Loss with h_{ice}

APPENDIX A

Salinity Measurements of Ice Cores Taken Along the Line of Interest

Notes on Core Samples:

C1-C9: Pulled on March 3, 1982 these cores were cut, multed, and measured for salinity on March 10, 1982. During the interim the cores were stored outside (typical outside temperatures were -30° during the day).

C1-C31: All snow was scraped off sides of cores before measurement. If the snow layer left on top of the core was sufficiently deep, it was scraped off and measured separately. Otherwise it was left on and measured as part of the surface sample.

"Snow" salinities refer to the snow stuck to the top of the ice core. "Surface" salinities refer to the snow/ice interface.

The depth listed for each sample of ice core is the top of the ice sample. Most samples were approximately 2.5 cm's thick.

C-11, 13, 19, 23, 26: These samples were cut using a band saw and contained some contamination from the sawblade.

Comparing Salinities of C-CORE and A.R.E.

To compare the salinity measurements of C-CORE and A.R.E. certain core samples were measured by both organizations. Those samples were then taken back to Memorial University and measured by the Chemistry Department as well.

The independent measurements were in general agreement (see following table). The higher salinities generally contained the greatest discrepancies.

In the field C-CORE used a YSI salinity meter for the above measurements. It is our understanding that A.R.E. used an Endeco salinometer for its measurements. The Chemistry Dept. of Memorial University used titration as its method of analysis.

Raw Salinity Data - C-CORE

Distance / Date / Core Depth	0.0 km 03/03/82	0.0 km 03/03/82	0.0 km 03/03/82	0.0 km 03/03/82	0.0 km 03/03/82	0.0 km 03/03/82	0.0 km 03/03/82	0.0 km 03/03/82	0.67 km 12/03/82	0.67 km 12/03/82	1.35 km 12/03/82	1.35 km 12/03/82	1.35 km 06/03/82	1.45 km 06/03/82	1.55 km 06/03/82
Snow												19.9			
Surface	11.0	9.2	9.4	10.1	7.4	1.9	8.7	9.4	13.8	11.2	12.8	9.1	12.0	10.2	13.6
5 cm									6.2	6.0	6.0	5.7			
10 cm									6.0	6.1	5.5				
15 cm									6.0	8.1	6.6	6.6			
20 cm	4.3	5.3	5.7	5.3	3.6	5.2	5.4	5.8					5.1	5.3	4.8
25 cm									5.2	5.4	5.9	6.1			
30 cm															
35 cm										3.8	4.0	4.3			
40 cm	3.3	3.1	4.7	3.6	3.8	3.7	3.5	4.1					4.0	3.5	3.8
45 cm									4.7	4.0		3.7			
50 cm															
55 cm									4.6	5.1	4.9	4.5			
60 cm	4.7	3.4	4.0	3.7		1.0	4.6	4.0					4.7	4.9	4.3
65 cm									4.8	4.9	4.8	3.8			
70 cm															
75 cm									4.8	5.2	4.1				
80 cm	4.3			3.5											
85 cm										5.2					

Distance / Date / Core Depth	1.65 km 06/03/82	1.75 km 06/03/82	1.85 km 12/03/82	1.85 km 12/03/82	1.95 km 06/03/82	2.45 km 12/03/82	2.45 km 12/03/82	2.45 km 06/03/82	3.0 km 12/03/82	3.0 km 12/03/82	3.50 km 06/03/82	3.5 km 12/03/82	3.5 km 12/03/82	4.6 km 12/03/82	4.6 km 12/03/82
Snow			11.0	17.8		18.1	16.0					16.9	16.7	16.7	
Surface	14.1		11.3	16.2	13.0	18.8	13.2	3.1	7.7	14.9	14.0	12.7		15.1	9.1
5 cm			5.7	6.3		7.4			3.4	3.7		3.5	4.9	5.9	6.0
10 cm			4.3	5.2		3.1	4.1		3.2	3.3		5.6	4.8	6.0	6.6
15 cm			4.2	4.1		4.3	3.4		3.2	4.8		5.7	4.9	6.7	5.2
20 cm	5.6	5.0			5.7			5.7			5.2				
25 cm			4.5	4.9		4.8	5.0		4.9			5.7	5.2	5.6	4.2
30 cm															
35 cm			4.7	4.9		4.2	3.8		4.0	3.9		4.8	4.6	4.2	4.0
40 cm	4.6	4.3			5.0			4.7			3.7				
45 cm			5.1	5.5		4.3	3.9		4.2	4.9		3.3	4.2	4.3	4.8
50 cm															
55 cm			5.8	5.3		5.2	3.7		3.2	4.8		4.8	4.2	5.0	
60 cm	4.9	4.5			5.2			4.2			4.9				
65 cm				4.3		5.1	4.4		4.3	5.0		4.3	4.8	4.1	
70 cm															
75 cm				4.9	4.9		4.3		4.9	6.4		4.7	4.9	4.6	4.8
80 cm								4.8			5.0				
85 cm							4.9		4.3						4.4

Salinity Measurements (A.R.E.):
March 10/82
Location: 6.9 km from transmit antenna
Snow Depth: 9.0 cm

Depth (cm)	Salinity (°/oo)	Depth (cm)	Salinity (°/oo)	Depth (cm)	Salinity (°/oo)
0	0.0	37.5	5.7	75.0	4.4
2.5	15.3	40.0	6.5	77.5	3.8
5.0	22.8	42.5	6.1	80.0	3.7
7.5	15.4	45.0	5.9	82.5	5.1
10.0	6.4	47.5	5.7	85.0	6.1
12.5	4.8	50.0	5.4	87.5	5.8
15.0	4.5	52.5	5.5	90.0	5.3
17.5	4.9	55.0	5.4	92.5	5.9
20.0	4.1	57.5	4.7	95.0	5.7
22.5	4.7	60.0	5.4	97.5	5.6
25.0	5.7	62.5	5.3	100.0	5.6
27.5	5.9	65.0	5.7	102.5	5.5
30.0	6.1	67.5	5.9	105.0	6.2
32.5	6.6	70.0	6.4	107.5	8.0
35.0	6.1	72.5	6.0		

Salinity Measurements (A.R.E.)
March 10/82
Location: 15.3 km from transmit antenna
Snow Depth: 8.7 cm

Depth (cm)	Salinity (°/oo)	Depth (cm)	Salinity (°/oo)	Depth (cm)	Salinity (°/oo)
0	9.9	37.5	5.8	75.0	6.1
2.5	6.7	40.0	5.9	77.5	6.6
5.0	5.6	42.5	7.1	80.0	5.9
7.5	6.0	45.0	6.9	82.5	5.5
10.0	5.9	47.5	6.7	85.0	6.1
12.5	5.2	50.0	7.3	87.5	6.1
15.0	6.0	52.5	7.9	90.0	5.5
17.5	6.1	55.0	7.8	92.5	4.9
20.0	5.8	57.5	8.1	95.0	5.1
22.5	5.0	60.0	7.3	97.5	5.1
25.0	5.0	62.5	7.3	100.0	6.1
27.5	4.9	65.0	7.1	102.5	6.3
30.0	4.5	67.5	6.9	105.0	6.3
32.5	5.6	70.0	6.8	107.5	9.5
35.0	5.2	72.5	5.9		

Comparison of Salinity Measurements

SAMPLE #	WAF #	location (distance from tent)	Core Date	Measured Salinity °/oo Chemistry Dept. (±0.2 °/oo)	Salinity via Salinometer	ARE Salinity
C-28 4-SM	1094	3.5 km	Mar. 12/82	18.2	16.9	19.0
C-28 4-S	1095	3.5 km	Mar. 12/82	14.4	12.7	14.4
C-28 4-5	1096	3.5 km	Mar. 12/82	3.7	3.5	5.8
C-28 4-10	1097	3.5 km	Mar. 12/82	6.0	5.6	6.2
C-28 4-15	1098	3.5 km	Mar. 12/82	5.9	5.7	6.1
C-28 4-25	1099	3.5 km	Mar. 12/82	6.1	5.7	6.4
C-28 4-35	1100	3.5 km	Mar. 12/82	4.8	4.8	5.4
C-28 4-45	1101	3.5 km	Mar. 12/82	4.8	3.3	4.0
C-28 4-55	1102	3.5 km	Mar. 12/82	3.9	4.8	5.5
C-28 4-65	1103	3.5 km	Mar. 12/82	5.0	4.3	5.0
C-28 4-75	1104	2.45 km	Mar. 12/82	4.5	4.7	4.8
C-23 1.5-S	1105	0.67 km	Mar. 12/82	4.9	18.8	
C-10 1.5-S	1106	1.35 km	Mar. 12/82	19.0	13.8	
C-13 2-S	1107	1.35 km	Mar. 12/82	14.7	9.1	
C-14 2-S	1108	1.85 km	Mar. 12/82	9.0	12.8	
C-20 2.5-S	1109	0.67 km	Mar. 12/82	14.7	11.3	
C-11 3.S	1110	3.0 km	Mar. 12/82	12.0	11.2	
C-25 3.5-S	1111	4.6 km	Mar. 12/82	11.4	7.7	
C-305-S	1112	4.6 km	Mar. 12/82	8.0	15.1	17.0
C-3/5-S	1113	0 km	Mar. 12/82	16.2	9.1	
C-4 4-S grid	1114	0 km	Mar. 12/82	9.5	9.4	
C-5 5/S grid	1115	0 km	Mar. 12/82	10.7	7.4	
C-9 9-S grid	1116	0 km	Mar. 3/82	8.4	9.4	
C-2/16-S grid	1117	2.45 km	Mar. 3/82	10.1	13.0	
C-231.5-SN	1118	1.35 km	Mar. 3/82	16.2	18.1	
C-132-SN	1119	1.85 km	Mar. 3/82	18.6	19.9	
C-192.5-SN	1120	1.85 km	Mar. 12/82	20.2	17.8	
C-202.5-SN	1121	0.67 km	Mar. 12/82	18.3	11.0	
C-11 3-SN	1122	2.45 km	Mar. 12/82	11.4	?	
C-24 3-SN	1123	3.5 km	Mar. 12/82	21.2	16.0	
C-29 4-SN	1124	4.6 km	Mar. 12/82	17.8	16.7	
C-305 SN	1125		Mar. 12/82	17.1	16.7	19.6
				18.2		

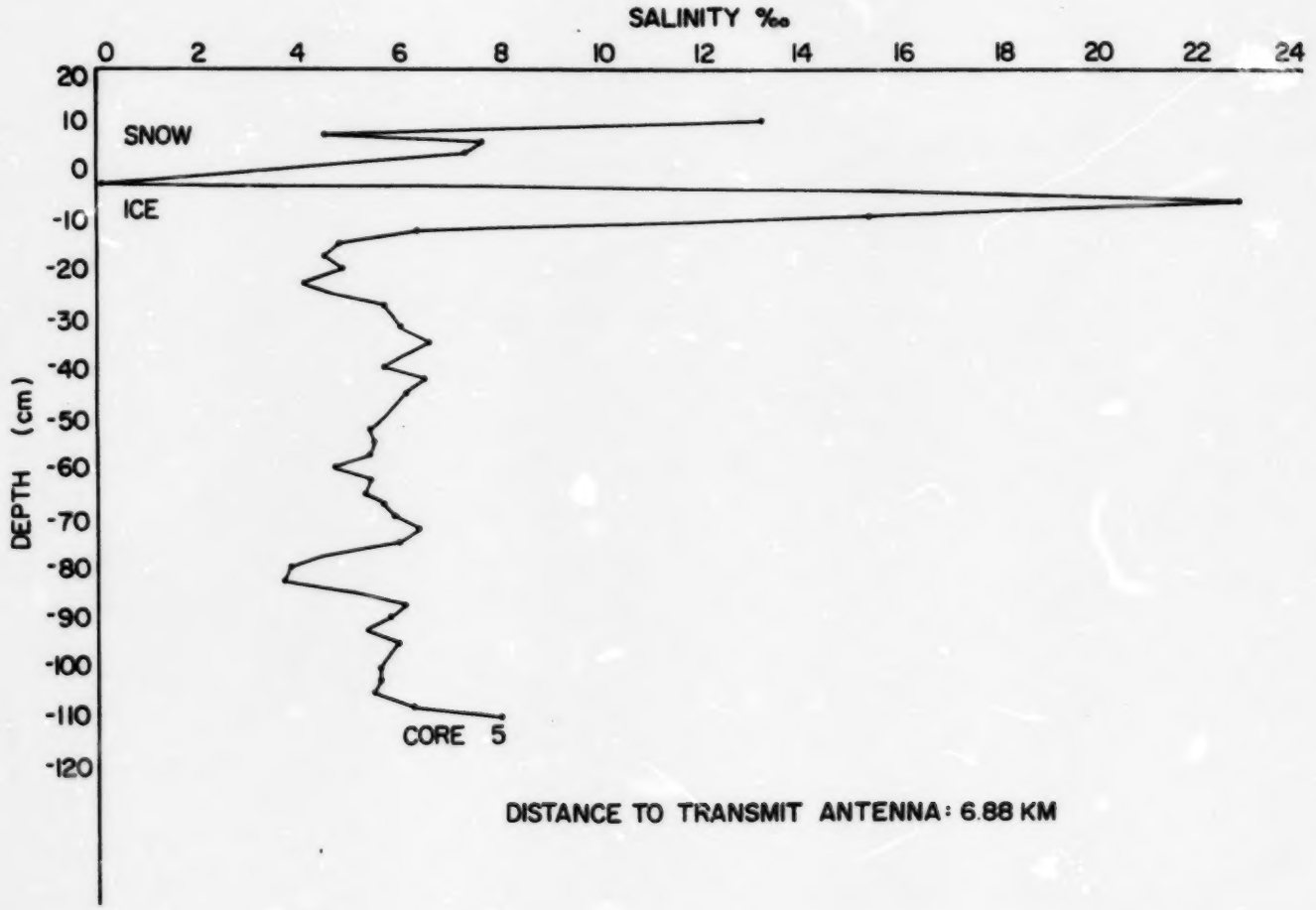

Figure A-1 Salinity Profile Core C-32
(ARE Data)

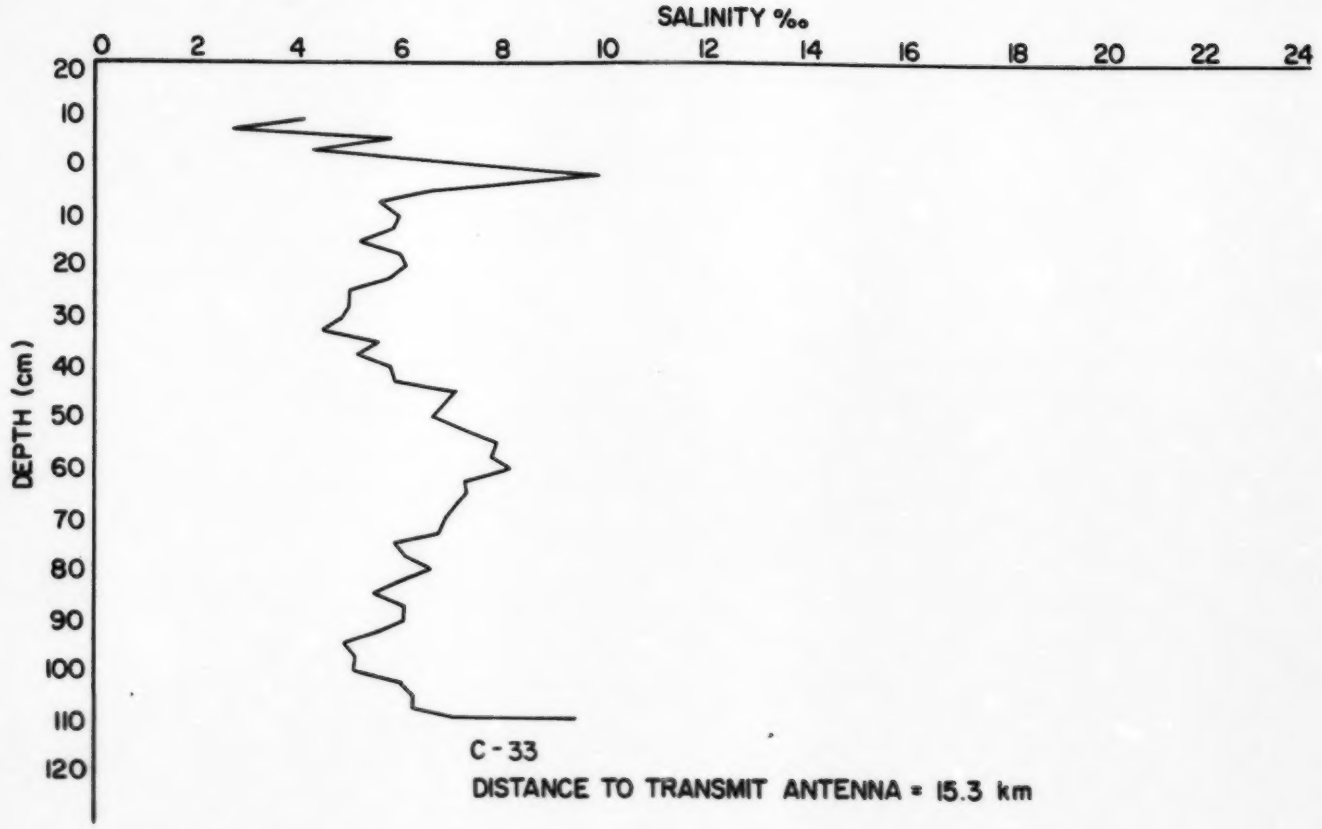

Figure A-2 Salinity Profile Core C-33
(ARE Data)

APPENDIX B

Temperature Data

Thermocouple Probes (A.R.E.): Readings were taken on March 10, 1982 from the two thermocouples (at 6.9 and 1.53 km from the transmit antenna.) by A.R.E. personnel. Each 2 metre probe contained 21 thermocouples using 10 cm spacings. The top thermocouple was level with the ice surface. Thermistor Probes (C-CORE): Hourly readings were taken prior to and during March 10, 1982 of the two thermistor probes located very close to the transmit antenna. The thermister depths (relative to ice surface) are given below;

STRING #1	STRING #2
+48 cm	-62 cm
+38 cm	-82 cm
+28 cm	-92 cm
+23 cm	-97 cm
+18 cm	-102 cm
+ 8 cm	-104 cm
- 2 cm	-106 cm
-12 cm	-108 cm
-32 cm	-110 cm
-52 cm	-112 cm
-72 cm	-114 cm
	-119 cm

Thermistor Data Extract (C-CORE) Location: Transmit Antenna (0 km)

DEPTH IN CM

DATE	TIME	+48	+38	+28	+23	+18	+8	-2	-12	-32	-52	-72
1003	957	-28.6	-28.9	-28.5	-28.4	-27.7	-26.2	-21.3	-19.3	-13.4	-10.0	-6.0
1003	1056	-29.4	-29.6	-29.1	-29.1	-28.7	-28.4	-21.8	-18.9	-13.4	-10.1	-6.6
1003	1155	-29.9	-29.2	-28.7	-27.9	-27.0	-26.1	-21.4	-19.0	-13.2	-10.3	-6.3
1003	1254	-27.6	-27.4	-27.1	-27.1	-27.1	-27.9	-21.6	-18.8	-12.7	-10.4	-6.5
1003	1353	-31.3	-31.2	-31.2	-32.0	-31.3	-31.7	-21.8	-18.3	-12.6	- 9.8	-5.9
1003	1452	-34.3	-34.5	-34.5	-34.5	-34.4	-33.8	-22.4	-18.7	-12.5	- 9.7	-6.2
1003	1551	-35.0	-34.8	-34.5	-34.8	-34.8	-34.4	-22.7	-18.5	-12.3	- 9.7	-5.8

DEPTH IN CM

DATE	TIME	62	82	92	97	102	104	106	108	110	112	114	119
1003	957	-10.1	-5.0	-3.4	-2.2	-1.7	-1.5	-1.5	-1.4	-1.6	-1.6	-1.6	-1.5
1003	1056	-10.1	-5.0	-3.4	-2.2	-1.7	-1.5	-1.5	-1.4	-1.5	-1.6	-1.6	-1.5
1003	1155	-10.0	-5.0	-3.3	-2.2	-1.6	-1.4	-1.4	-1.4	-1.5	-1.5	-1.5	-1.6
1003	1254	-10.0	-5.1	-3.3	-2.3	-1.7	-1.6	-1.5	-1.5	-1.6	-1.6	-1.6	-1.6
1003	1353	-10.1	-5.1	-3.3	-2.4	-1.8	-1.5	-1.4	-1.4	-1.6	-1.7	-1.7	-1.6
1003	1452	-10.1	-5.1	-3.4	-2.4	-1.7	-1.6	-1.5	-1.5	-1.6	-1.7	-1.7	-1.6
1003	1551	-10.1	-5.2	-3.4	-2.3	-1.8	-1.7	-1.5	-1.5	-1.6	-1.7	-1.7	-1.6

Thermocouple Data (A.R.E.):

Location: 6.9 km from transmit antenna
Date: March 10, 1982
Time: 15:20 E.S.T.

Depth (cm)	Temperature ^{o}C
0	-15.71
10	-13.93
20	-12.50
30	-10.90
40	- 9.25
50	- 6.41
60	- 6.01
70	- 4.62
80	- 3.23
90	- 1.87
100	- 1.87
110	- 1.87
120	- 1.87
130	- 1.87
140	- 1.87
150	- 1.87
160	- 1.87
170	- 1.87
180	- 1.87
190	- 1.87
200	- 1.87

Location: 15.3 km from transmit antenna
Date: March 10, 1982
Time: 14:16 E.S.T.

Depth (cm)	Temperature ^{o}C
0	-22.77
10	-20.60
20	-18.36
30	-16.14
40	-13.90
50	-11.97
60	- 9.99
70	- 8.08
80	- 6.38
90	- 4.12
100	- 2.39
110	- 2.39
120	- 2.39
130	- 2.39
140	- 2.39
150	- 2.39
160	- 2.39
170	- 2.39
180	- 2.39
190	- 2.39
200	- 2.39

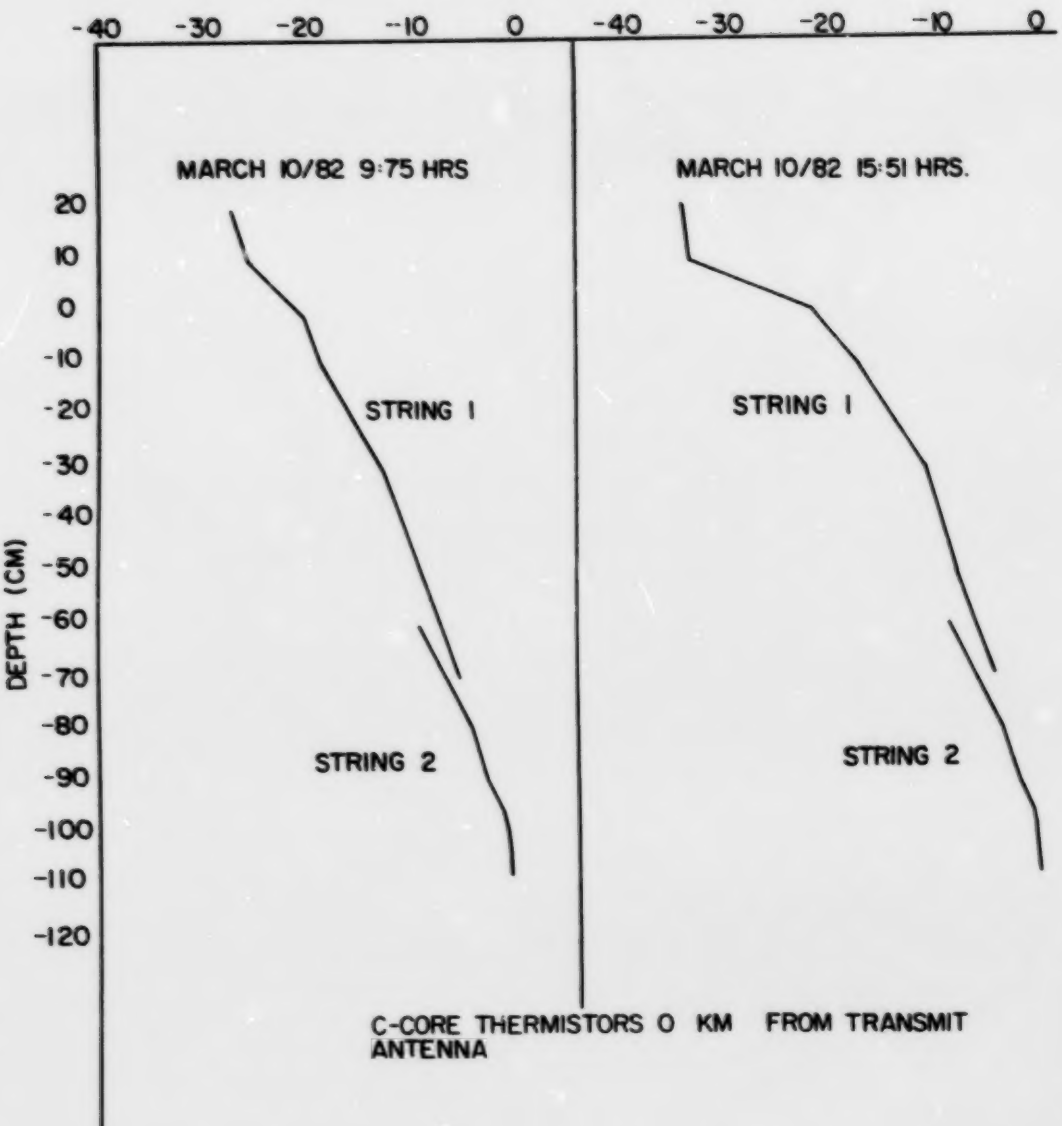
-40 -30 -20 -10 0 -40 -30 -20 -10 0
MARCH 10/82 9:75 HRS
MARCH 10/82 15:51 HRS.
20
10
0
-10
-20
-30
-40
-50
-60
-70
-80
-90
-100
-110
-120
DEPTH (CM)
STRING 1
STRING 2
STRING 1
STRING 2
C-CORE THERMISTORS 0 KM FROM TRANSMIT ANTENNA

APPENDIX C

Calculation of Receiver Gains

During the course of the experiment a number of different gains were used on the receiver. It is therefore necessary to know the absolute receiver gain as a function of the front panel gain setting on the receiver.

In the summer of /82 the receiver was sent down to Erbtech Engineering in the U.S.A. for modifications. Prior to the modifications the original receiver gains as used in Pond Inlet were measured.

Method of Measurement: Lee Erb (Erbtech Engineering) described the method as follows:

The input to the receiver was adjusted to provide a fixed receiver output for each front panael gain setting. With the receiver operating at 25.400 MHz the input, 25.401 MHz, was adjusted to produce 3 volts r.m.s. @ Khz) on one of the "I" (in phase) or "Q" (quadrature) channels, with the unused channel nulled. (The output was found to be independent of the channel used.)

Calculations: With the following nomenclature,

V_{in} = r.m.s. input voltage (volts)
P_{in} = input power (watts)
V_{out} = 3 Volts r.m.s.
Gain = $20 \text{ Log } \left[\frac{V_{out}}{V_{in}}\right]$ (dB)

and Z_{in} = 50 ohms (receiver input impedance) then for a given input of x dBm,

$$P_{in} = 10^{(\frac{x}{10}-3)} \text{ watts}$$

(from XdBm = 10 log $\left[\frac{P_{in}}{10^{-3} \text{ Watts}}\right]$

Since $P_{in} = \frac{V_{in}^2}{50 \text{ ohms}}$ therefore it follows that,

$$V_{in}^2 = (50 \text{ ohms})\ 10^{(\frac{x}{10}-3)} \text{ watts}$$

or $V_{in} = 5^{1/2} \times 10^{(\frac{x}{20}-1)}$ watts

yielding, Gain (dB) = $20 \text{ Log } \left[\frac{3}{5^{1/2} \cdot 10^{(\frac{x}{20}-1)}}\right]$

The following results were obtained;

Receiver front panel setting	Required Input (25.401 MHz) to produce 3 Vr.m.s. output	Gain (dB)
090	-25.1 dBm ± .5 dBm	47.65
095	-29.1 dBm	51.65
100	-33.0 dBm	55.55
110	-40.2 dBm	62.75
140	-54.9 dBm	77.45
160	-58.25 dBm	80.80
184	-68.9 dBm	91.45
190	-73.0 dBm	95.55
200	-78.5 dBm	101.05
206	-82.1 dBm	104.65
215	-86.0 dBm	108.55
220	-87.6 dBm	110.15
223	-88.6 dBm	111.15

APPENDIX D

Intermediate Results from Integrated Digital I & Q Wave Forms

Range (km)	Δt (sec)	Σ I	Σ Q	20 Log $\sqrt{(\Sigma I)^2 + (\Sigma Q)^2}$ (dB)
0.64	33.75	-13.99	-76.52	37.82
0.67	33.75	- 4.73	-50.48	34.10
1.32	33.75	4.818	-34.32	30.80
1.87	33.75	34.59	-11.87	31.26
1.90	33.75	54.00	10.79	34.82
2.45	33.75	- 8.34	36.41	31.45
2.97	33.75	- 3.20	-28.32	29.10
3.00	33.75	- 0.53	-26.09	28.33
3.51	33.75	10.39	- 6.62	21.81
3.54	33.75	15.11	2.31	23.69
5.73	35.00	7.83	- 8.77	21.41
6.88	33.75	5.90	3.96	17.03
(m)				
210.6	32.50	-20.68	- 4.64	26.52
180.0	32.50	- 2.01	-21.76	26.79
150.5	32.50	- 4.19	17.23	24.98
120.4	32.50	30.27	- 0.49	29.62
89.6	32.50	37.89	1.94	31.58
59.7	32.50	5.66	-52.81	34.50

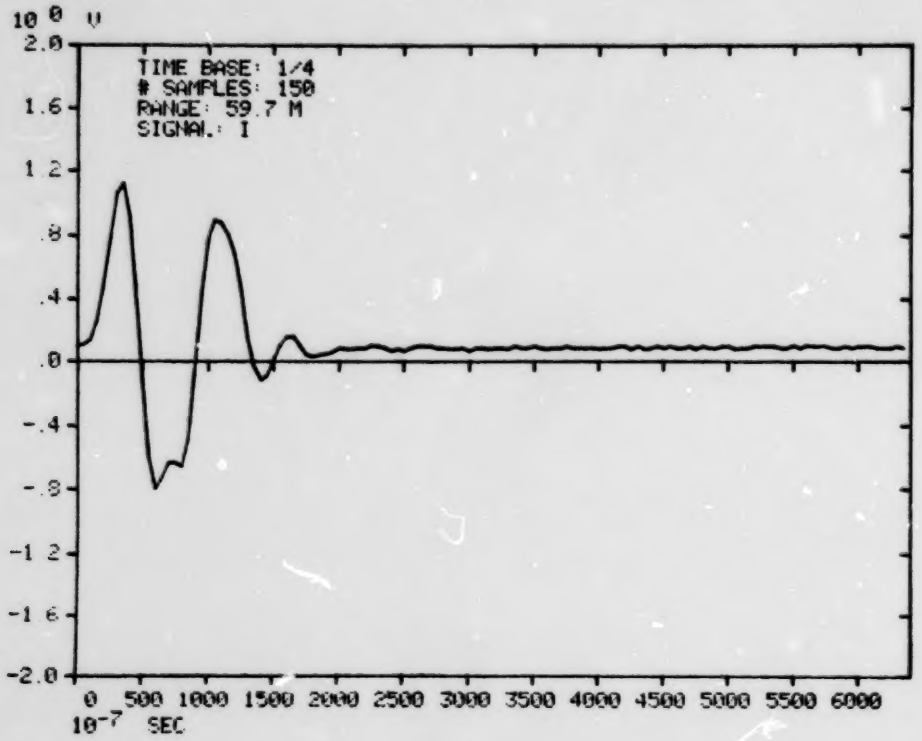
10 0 V
2.0
1.6
1 2
.8
.4
.0
-.4
-.8
-1 2
-1 6
-2.0
TIME BASE: 1/4
SAMPLES: 150
RANGE: 59.7 M
SIGNAL: I
0 500 1000 1500 2000 2500 3000 3500 4000 4500 5000 5500 6000
10-7 SEC

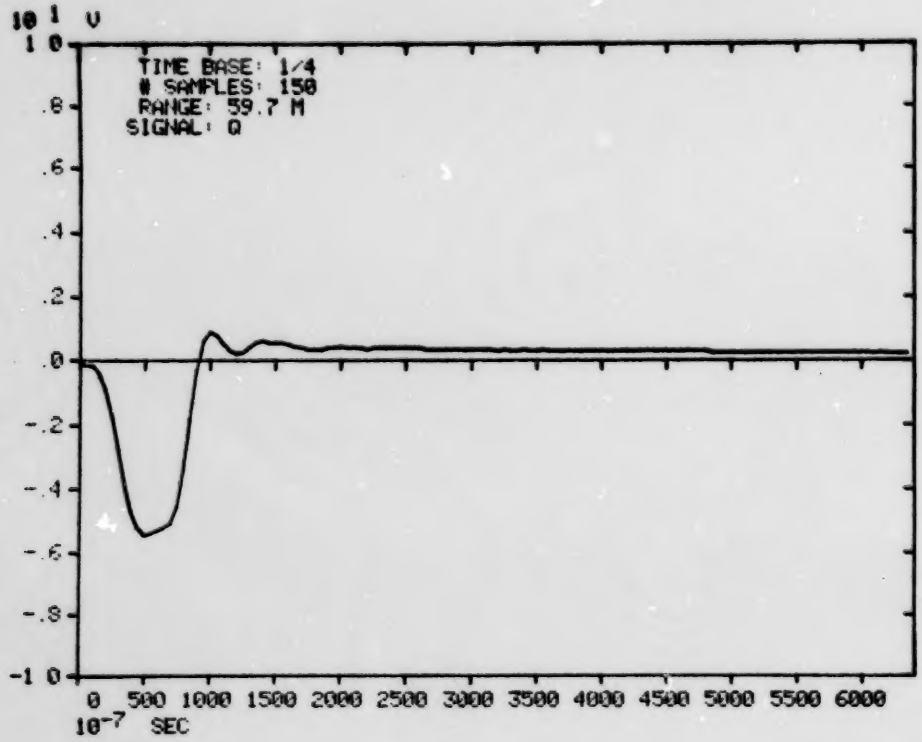
10 1 V
1 0
.8
.6
.4
.2
.0
-.2
-.4
-.6
-.8
-1 0
TIME BASE: 1/4
SAMPLES: 150
RANGE: 59.7 M
SIGNAL: Q
0 500 1000 1500 2000 2500 3000 3500 4000 4500 5000 5500 6000
10-7 SEC

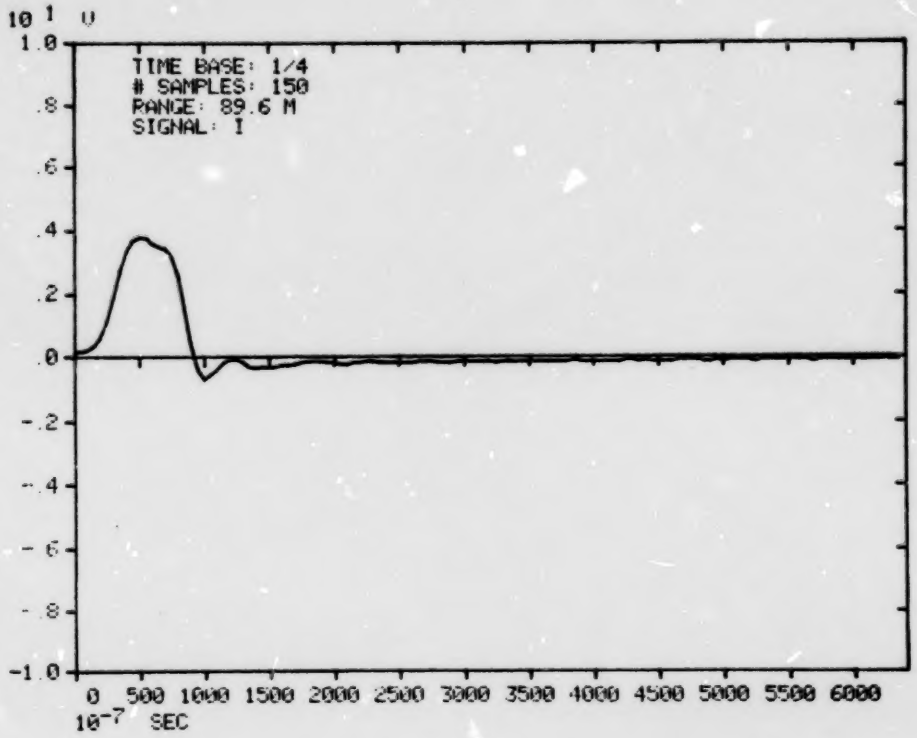
10 1 V
TIME BASE: 1/4
SAMPLES: 150
RANGE: 89.6 M
SIGNAL: I
1.0
.8
.6
.4
.2
.0
-.2
-.4
-.6
-.8
-1.0
0 500 1000 1500 2000 2500 3000 3500 4000 4500 5000 5500 6000
10-7 SEC

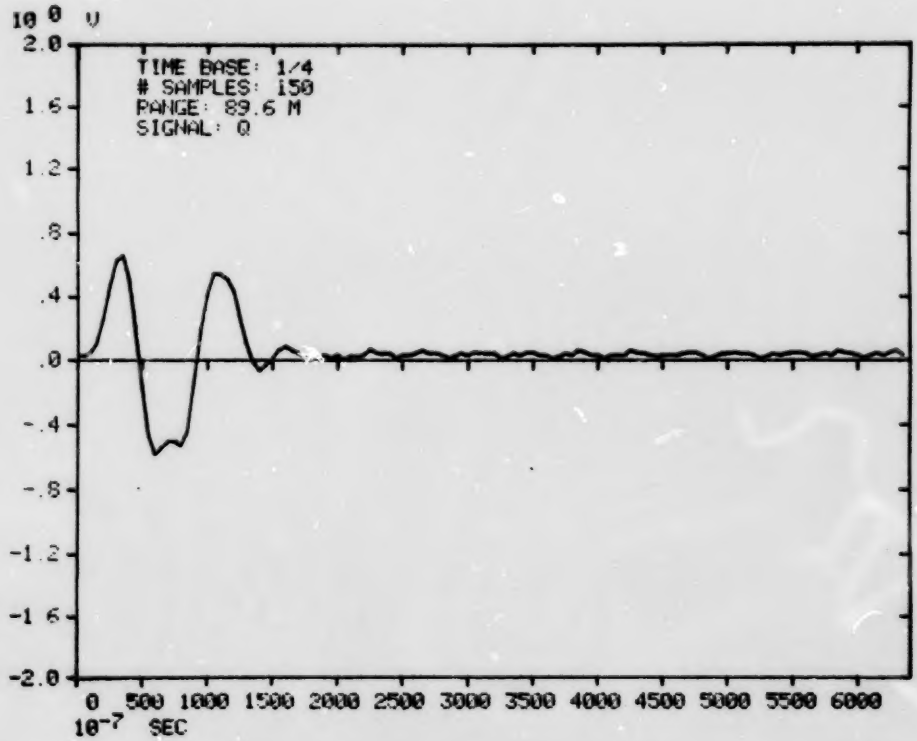
10 0 V
TIME BASE: 1/4
SAMPLES: 150
RANGE: 89.6 M
SIGNAL: Q
2.0
1.6
1.2
.8
.4
.0
-.4
-.8
-1.2
-1.6
-2.0
0 500 1000 1500 2000 2500 3000 3500 4000 4500 5000 5500 6000
10-7 SEC

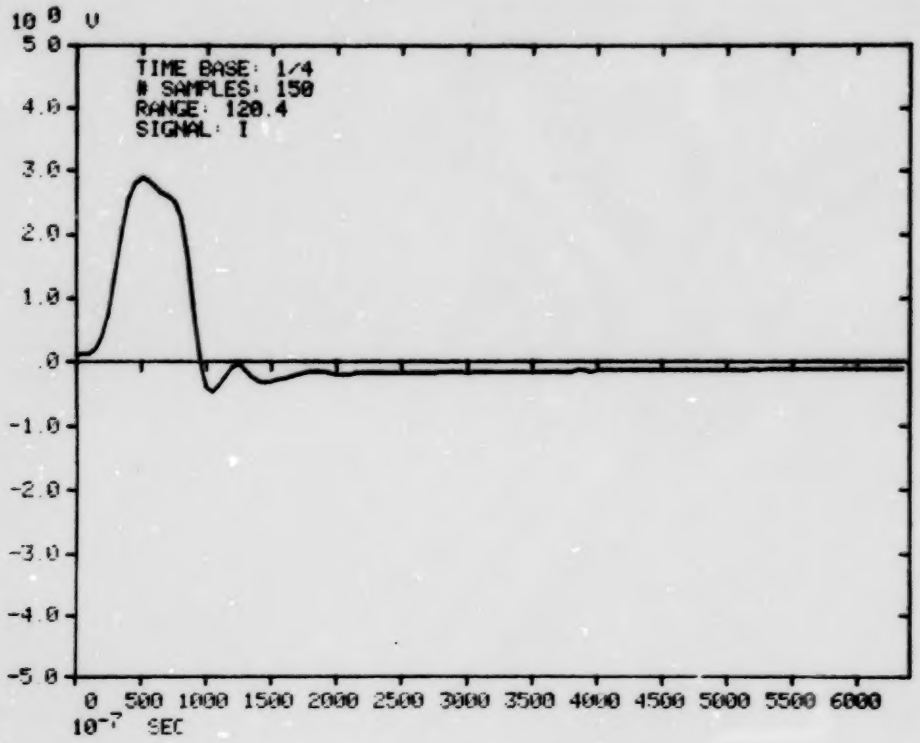
10 0 V
5.0
4.0
3.0
2.0
1.0
.0
-1.0
-2.0
-3.0
-4.0
-5.0
TIME BASE: 1/4
SAMPLES: 150
RANGE: 120.4
SIGNAL: I
0 500 1000 1500 2000 2500 3000 3500 4000 4500 5000 5500 6000
10-7 SEC

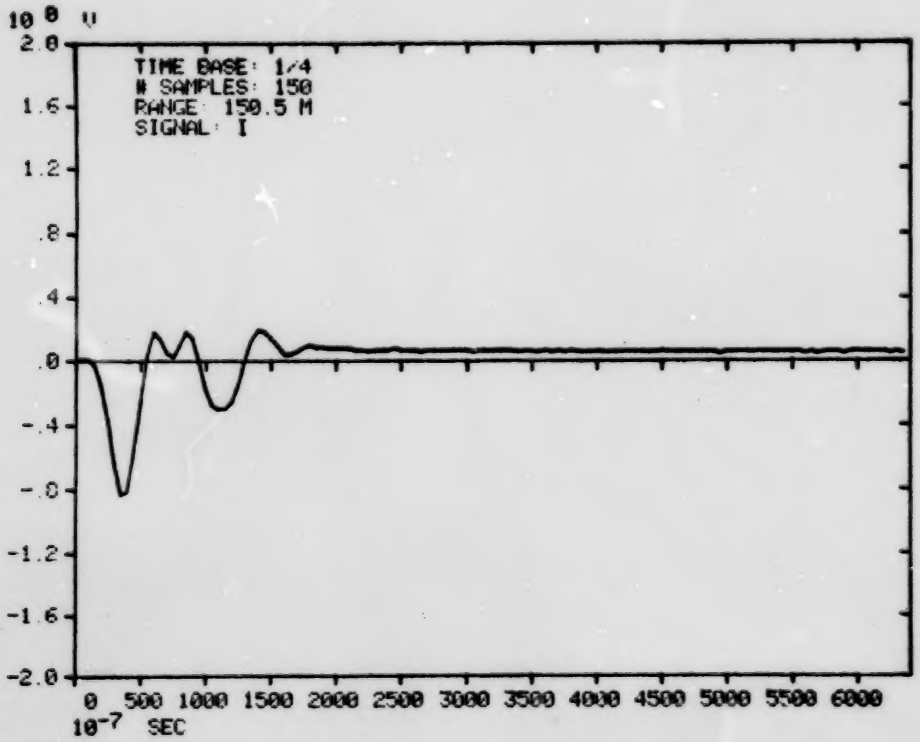
10 0 V
2.0
1.6
1.2
.8
.4
.0
-.4
-.8
-1.2
-1.6
-2.0
TIME BASE: 1/4
SAMPLES: 150
RANGE: 150.5 M
SIGNAL: I
0 500 1000 1500 2000 2500 3000 3500 4000 4500 5000 5500 6000
10-7 SEC

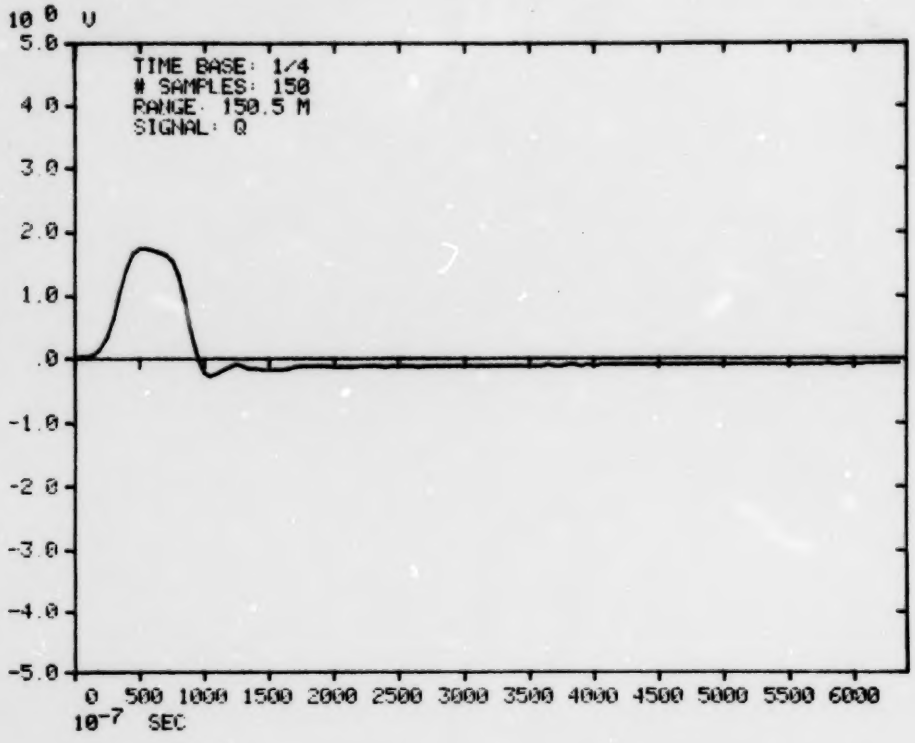
10 0 V
5.0
4.0
3.0
2.0
1.0
.0
-1.0
-2.0
-3.0
-4.0
-5.0
TIME BASE: 1/4
SAMPLES: 150
RANGE 150.5 M
SIGNAL: Q
0 500 1000 1500 2000 2500 3000 3500 4000 4500 5000 5500 6000
10-7 SEC

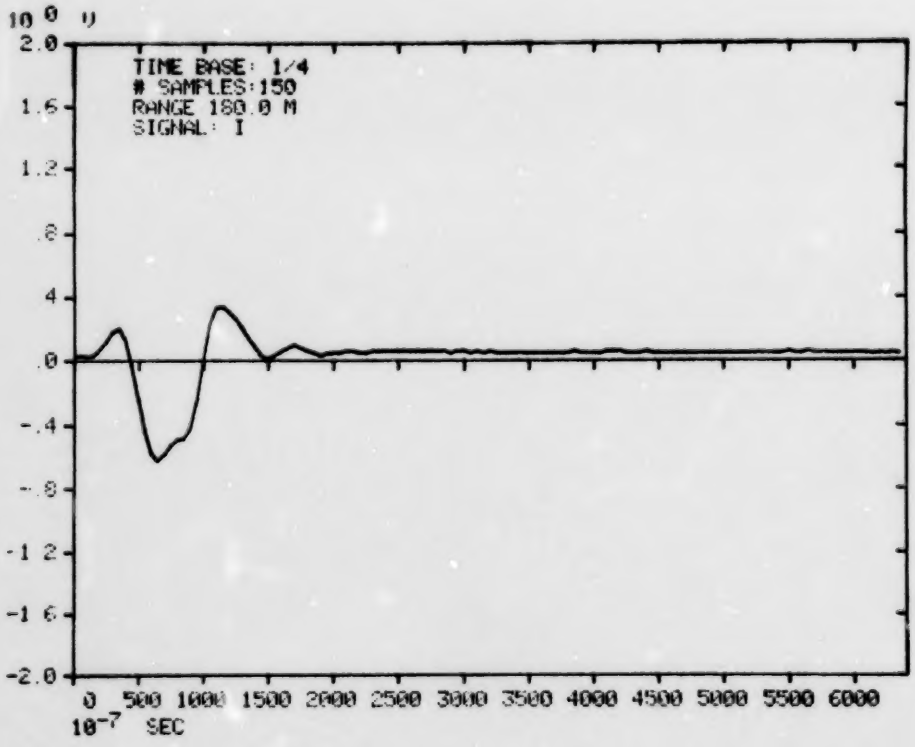
10 0 V
2.0
1.6
1.2
.8
4
.0
-.4
-.8
-1.2
-1.6
-2.0
TIME BASE: 1/4
SAMPLES:150
RANGE 180.0 M
SIGNAL: I
0 500 1000 1500 2000 2500 3000 3500 4000 4500 5000 5500 6000
10-7 SEC

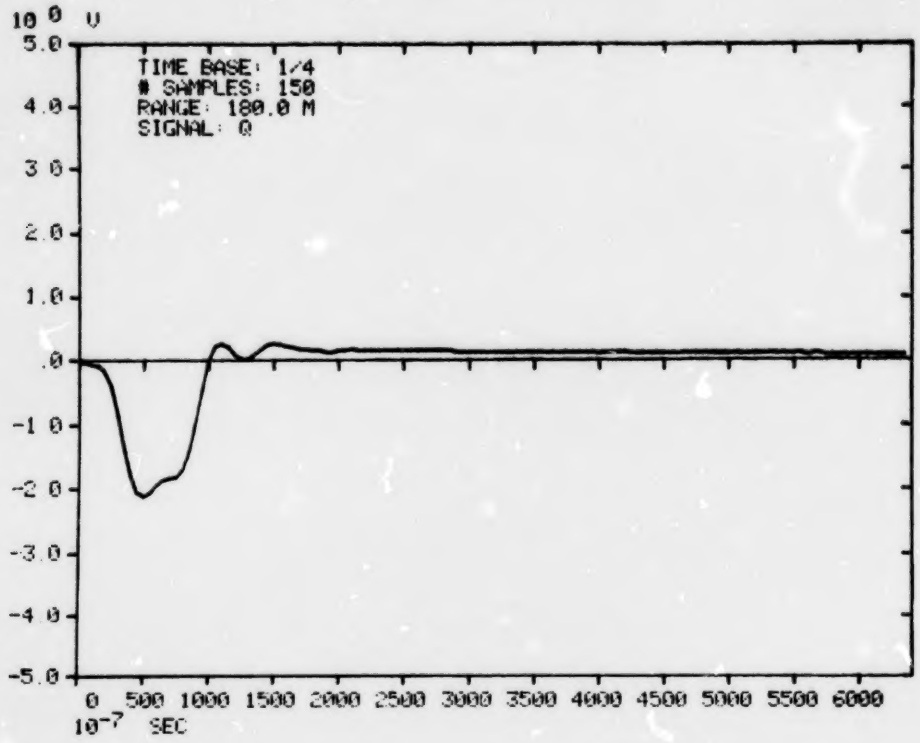
10 0 V
5.0
4.0
3.0
2.0
1.0
.0
-1.0
-2.0
-3.0
-4.0
-5.0
TIME BASE: 1/4
SAMPLES: 150
RANGE: 180.0 M
SIGNAL: Q
0 500 1000 1500 2000 2500 3000 3500 4000 4500 5000 5500 6000
10-7 SEC

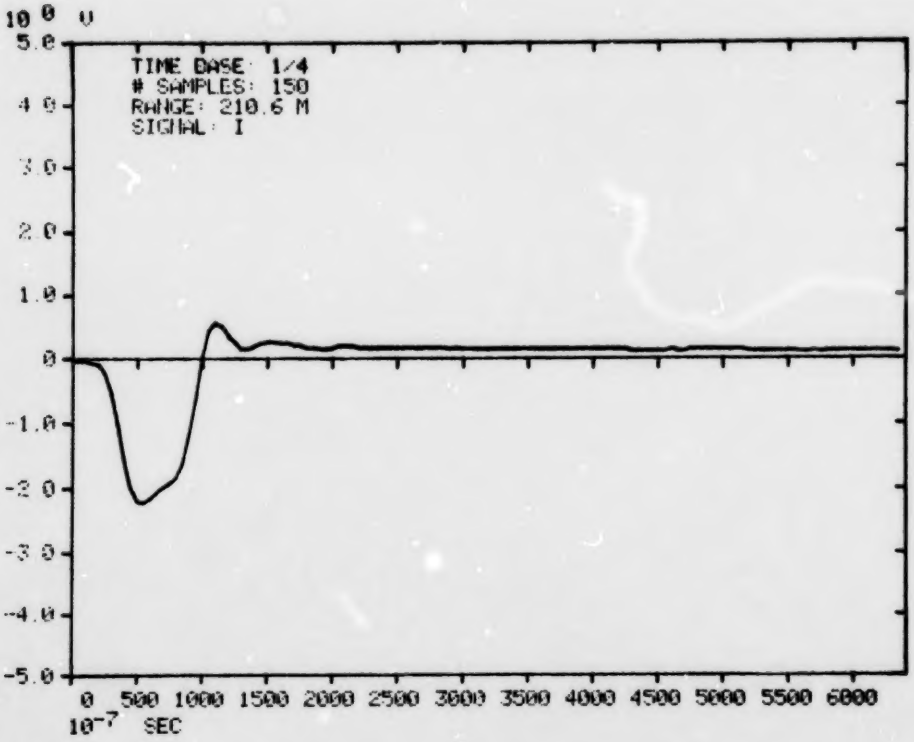
10 0 V
5.0
4.0
3.0
2.0
1.0
0
-1.0
-2.0
-3.0
-4.0
-5.0
TIME BASE: 1/4
SAMPLES: 150
RANGE: 210.6 M
SIGNAL: I
0 500 1000 1500 2000 2500 3000 3500 4000 4500 5000 5500 6000
10-7 SEC

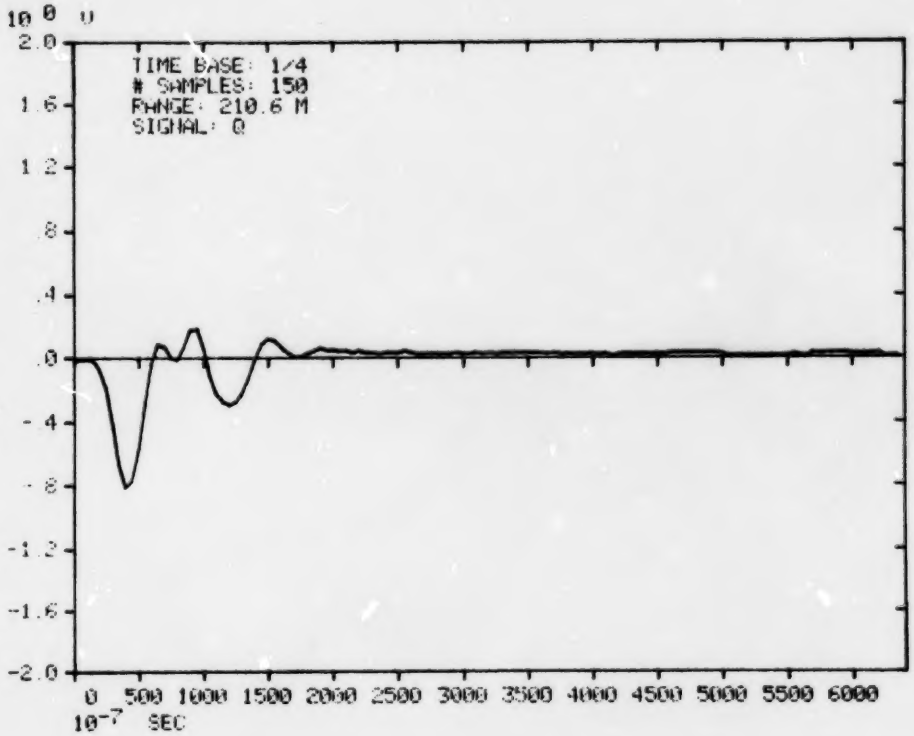
10 0 V
2.0
1.6
1.2
.8
.4
.0
-.4
-.8
-1.2
-1.6
-2.0
TIME BASE: 1/4
SAMPLES: 150
RANGE: 210.6 M
SIGNAL: Q
0 500 1000 1500 2000 2500 3000 3500 4000 4500 5000 5500 6000
10-7 SEC

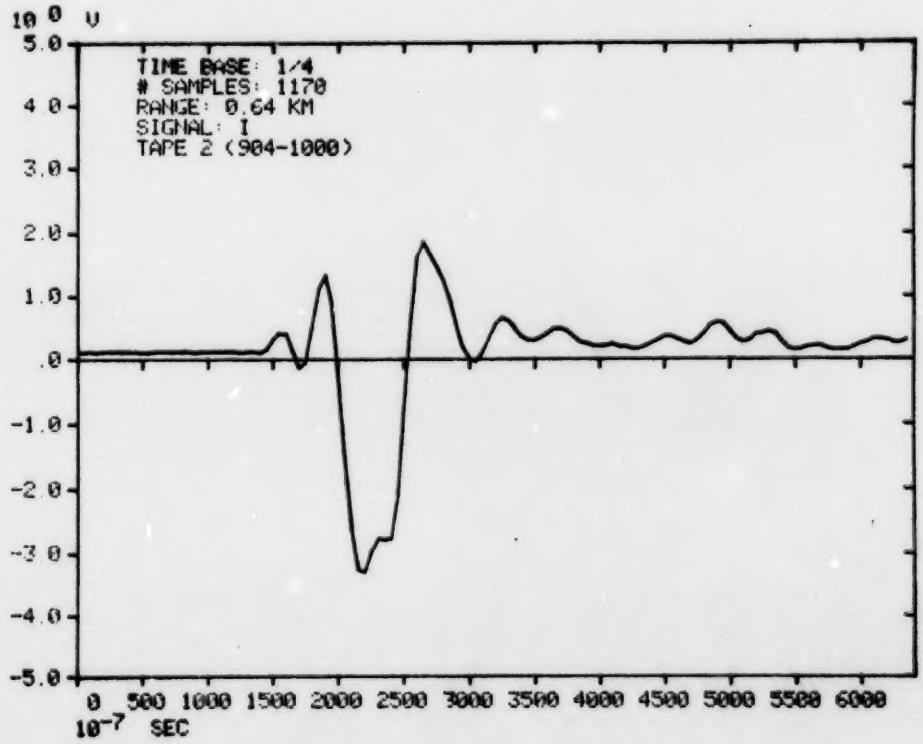
10 0 V
5.0
4.0
3.0
2.0
1.0
.0
-1.0
-2.0
-3.0
-4.0
-5.0
TIME BASE: 1/4
SAMPLES: 1170
RANGE: 0.64 KM
SIGNAL: I
TAPE 2 (904-1000)
0 500 1000 1500 2000 2500 3000 3500 4000 4500 5000 5500 6000
10-7 SEC

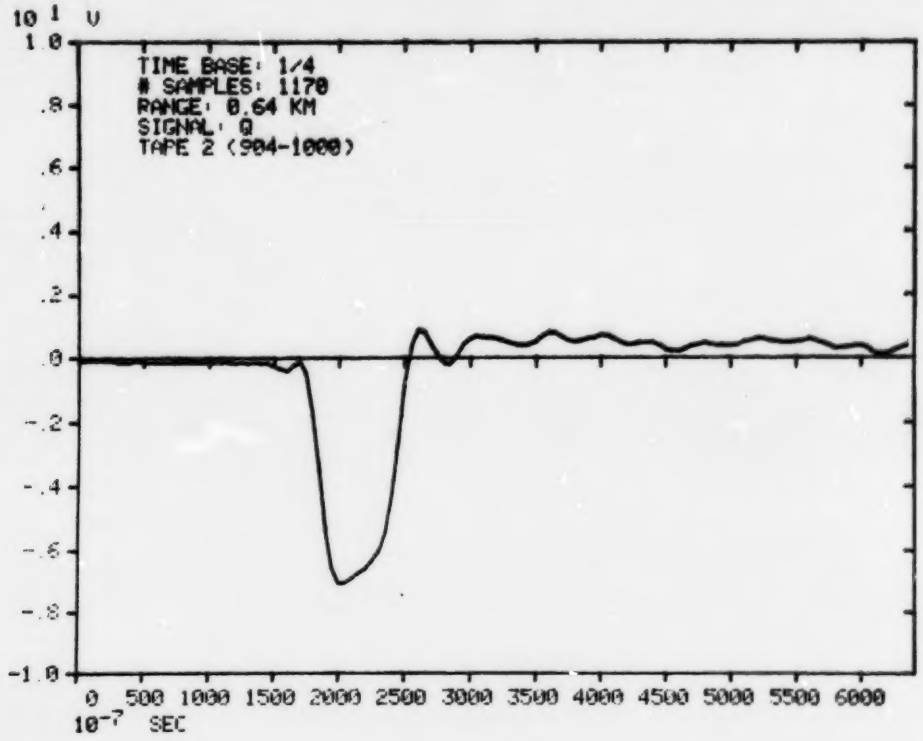
10 1 V
1 0
.8
.6
.4
.2
.0
-.2
-.4
-.6
-.8
-1.0
TIME BASE: 1/4
SAMPLES: 1170
RANGE: 0.64 KM
SIGNAL: Q
TAPE 2 (904-1000)
0 500 1000 1500 2000 2500 3000 3500 4000 4500 5000 5500 6000
10-7 SEC

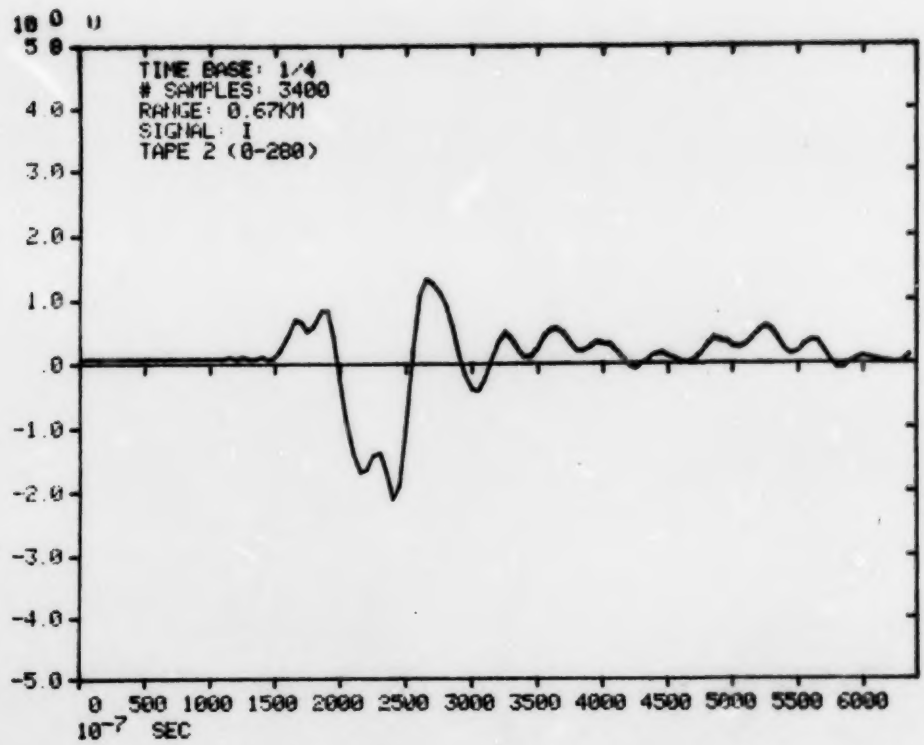
10 0 V
5 0
4 0
3.0
2.0
1.0
.0
-1.0
-2.0
-3.0
-4.0
-5.0
TIME BASE: 1/4
SAMPLES: 3400
RANGE: 0.67KM
SIGNAL: I
TAPE 2 (0-280)
0 500 1000 1500 2000 2500 3000 3500 4000 4500 5000 5500 6000
10-7 SEC

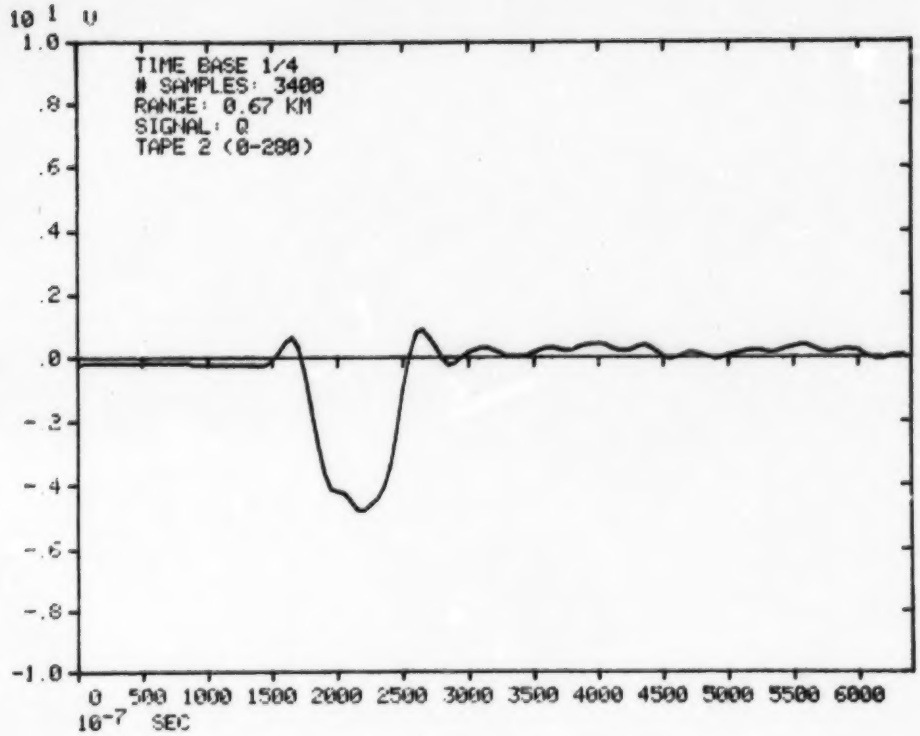
10 1 U
TIME BASE 1/4
SAMPLES: 3400
RANGE: 0.67 KM
SIGNAL: Q
TAPE 2 (0-200)
1.0
.8
.6
.4
.2
.0
-.2
-.4
-.6
-.8
-1.0
0 500 1000 1500 2000 2500 3000 3500 4000 4500 5000 5500 6000
10-7 SEC

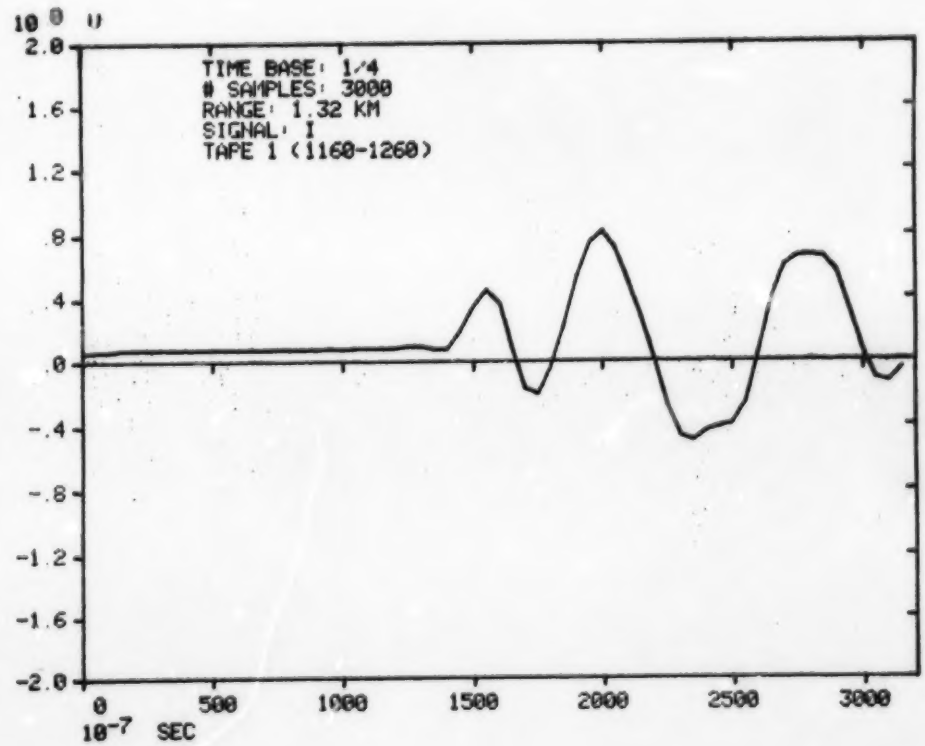
10 0 U
TIME BASE: 1/4
SAMPLES: 3000
RANGE: 1.32 KM
SIGNAL: I
TAPE 1 (1160-1260)
2.0
1.6
1.2
.8
.4
.0
-.4
-.8
-1.2
-1.6
-2.0
0 500 1000 1500 2000 2500 3000
10-7 SEC

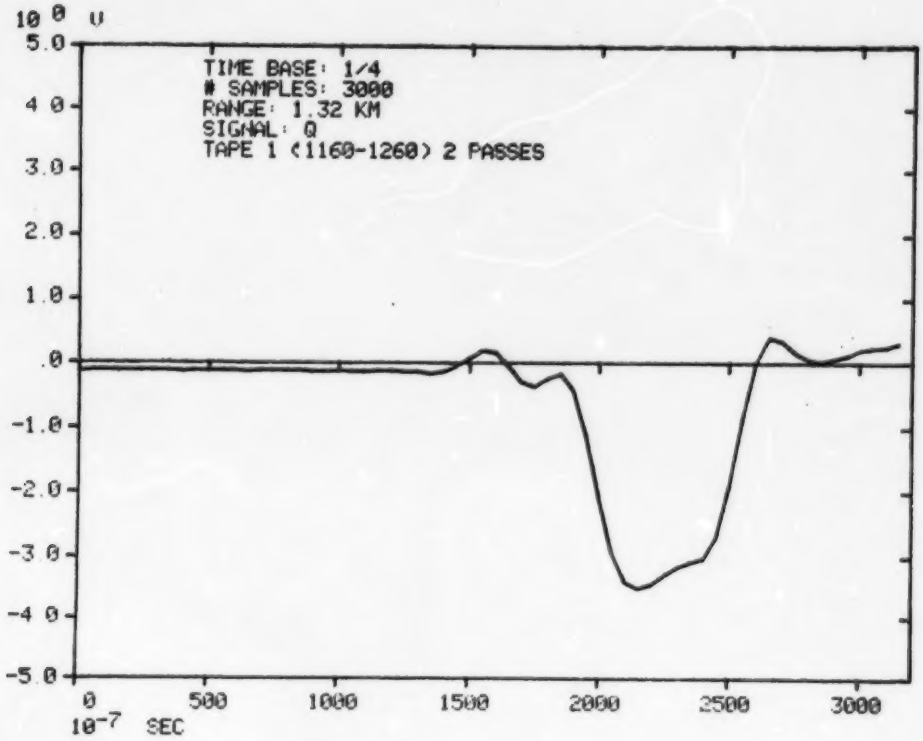
10 0 V
5.0
4.0
3.0
2.0
1.0
.0
-1.0
-2.0
-3.0
-4.0
-5.0
TIME BASE: 1/4
SAMPLES: 3000
RANGE: 1.32 KM
SIGNAL: Q
TAPE 1 (1160-1260) 2 PASSES
0
500
1000
1500
2000
2500
3000
10-7 SEC

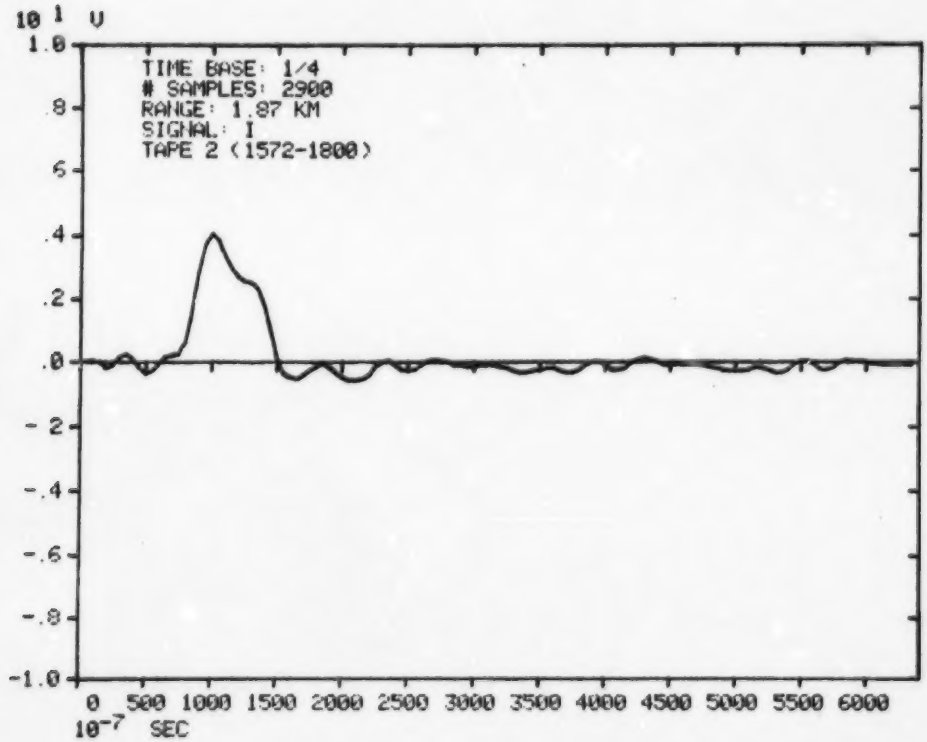
10 1 V
1.0
.8
.6
.4
.2
.0
-.2
-.4
-.6
-.8
-1.0
TIME BASE: 1/4
SAMPLES: 2900
RANGE: 1.87 KM
SIGNAL: I
TAPE 2 (1572-1800)
0 500 1000 1500 2000 2500 3000 3500 4000 4500 5000 5500 6000
10-7 SEC

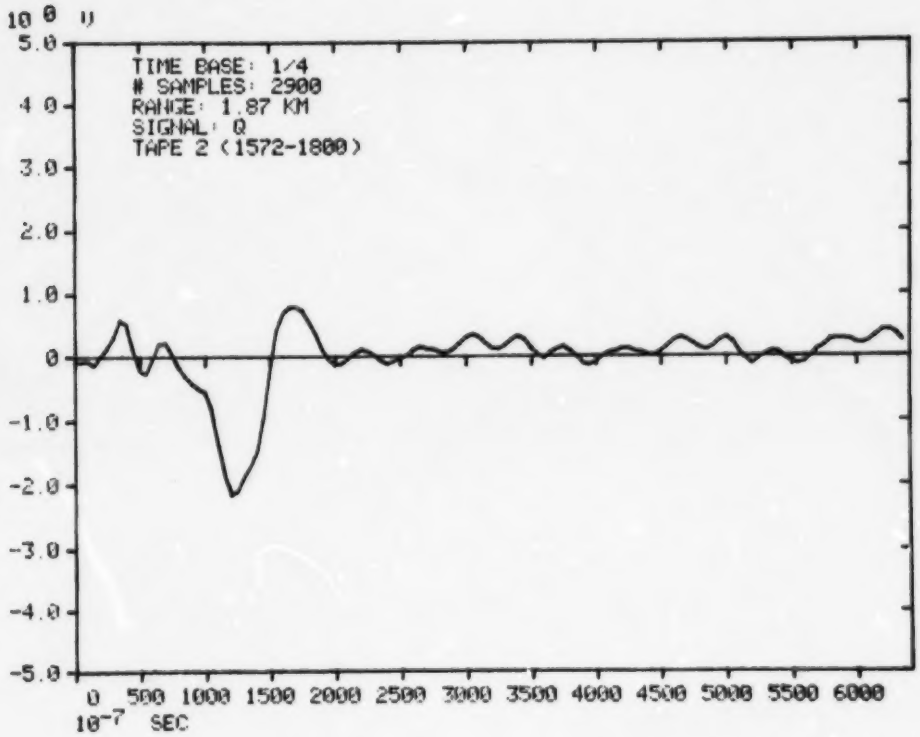
10 0 V
5.0
4.0
3.0
2.0
1.0
0
-1.0
-2.0
-3.0
-4.0
-5.0
TIME BASE: 1/4
SAMPLES: 2900
RANGE: 1.87 KM
SIGNAL: Q
TAPE 2 (1572-1800)
0 500 1000 1500 2000 2500 3000 3500 4000 4500 5000 5500 6000
10-7 SEC

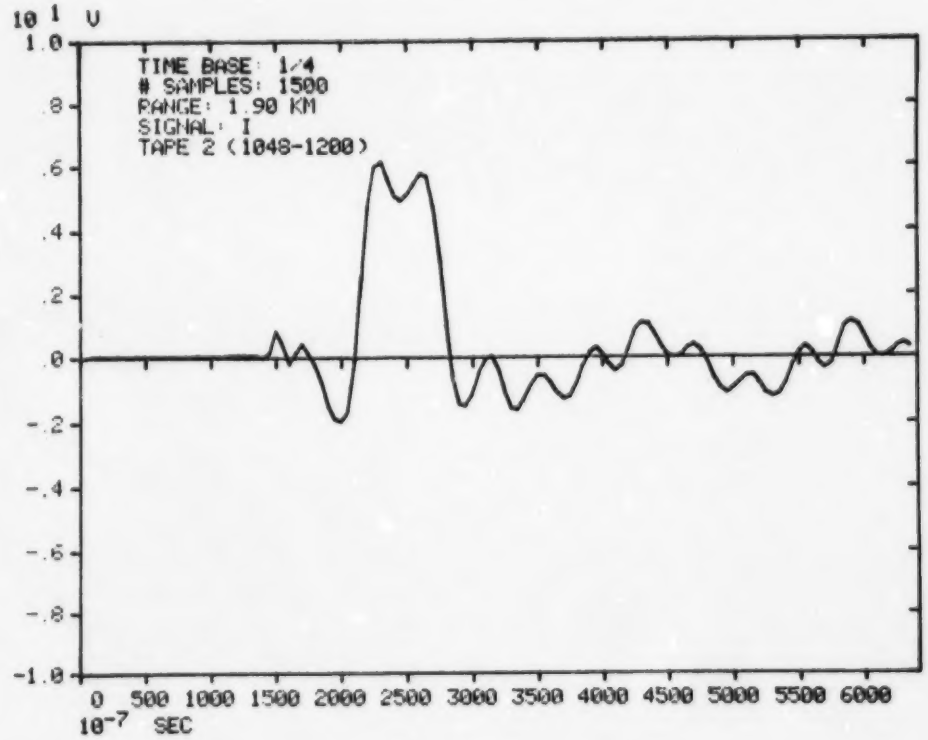
10 1 V
1.0
.8
.6
.4
.2
0
-.2
-.4
-.6
-.8
-1.0
TIME BASE: 1/4
SAMPLES: 1500
RANGE: 1.90 KM
SIGNAL: I
TAPE 2 (1048-1200)
0 500 1000 1500 2000 2500 3000 3500 4000 4500 5000 5500 6000
10-7 SEC

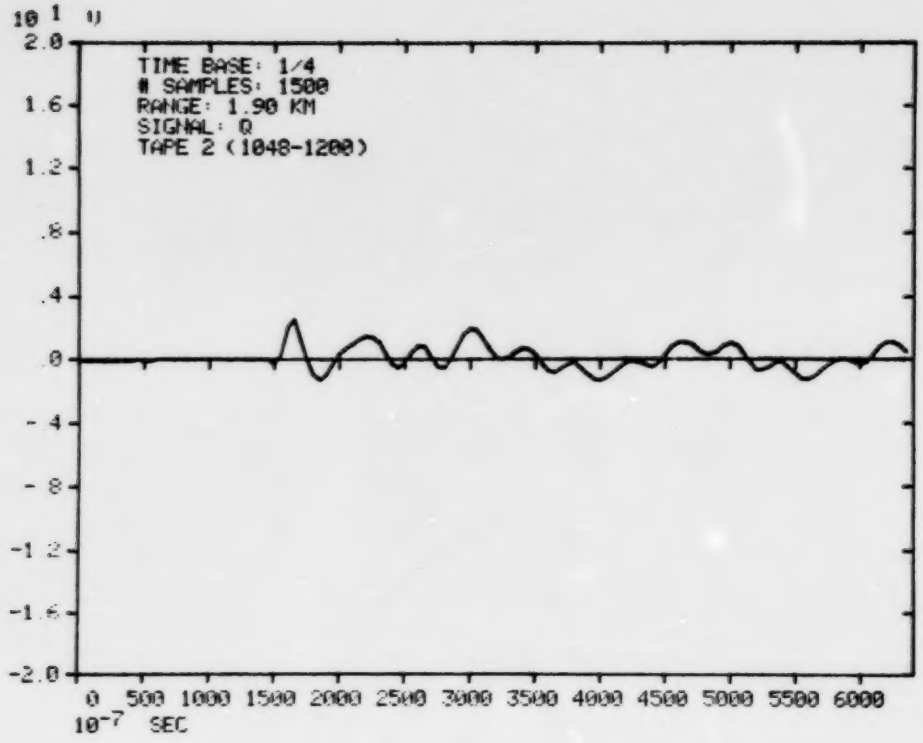
10 1 U
TIME BASE: 1/4
SAMPLES: 1500
RANGE: 1.90 KM
SIGNAL: Q
TAPE 2 (1048-1200)
2.0
1.6
1.2
.8
.4
.0
-.4
-.8
-1.2
-1.6
-2.0
0 500 1000 1500 2000 2500 3000 3500 4000 4500 5000 5500 6000
10-7 SEC

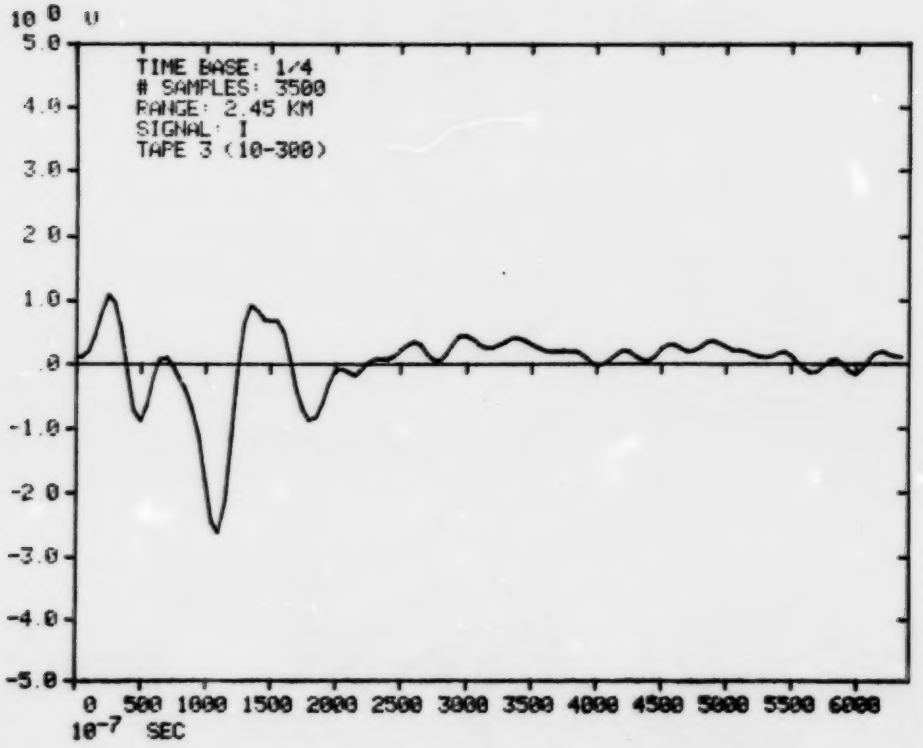
10 0 U
TIME BASE: 1/4
SAMPLES: 3500
RANGE: 2.45 KM
SIGNAL: I
TAPE 3 (10-300)
5.0
4.0
3.0
2.0
1.0
.0
-1.0
-2.0
-3.0
-4.0
-5.0
0 500 1000 1500 2000 2500 3000 3500 4000 4500 5000 5500 6000
10-7 SEC

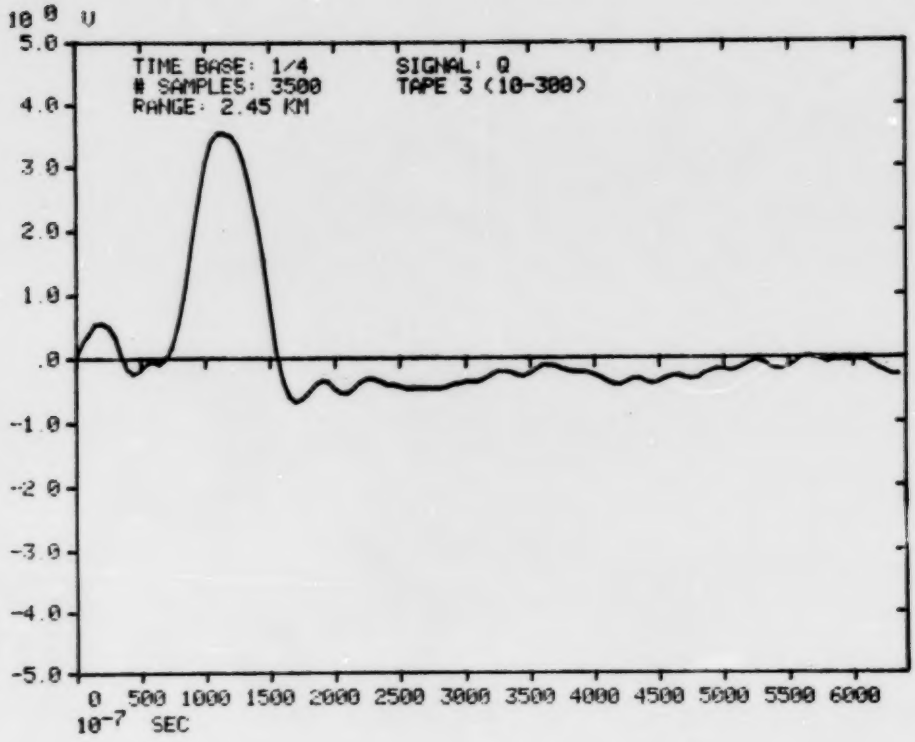
10 0 V
5.0
4.0
3.0
2.0
1.0
.0
-1.0
-2.0
-3.0
-4.0
-5.0
TIME BASE: 1/4
SAMPLES: 3500
RANGE: 2.45 KM
SIGNAL: Q
TAPE 3 (10-300)
0 500 1000 1500 2000 2500 3000 3500 4000 4500 5000 5500 6000
10-7 SEC

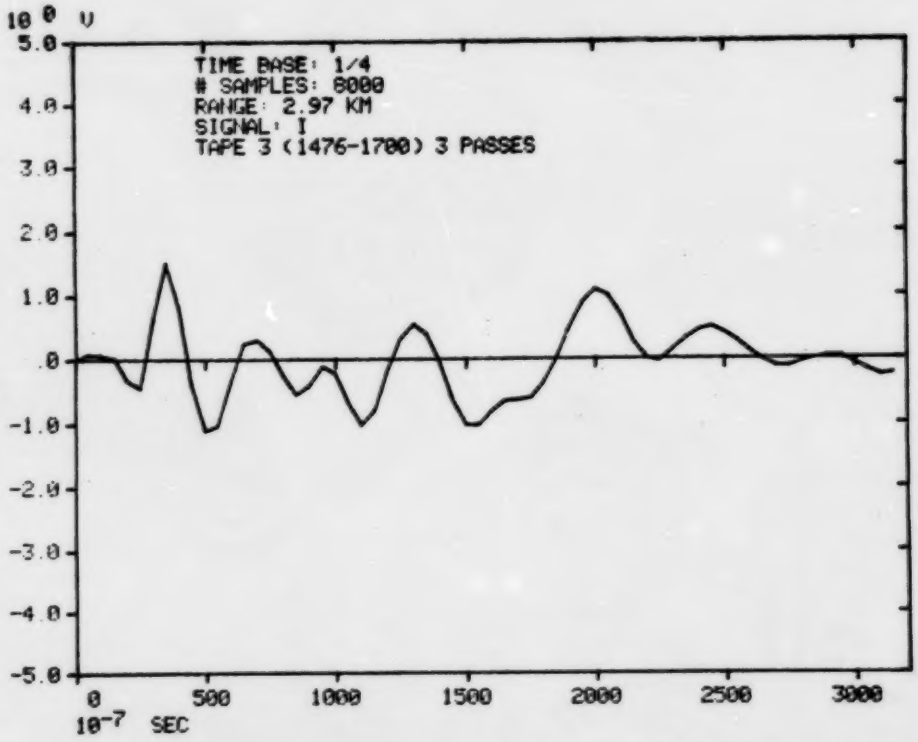
10 0 V
5.0
4.0
3.0
2.0
1.0
.0
-1.0
-2.0
-3.0
-4.0
-5.0
TIME BASE: 1/4
SAMPLES: 8000
RANGE: 2.97 KM
SIGNAL: I
TAPE 3 (1476-1700) 3 PASSES
0 500 1000 1500 2000 2500 3000
10-7 SEC

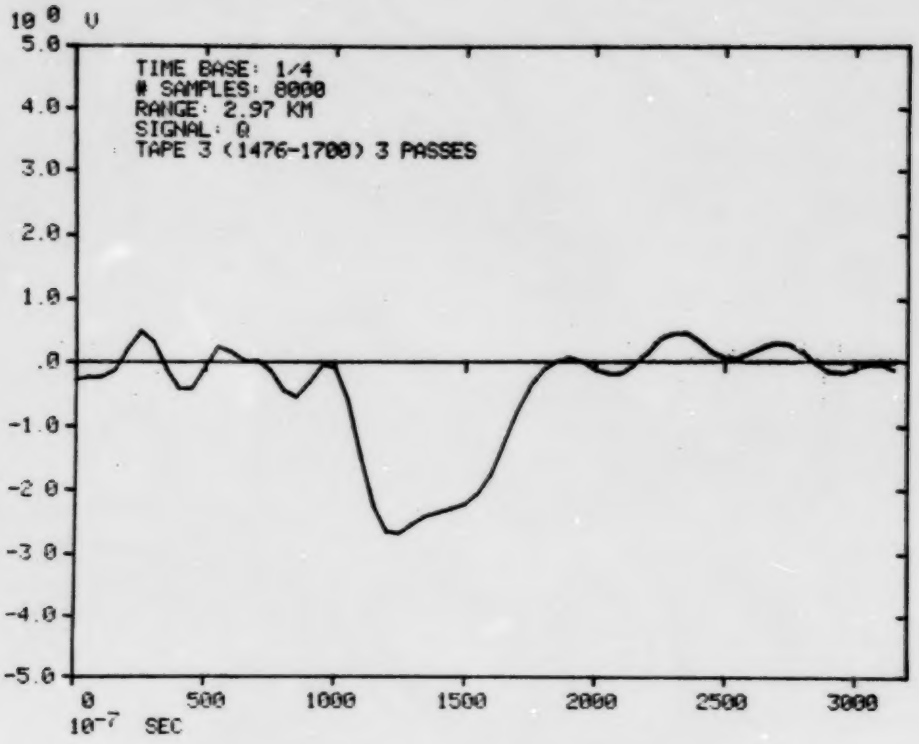
10 0 V
5.0
4.0
3.0
2.0
1.0
.0
-1.0
-2.0
-3.0
-4.0
-5.0
TIME BASE: 1/4
SAMPLES: 8000
RANGE: 2.97 KM
SIGNAL: Q
TAPE 3 (1476-1700) 3 PASSES
0
500
1000
1500
2000
2500
3000
10-7 SEC

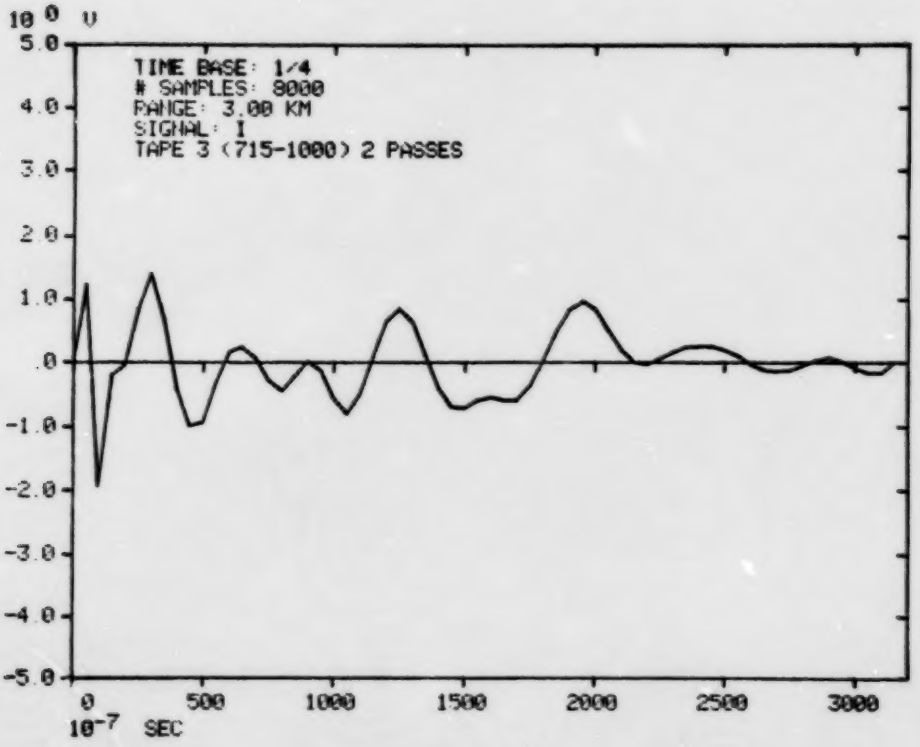
10 0 V
5.0
4.0
3.0
2.0
1.0
.0
-1.0
-2.0
-3.0
-4.0
-5.0
TIME BASE: 1/4
SAMPLES: 8000
RANGE: 3.00 KM
SIGNAL: I
TAPE 3 (715-1000) 2 PASSES
0
500
1000
1500
2000
2500
3000
10-7 SEC

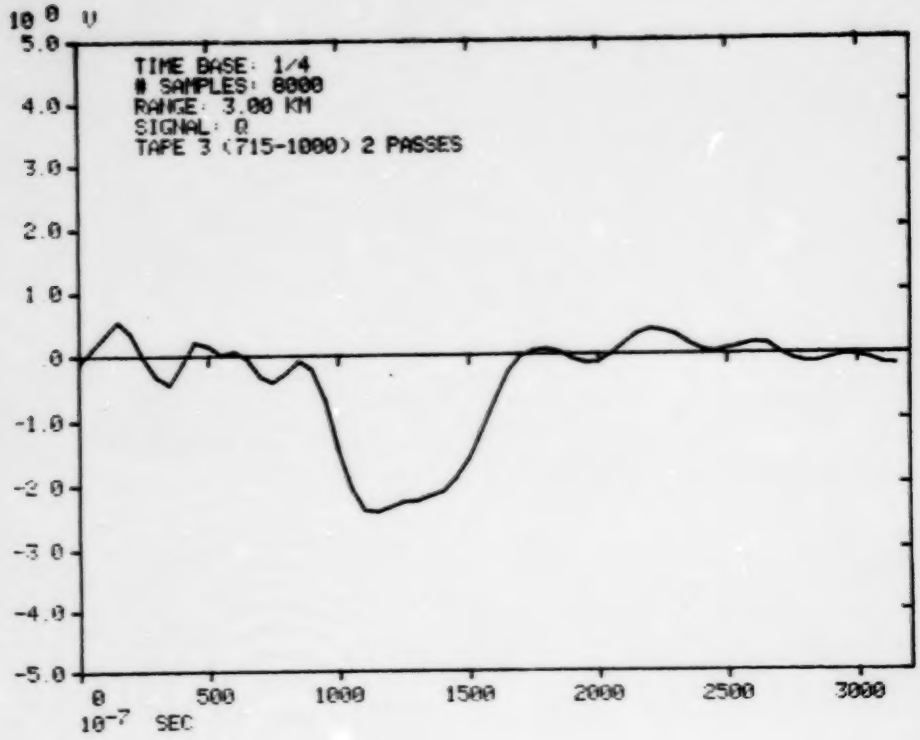
10 0 V
5.0
4.0
3.0
2.0
1.0
0
-1.0
-2.0
-3.0
-4.0
-5.0
TIME BASE: 1/4
SAMPLES: 8000
RANGE: 3.00 KM
SIGNAL: Q
TAPE 3 (715-1000) 2 PASSES
0
500
1000
1500
2000
2500
3000
10-7 SEC

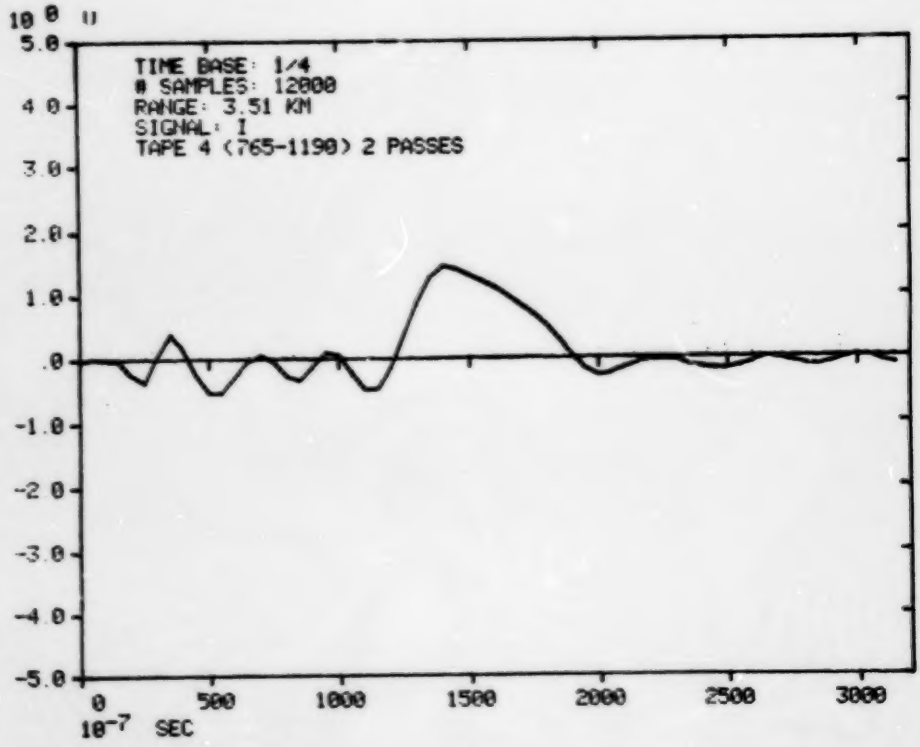
10 0 V
5.0
4.0
3.0
2.0
1.0
.0
-1.0
-2.0
-3.0
-4.0
-5.0
TIME BASE: 1/4
SAMPLES: 12000
RANGE: 3.51 KM
SIGNAL: I
TAPE 4 (765-1190) 2 PASSES
0
500
1000
1500
2000
2500
3000
10-7 SEC

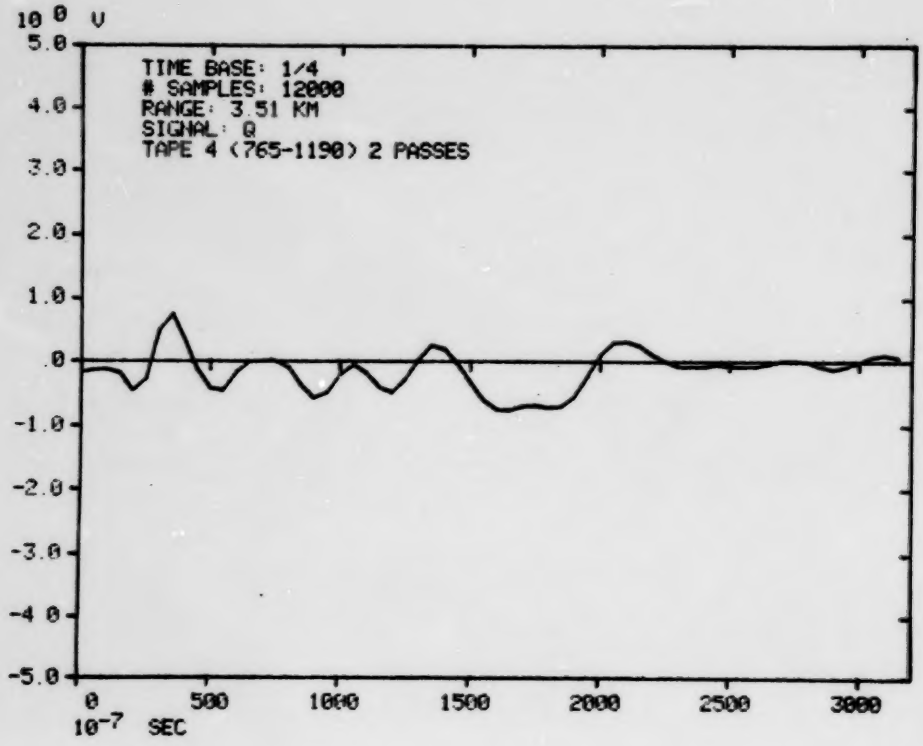
10 0 V
5.0
4.0
3.0
2.0
1.0
.0
-1.0
-2.0
-3.0
-4.0
-5.0
TIME BASE: 1/4
SAMPLES: 12000
RANGE: 3.51 KM
SIGNAL: Q
TAPE 4 (765-1190) 2 PASSES
0
500
1000
1500
2000
2500
3000
10-7 SEC

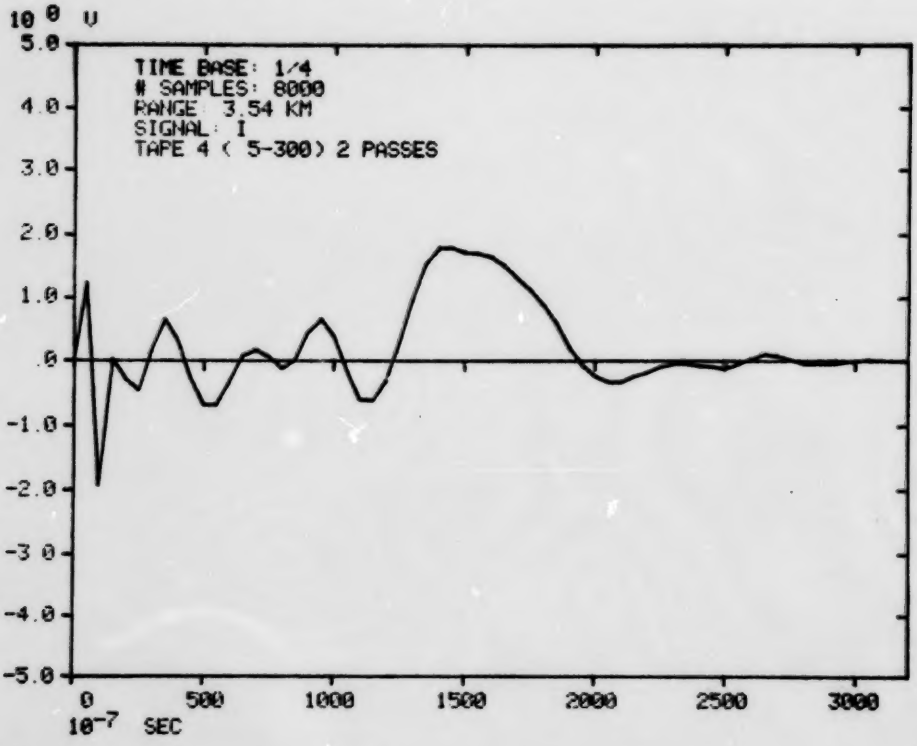
10 0 V
5.0
4.0
3.0
2.0
1.0
.0
-1.0
-2.0
-3.0
-4.0
-5.0
TIME BASE: 1/4
SAMPLES: 8000
RANGE 3.54 KM
SIGNAL: I
TAPE 4 (5-300) 2 PASSES
0
500
1000
1500
2000
2500
3000
10-7 SEC

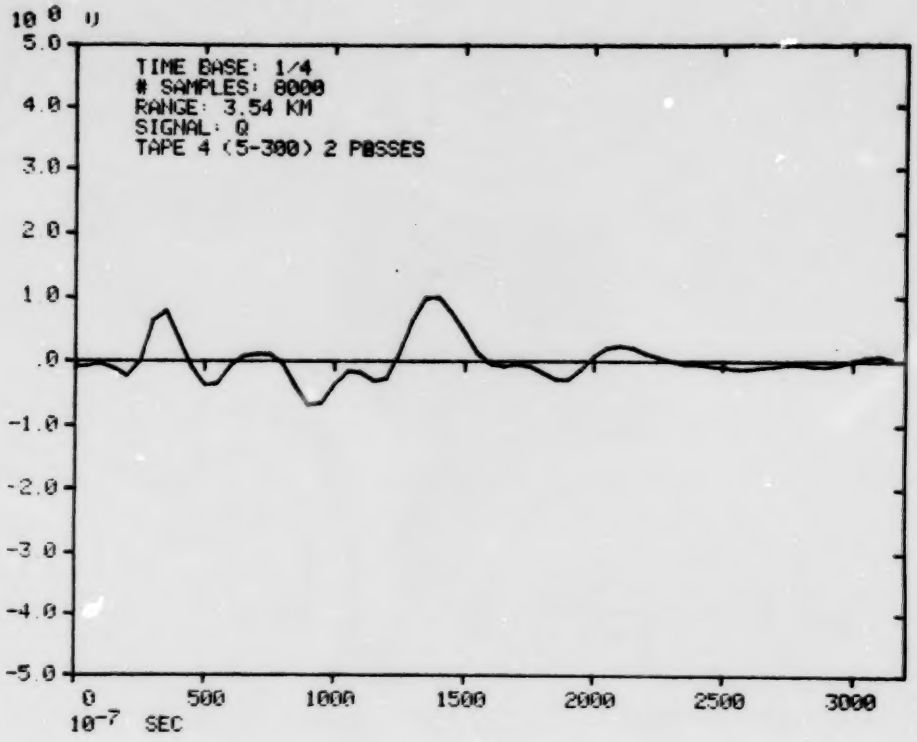
10 0 V
5.0
4.0
3.0
2.0
1.0
.0
-1.0
-2.0
-3.0
-4.0
-5.0
TIME BASE: 1/4
SAMPLES: 8000
RANGE: 3.54 KM
SIGNAL: Q
TAPE 4 (5-300) 2 PASSES
0
500
1000
1500
2000
2500
3000
10-7 SEC

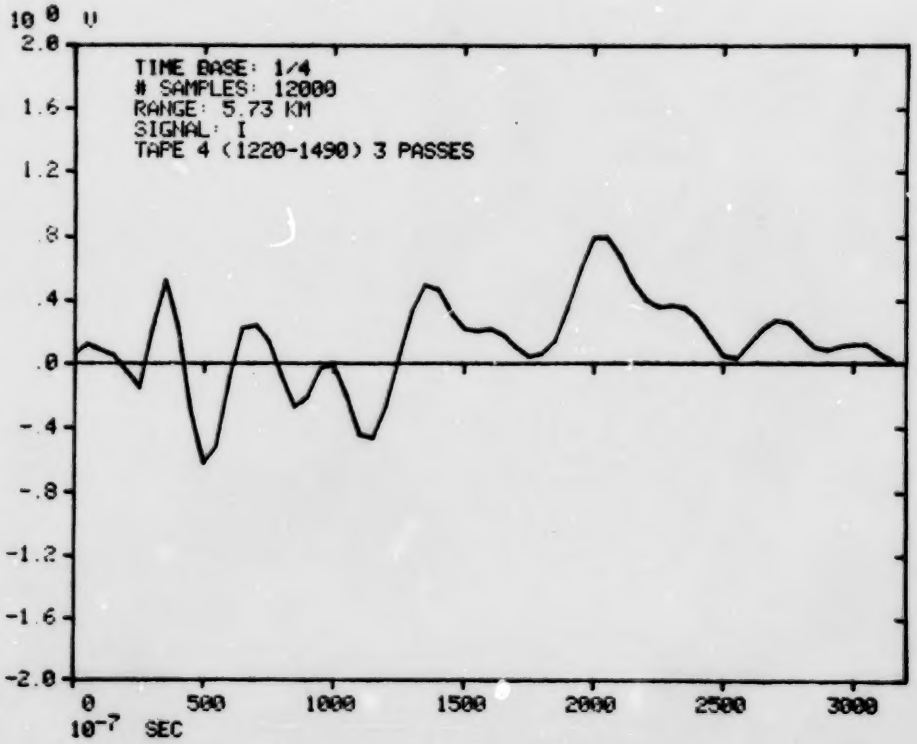
10 0 V
2.0
1.6
1.2
.8
.4
.0
-.4
-.8
-1.2
-1.6
-2.0
TIME BASE: 1/4
SAMPLES: 12000
RANGE: 5.73 KM
SIGNAL: I
TAPE 4 (1220-1490) 3 PASSES
0
500
1000
1500
2000
2500
3000
10-7 SEC

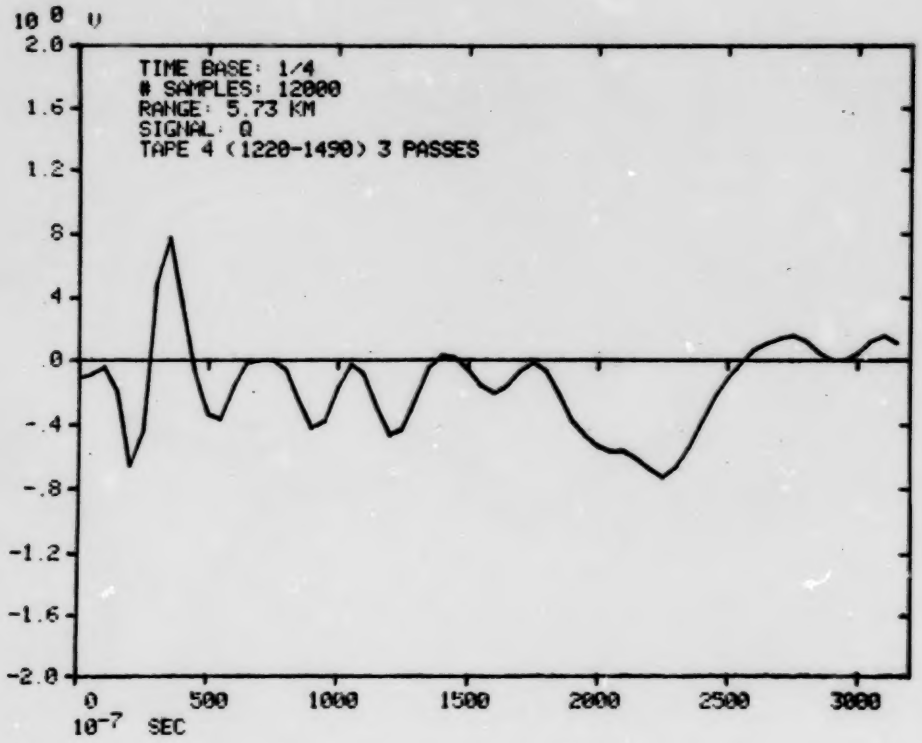
10 0 V
2.0
1.6
1.2
8
4
0
-.4
-.8
-1.2
-1.6
-2.0
TIME BASE: 1/4
SAMPLES: 12000
RANGE: 5.73 KM
SIGNAL: Q
TAPE 4 (1220-1490) 3 PASSES
0
500
1000
1500
2000
2500
3000
10-7 SEC

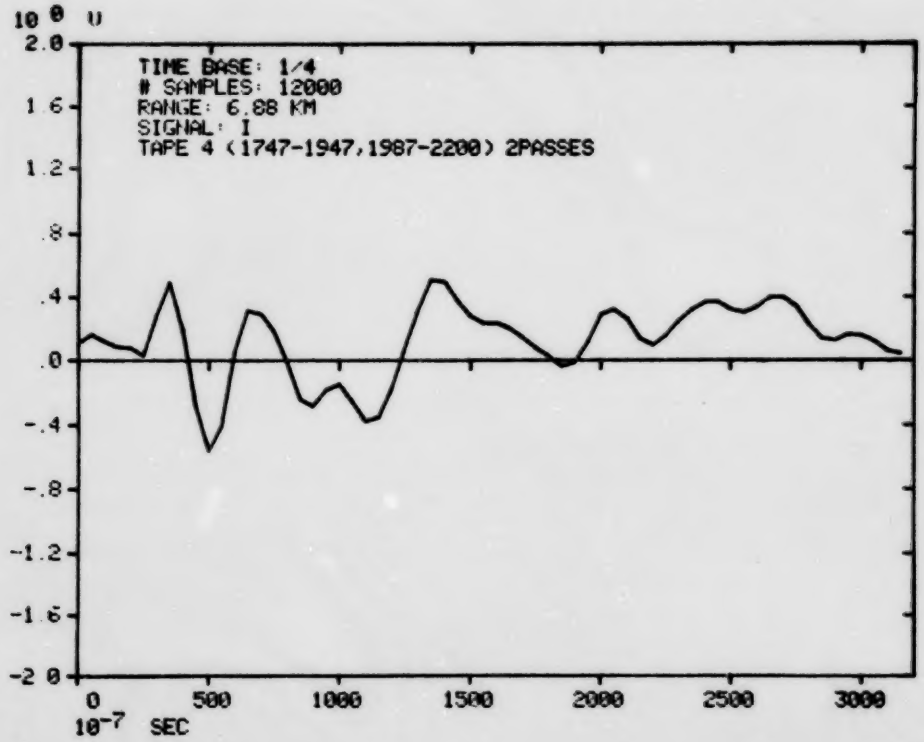
10 0 V
2.0
1.6
1.2
.8
.4
.0
-.4
-.8
-1.2
-1.6
-2.0
TIME BASE: 1/4
SAMPLES: 12000
RANGE: 6.88 KM
SIGNAL: I
TAPE 4 (1747-1947,1987-2200) 2PASSES
0
500
1000
1500
2000
2500
3000
10-7 SEC

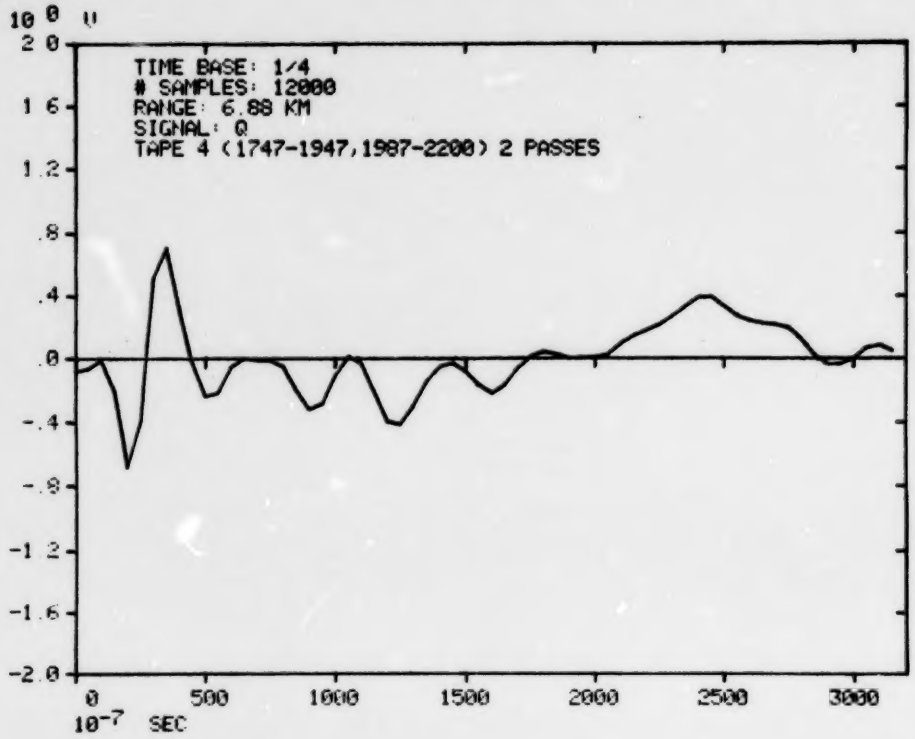
10 0 U
2 0
1 6
1.2
.8
.4
.0
-.4
-.8
-1 2
-1.6
-2.0
TIME BASE: 1/4
SAMPLES: 12000
RANGE: 6.88 KM
SIGNAL: 0
TAPE 4 (1747-1947,1987-2200) 2 PASSES
0
500
1000
1500
2000
2500
3000
10-7 SEC

APPENDIX E

Computerized Model

```
!       ************************************************************
!       **                      NEWPROP                           **
!       **              Written By : Joe Ryan                     **
!       **              Revised By : Wayne Collins                **
!       **         This Version Created : April 27,1983           **
!       ************************************************************
!
!       This program computes the transmission loss with distance
!       of a vertically  polarized H.F. E/M wave propogating over
!       a horozontally  uniform semi-infinite medium, assuming an
!       infinitesimal  dipole  source, and receive  antennas with
!       large  separation, compared  to  the  individual  antenna
!       elevations, given: (1) Antenna  Height  (Transmitter  and
!       Receiver), (2) Distance between transmitter and Receiver,
!       (3) Frequency, (4) Permittivity anc Conductivity for each
!       layer, and (5) Number  of layers (The  lowest layer being
!       semi-infinite seawater). A graph and transmission loss vs.
!       Distance can be plotted if desired.
!       This program requires two data files:
!
!                 Data File #1                        Data File #2
!       ------------------------------------      ----------------
!       Graph Label                [chr string]   # of points
!       # of points                [integer]      Dist.(km),Loss(dB)
!       Distance (km)              [real]               "
!       Starting Point             [real]               "
!       Transmitter Height (m)     [real]               "
!       Receiver Height (m)        [real]               "
!       Frequency (Mhz.)           [real]               "
!       # of layers                [integer]            "
!       # of runs                  [integer]            "
!       Permittivity layer n       [real]               "
!       Conductivity layer n       [real]               "
!       Thickness layer n (m)      [real]               "
!       Permittivity layer n-1     [real]               "
!       Conductivity layer n-1     [real]               "
!       Thickness layer n-1 (m)    [real]               "
!       etc.
!
!       Note: Data File #2 is required only when Observed Data is
!             to be plotted on the graph.
!
!!!
```

```
      COMPLEX CG1,CMUOU,CGAM1,CG2,CGAM2,ZLAYER,ZBELOW,ZEFF,CFREM
      COMPLEX ZO,CCON1,CSEANG,P,CX ,ROTT,ROT,RV,CPI,C2,CFTRM,CZERO
      COMPLEX T,FTERM,CTNICK,CC1,CAPS1,C1,CAPSR,CTHE,EZR,CN1,ZEFFN
      COMPLEX CHECK,CHEK,CPERML,CFACT(500),PCFAC,TANHT,CP2,CH
      REAL EOU,CCHEK,LOSS,CST,IPERML,FACTOR,CONDSE,H1,H2,ELEV,D2,IEZR
      REAL PI,MUO,LAMDA,U,FRQ,D,PERMLR,PERMSE,CONDLR,EPHA,MOPERM
      REAL G2,WAVEN,CON1,TNICK,SELANG,REALP,IMAGP,DPERML,MAGP,REZR
      REAL START,SCALE,DIST,MUOU,ELANGL,THE,X,G1,EMAG,TOU,CONST1
      INTEGER EN,NTHLYR,NRUNS,NPOINT,E,LAYERN,NCHRS,MCHRS,J,COLOR
      CHARACTER*20 DATE,DATA,LABEL,FILE,TRUE,PLTFIL,TEROUT
      CHARACTER GRPH,OBSERV,AXFLG,CLRF,NEWSIG,TO,IC,SW,CLAB

!ZZZ
```

```
950 OPEN (UNIT=3,NAME=FILE,TYPE='OLD')   ! opens data file.
    READ(3,203)DATA    ! graph title.
    READ(3,13)NPOINT   ! # of points calculated ?
    READ(3,45)DIST     ! max. range of interest ?
    READ(3,45)START    ! min. range of interest ?
    READ(3,45)H1       ! first antenna height ?
    READ(3,45)H2       ! second antenna height ?
    READ(3,45)FRQ      ! frequency of interest ?
    READ(3,13)NTHLYR   ! establish number of layers
    READ(3,13)NRUNS    ! number of independent runs with
                       !    this layering
    PERMSE=80          ! set permittivity of sea water
    IF(NEWSIG.NE.'Y'.AND.NEWSIG.NE.'y')THEN
       CONDSE=4        ! set conductivity of sea water.
    ELSE
       WRITE(5,199)'              CONDUCTIVITY ?:'
       ACCEPT *,CONDSE
    END IF
    PI=3.14159         ! constant
    TOW=1.39078/(25*10**3)  ! epsilon(freespace) * 2pi * 10**6
    EOW=TOW*FRQ        ! epsilon(freespace) * onega
    MU0=4*PI/(10**7)   ! permiability of freespace
    LAMDA=300./FRQ     ! freespace wavelength
    W=2*PI*FRQ*10**6   ! angular frequency
    Z0= CMPLX(377.,0.)! complex impedence of freespace
    CZERO=CMPLX(0.,0.) !
    CPI=CMPLX(PI,0.)   !
    CP2=CMPLX(2.,0.)   ! complex constants
    C2=CMPLX(0.,-2.)   !
    C1=CMPLX(0.,1.)    !
    CC1=CMPLX(1.,0.)   !
    MU0W=MU0*W
    CMU0W=CMPLX(0.,MU0W)
    WAVEN=W/(3*10**8) ! free space wavenumber (2pi/lamda)
    IPEN=3
    COLOR=1
    SCALE=(DIST)/10.  ! scale range of interest to 10 inch graph
    IF(TO.NE.'Y'.AND.TO.NE.'y')GOTO 965
       OPEN(UNIT=1,NAME=TEROUT,TYPE='NEW')
965 IF(IC.NE.'Y'.AND.IC.NE.'y')GOTO 970
       CALL INDATA(GRPH,NPOINT,DIST,START,H1,H2,FRQ,NTHLYR,NRUNS,DATE)
       !  print input data as read from data file.
970 IF(GRPH.NE.'Y'.AND.GRPH.NE.'y')GOTO 980
    OPEN(UNIT=4,NAME=PLTFIL,TYPE='NEW')
    CALL PLOTS (53,1,4)
    IF(AXFLG.EQ.'Y'.OR.AXFLG.EQ.'y')CALL GRAPH(SCALE,NCHRS,DATA,DATE)
    ! draw axis

!XXXX
```

```
980 DO 900 J=1,NRUNS
      IF(GRPH.NE.'Y'.AND.GRPH.NE.'y')GOTO 990
      IF(CLAB.EQ.'Y'.OR.CLAB.EQ.'y')THEN
         WRITE(5,197)'            CURVE ',J,'  LABEL :'
         ACCEPT 202,LABEL   ! Curve Label for multiple curve plots
      ELSE
         LABEL='  '
      END IF
      CALL NEWPEN(COLOR)
990   IPEN=3
      D = START*1000.  ! converts from km. to m.

!   This loop (888) computes the normalized surface impedence
!   for each layer.

      DO 888 N=1,NTHLYR  ! first layer on top of sea water
         LAYERN=1+NTHLYR-N  ! nth layer=uppermost layer
         IF(NEWSIG.NE.'Y'.AND.NEWSIG.NE.'y')THEN
            IF(SW.EQ.'Y'.OR.SW.EQ.'y')THEN
               PERMLR=80.0
               CONDLR=4.0
               THICK=0.01
            ELSE
               READ(3,10)PERMLR   ! set relative permittivity of layer
               READ(3,10)CONDLR   ! set conductivity of layer
               READ(3,10)THICK    ! set thickness of layer
            END IF
         ELSE
            PERMLR=80.0
            CONDLR=CONDSE
            THICK=0.01
         END IF
         IPERML=CONDLR/EOW  ! imaginary part of layer
                            !    complex permittivity
         CPERML=CMPLX(PERMLR,-IPERML)  ! layer complex permittivity
         MGPERM=CABS(CPERML)! magnitude of layer complex
                            !    permittivity
         IF(MGPERM.GT.10)GOTO 77
         IF(IC.NE.'Y'.AND.IC.NE.'y')GOTO 77
         WRITE(1,*)' '          !  prints a space.
         WRITE(1,112)LAYERN,MGPERM
77       G1=PERMLR*EOW      ! epsilon(layer) * omega
         G2=PERMSE*EOW      ! epsilon(sea) * omega
         CONST1=60*CONDLR*LAMDA

!   Calculate propagation consts.

         CG1=CMPLX(CONDLR,G1)
         CG2=CMPLX(CONDSE,G2)
         CGAM2=CMUOW*CG2
         CGAM1=CMUOW*CG1
         ZLAYER=CMUOW*CSQRT(CGAM1+WAVEN**2)/CGAM1
         !     =surface impedence of current layer
         IF(N.GT.1)GOTO 44! if lowest layer zbelow=(seawater)
         ZBELOW=CMUOW*CSQRT(CGAM2+WAVEN**2)/CGAM2
         !     =surface impedence of seawater
44       CTHICK=CMPLX(THICK,0.)
         T=CTHICK*CSQRT(CGAM1+WAVEN**2)
         TANHT=(CEXP(T)-CEXP(-T))/(CEXP(T)+CEXP(-T))
```

```
            !    =hyperbolic tangent of T
            IF(IC.EQ.'Y'.OR.IC.EQ.'y')CALL OUTPUT(ZLAYER,ZBELOW,T,
     +      TANHT,LAYERN,PERMLR,CONDLR,THICK)

!    Compute cumulative surface impedence layer by layer

            ZEFF=ZLAYER*(ZBELOW+ZLAYER*TANHT)/(ZLAYER+ZBELOW*TANHT)
            !   =effective surface impedence,
            !      including current layer
            ZBELOW=ZEFF  ! zbelow now includes current layer
            AZEFF=CABS(ZEFF)/377 ! normalized surface impedence.
            ZEFFN=ZEFF/Z0
          IF(IC.EQ.'Y'.OR.IC.EQ.'y')WRITE(1,93)ZEFFN
 888      CONTINUE

!ZZZ
```

```
!    Asymptotic series expansion (b - positive)

   89       CFTRM=C2*CSQRT(CPI*P)*CEXP(-P)
            !    =extra term for b-positive case

!    Asymptotic series expansion  b(+/-)

   90       CN=CC1  ! asymptotic series evaluation continues
            CFREM=CZERO
            EN=1
  100       CHECK=CABS(CFREM)  ! store old series value
               CFREM=-CN/((CP2*P)**EN)+CFREM  !add next term in series
               CN1=CN1+CP2  ! increment by 2
               CN=CN*CN1! adjust series coefficient next term
               EN=EN+1  ! adjust series power next term
               CHEK=CABS(CFREM)  ! store new series value
               CCHEK=ABS(CHECK-CHEK) ! calculate effect of
                                     !   last term in series
               IF(CCHEK.GT.0.0001)GOTO 100
               !  if series is oscillating, continue
            FTERM=CFTRM+CFREM  ! final value of series
            GOTO 300

!zzzz
```

```
!       For some values of "rezr" and "iezr" the calculation of "emag"
!    will produce numbers too large to be represented by the computer,
!    i.e.(greater than 1.7E+38).The following program segment will check
!    to see if such a situation exists. If so, it will then scale down
!    "rezr" and "iezr",perform the calculation, and rescale "emag".

        IF(((ABS(REZR)).GT.(1.7E-19)).AND.
     +  ((ABS(IEZR)).GT.(1.7E-19)))GOTO 349
           TYPE *,' COMPONENT OF EZR TOO SMALL'
  349      FACTOR=1
  350      IF(((ABS(REZR)).LT.(1.0E+18)).AND.((ABS(IEZR)).LT
     +     .(1.0E+18)))GOTO 410
           ! checks size of EZR ie.(is scaling necessary ?)
              REZR=REZR/10 ! scale down REZR by factor of 10
              IEZR=IEZR/10 ! scale down IEZR by factor of 10
              FACTOR=FACTOR*10 ! adjusts scaling factor
              GOTO 350 ! recheck size of EZR
  410      EMAG=SQRT(REZR**2+IEZR**2)
           ! compute modulus of EZR
           EPHA=ATAN2(IEZR,REZR) ! compute arguement of EZR
           CST=(EMAG*LAMDA)/(4*PI*D)
           LOSS=-20*(ALOG10(CST)+ALOG10(FACTOR)) ! calculate loss in dB.
           Y=1.+(175.-LOSS)*7./175  ! y-coordinate of graph.
           D2=D/1000.
           X=1.+(D2)/SCALE          ! x-coordinate of graph.
           IF(TO.NE.'Y'.AND.TO.NE.'y')GOTO 500
              WRITE(1,301) B,MAGP,EMAG,FACTOR,EPHA,LOSS,D
  500      D=D+((DIST-START)*1000.)/(NPOINT-1) ! increment dist
           IF(GRPH.NE.'Y'.AND.GRPH.NE.'y')GOTO 800
           CALL PLOT(X,Y,IPEN)
           IPEN=2
  800    CONTINUE
         IF(GRPH.NE.'Y'.AND.GRPH.NE.'y')GOTO 900
         CALL NEWPEN(1)
         CALL SYMBOL(X+.1,Y-.025,.05,LABEL,0.,20)
         IF(CLRF.EQ.'Y'.OR.CLRF.EQ.'y')COLOR=COLOR+1
         IF(COLOR.GE.5)COLOR=1
  900 CONTINUE
      CLOSE (UNIT=3)
      IF(TO.EQ.'Y'.OR.TO.EQ.'y')CLOSE (UNIT=1)
      IF(GRPH.NE.'Y'.AND.GRPH.NE.'y')GOTO 901
         IF(OBSERV.EQ.'Y'.OR.OBSERV.EQ.'y')CALL DATPLT(SCALE,TRUE)
         CALL PLOT(0.,0.,999)
         CLOSE (UNIT=4)
  901 CONTINUE
   10 FORMAT(F10.5)
   12 FORMAT(I1)
   13 FORMAT(X,I2)
   15 FORMAT(X,I1)
   45 FORMAT(X,F5.2)
   93 FORMAT('          NORMALIZED SURFACE IMPEDENCE =',
     +       F10.7,' +',F10.7,' i '//)
  111 FORMAT(' SURFACE IMPEDENCE ',F15.7)
  112 FORMAT(' MAGNITUDE OF COMPLEX PERMITTIVITY FOR LAYER ',
     +   I2,' = ',F10.7)
```

```
  190 FORMAT(A1)
  197 FORMAT($,A18,I2,A9)
  198 FORMAT($,A22)
  199 FORMAT($,A29)
  200 FORMAT($,A15)
  201 FORMAT(X,A20)
  202 FORMAT(A15)
  203 FORMAT(A20)
  301 FORMAT(F8.5,F12.3,4X,E10.5,1X,E10.5,1X,F12.6,1X,F9.2,F10.2)
  305 FORMAT(2X,'NUMERICAL DISTANCE',9X,'ELECTRIC FIELD',21X
     +   ,'LOSS',3X,'DISTANCE')
  306 FORMAT(' PHASE (RAD)',2X,'MAGNTD',6X,'MAGNTD',6X,'FACTOR',
     +   9X,'PHASE',6X,'(DB)',3X,'(METERS)'//)
  801 STOP
      END

!ZZZ
```

```
      SUBROUTINE OUTPUT(ZLAYER,ZBELOW,T,TANHT,LAYERN,
     + PERMLR,CONDLR,THICK)
           COMPLEX ZLAYER,ZBELOW,T,TANHT
           INTEGER LAYERN
           WRITE(1,600)'  EPSILON FOR LAYER ',LAYERN,' = ',PERMLR
           WRITE(1,600)'    SIGMA FOR LAYER ',LAYERN,' = ',CONDLR
           WRITE(1,600)' THICKNESS OF LAYER ',LAYERN,' = ',THICK
           WRITE(1,666)LAYERN,ZLAYER
           WRITE(1,676)ZBELOW
           WRITE(1,686)T
           WRITE(1,696)TANHT
  600    FORMAT(25X,A20,I2,A3,F10.7)
  666    FORMAT('         COMPLEX IMPEDENCE OF LAYER ',I2,' =',
     +         F10.4,' +',F10.4,' i')
  676    FORMAT(' COMPLEX IMPEDENCE OF ALL LAYERS BELOW =',
     +         F10.4,' +',F10.4,' i')
  686    FORMAT('                                        T =',
     +         F10.7,' +',F10.7,' i')
  696    FORMAT('                HYPERBOLIC TANGENT OF T =',
     +         F10.7,' +',F10.7,' i')
      RETURN
      END

!zzzz
```

POOR

QUALITY

ORIGINAL